Assembly of cytochrome *c* oxidase: the role of hSco1p and hSco2p

Dissertation

zur Erlangung des akademischen Grades Doktor der Naturwissenschaften (Dr. rer. nat.)

eingereicht an der Fakultät Mathematik und Naturwissenschaften der Technischen Universität Dresden

von

Claudia Paret

aus Turin

Dresden, Oktober 2001

Gutachter:	1. Prof. Dr. Gerhard Rödel 2. Prof. Dr. Michael Göttfert 3. Dr. Michaela Jaksch
Eingereicht am:	15.10.2001
Tag der Verteidigung:	17.12.2001

Part of this work was published:

Paret, C., Ostermann, K., Krause-Buchholz, U., Rentzsch, A. and Rödel, G. (1999) Human members of the *SCO1* gene family: complementation analysis in yeast and intracellular localization. *FEBS Lett* **447**, 65-70.

Paret, C., Lode, A., Krause-Buchholz, U. and Rödel, G. (2000) The P(174)L mutation in the human *hSCO1* gene affects the assembly of cytochrome *c* oxidase. *Biochem Biophys Res Commun* **279**, 341-7.

Jaksch, M., Paret, C., Stucka, R., Horn, N., Mueller-Hoecker, J., Horvath, R., Trepesch, N., Stecker, G., Freisinger, P., Thirion, C., Müller, J., Lunkwitz, R., Rödel, G., Shoubridge, E.A. and Lochmüller, A. (2001) Cytochrome *c* oxidase deficiency due to mutations in *SCO2*, encoding a mitochondrial copper chaperone, is rescued by copper in human myoblasts. *Hum Mol Gen* **in press**.

Contents

Abbreviations

Aa	Amino acid
ADH	Alcohol dehydrogenase
APS	Ammoniumperoxidisulfat
ATP	Adenosine triphosphate
BCS	Bathocuproine sulfonate
BSA	Bovine serum albumin
CMV	Cytomegalovirus
CMXRos	Chloromethyl-X-rosamine
Conc	Concentration
COX	Cytochrome *c* oxidase
C-terminus	Carboxyl-terminus
Cu	Copper
DMEM	Dulbecco's Modified Eagle medium
DMSO	Dimethyl sulfoxide
DNA	Deoxyribonuleic acid
dNTP	Deoxynucleosidtriphosphate
DTT	Dithiothreitol
EDTA	Ethylendiamine-tetraacetic acid
EGFP	Enhanced green fluorescent protein
$FADH_2$	Flavin adenine dinucleotide (reduced form of FAD)
FCS	Fetal Calf Serum
Gal	Galactose
GSH	Glutathione
GST	Glutathione S-transferase
HRP	Horseradish-peroxidase
IM	Inner membrane
IMS	Intermembrane space
IPTG	Isopropyl-1-thio-ß-D-galactopyranoside
Kan	Kanamycin
kDa	Kilodalton
MCS	Multiple cloning site
mt	Mitochondrial
MT	Metallothionein
n	Nuclear
NADPH	Nicotinamide adenine dinucleotide phosphate (reduced form of $NADP^+$)
Neo	Neomycin
NP-40	Nonidet P-40
N-terminus	Amino-terminus
OD	Optical density
PAGE	Polyacrylamide gel electrophoresis
PBS	Phosphate buffered saline
PCR	Polymerase chain reaction
PMSF	Phenylmethylsulfonyl fluoride
PVDF	Polyvinylidene difluoride
RT	Room temperature
SDS	Sodium dodecyl sulphate

SDS-PAGE	Sodium dodecyl sulfate polyacrylamide gel electrophoresis
TEMED	N,N,N',N'-Tetramethylethylenediamine
TM	Transmembrane
Tris	Tris(hydroxymethyl)aminomethane
v/v	Volume per volume
w/v	Weight per volume

Amino acids

A	Ala	alanine	M	Met	methionine
C	Cys	cysteine	N	Asn	asparagine
D	Asp	aspartate	P	Pro	proline
E	Glu	glutamate	Q	Gln	glutamine
F	Phe	phenylalanine	R	Arg	arginine
G	Gly	glycine	S	Ser	serine
H	His	histidine	T	Thr	threonine
I	Ile	isoleucine	V	Val	valine
K	Lys	lysine	W	Trp	tryptophan
L	Leu	leucine	Y	Tyr	tyrosine

Aim of the work

Human cytochrome *c* oxidase (COX), the last enzyme of the respiration pathway in mitochondria, is a complex enzyme constituted from at least 13 subunits, 3 of which are encoded by the mitochondrial DNA. The assembly process requires the involvement of different chaperones. The catalytic core of the enzyme, consisting of the three mitochondrially encoded subunits Cox1p, Cox2p and Cox3p, contains three copper atoms and two heme groups. Because free copper is not available in the cells, specific copper chaperones are necessary to deliver copper to the mitochondria and to COX. Studies in yeast suggest that the transfer of copper to the mitochondria requires yCox17p* and that two proteins, ySco1p and ySco2p, representatives of a large protein family, are involved in the insertion of copper in COX. Sco proteins could perform this function by binding copper and transferring it to COX. Alternatively, they could allow COX to assume a three-dimensional structure necessary for the insertion of copper from another chaperone. This last function is performed in bacteria by thioredoxin-like proteins. In human, two Sco proteins have been identified. Mutations in these proteins have been associated with lethal COX deficiency in infants.

This work will be focused on the characterisation of both hSco proteins and of some mutant forms found in patients. The intracellular localisation and the ability of the hSco proteins to substitute for the yeast homologues should be analysed. It is planned to develop a yeast model to characterise *hSCO* mutations. Recombinant hSco1p, hSco2p and mutant forms should be purified and analysed for their ability to bind copper and to act as thioredoxins. To define the pathway of the copper insertion, interaction with hCox17p and Cox2p will be analysed. Moreover, the ability of the two proteins to form homomers and heteromers should be examined.

*To distinguish between human and yeast, y is used to denote the yeast genes and proteins while h is used to denote the mammal genes and proteins.

1 INTRODUCTION

Mitochondria are small intracellular organelles present in the cytoplasm of aerobic eukaryotic cells. They are surrounded by a double membrane, the outer membrane separates the mitochondrion from the cytosol, the inner membrane is invaginated to form cristae which protrude into and define the matrix of the organelle. Most human cells contains 500 to 2000 mitochondria, often dynamically interconnected in a complex reticular network. Some cell types, like platelets, have only few mitochondria and red blood cells do not contain mitochondria. In the last decade, a considerable body of evidence has accumulated implicating defects in the mitochondrial (mt) energy-generating pathway, oxidative phosphorylation (OXPHOS), in a wide variety of degenerative diseases. The ubiquitous nature of mitochondria, the dual genetic control of the respiratory chain, and the peculiar rules of mt genetics contribute to explain the extraordinary clinical heterogeneity of disorders associated with defects of OXPHOS [1]. Abnormalities of the electron transport and OXPHOS system are probably the most common cause of mt diseases.

1.1 The OXPHOS System

The OXPHOS system is the main process responsible for the production of energy in the form of ATP in most animal tissues under most conditions. The human OXPHOS system contains at least 83 polypeptides, 13 of which are encoded by mtDNA genes. From a genetic point of view, the respiratory chain results from a coordinate expression of the nuclear (n) genome and the mt genome. The human mtDNA is a circular double-stranded molecule of 16,569 base pairs. It encodes 13 proteins, 2 rRNAs and 22 tRNAs [2]. Introns are absent and all coding sequences are contiguous with each other and lack significant untranslated flanking regions. All proteins encoded from mtDNA are directly involved in OXPHOS and include components of complex I (encoded by ND1, ND2, ND3, ND4, ND4L, ND5, ND6), III (encoded by CYT b), IV (encoded by COX1, COX2 and COX3) and V (encoded by A6 and A8). All other mt proteins (around 1100) are transcribed from the respective nuclear genes, translated in the cytoplasm and their products are imported into mitochondria.

The five multi-protein complexes involved in OXPHOS are located in the mt inner membrane. Substrates feed electrons into the respiratory chain at different points. Electrons are passed down the chain and protons are pumped into the mt intermembrane space. This creates the electrochemical membrane potential which is used to drive ATP production through re-entry of

protons via complex V. Complex I oxidises NADH, transfers electrons to ubiquinone (or coenzyme Q, CoQ) and pumps protons to the intermembrane space. Complex II links the tricarboxylic acid cycle and the respiratory chain: it converts succinate to fumarate, producing reducing equivalents as FADH2 and transferring electrons to ubiquinone. Complex III transfers electrons from ubiquinone to cytochrome c (cyt c) while pumping protons to the intermembrane space. Complex IV transfers electrons from cyt c to molecular oxygen and pumps protons to the intermembrane space. Complex V couples the proton gradient generated by the respiratory chain to ATP synthesis. Fig. 1 shows the OXPHOS complexes and denotes the associated diseases.

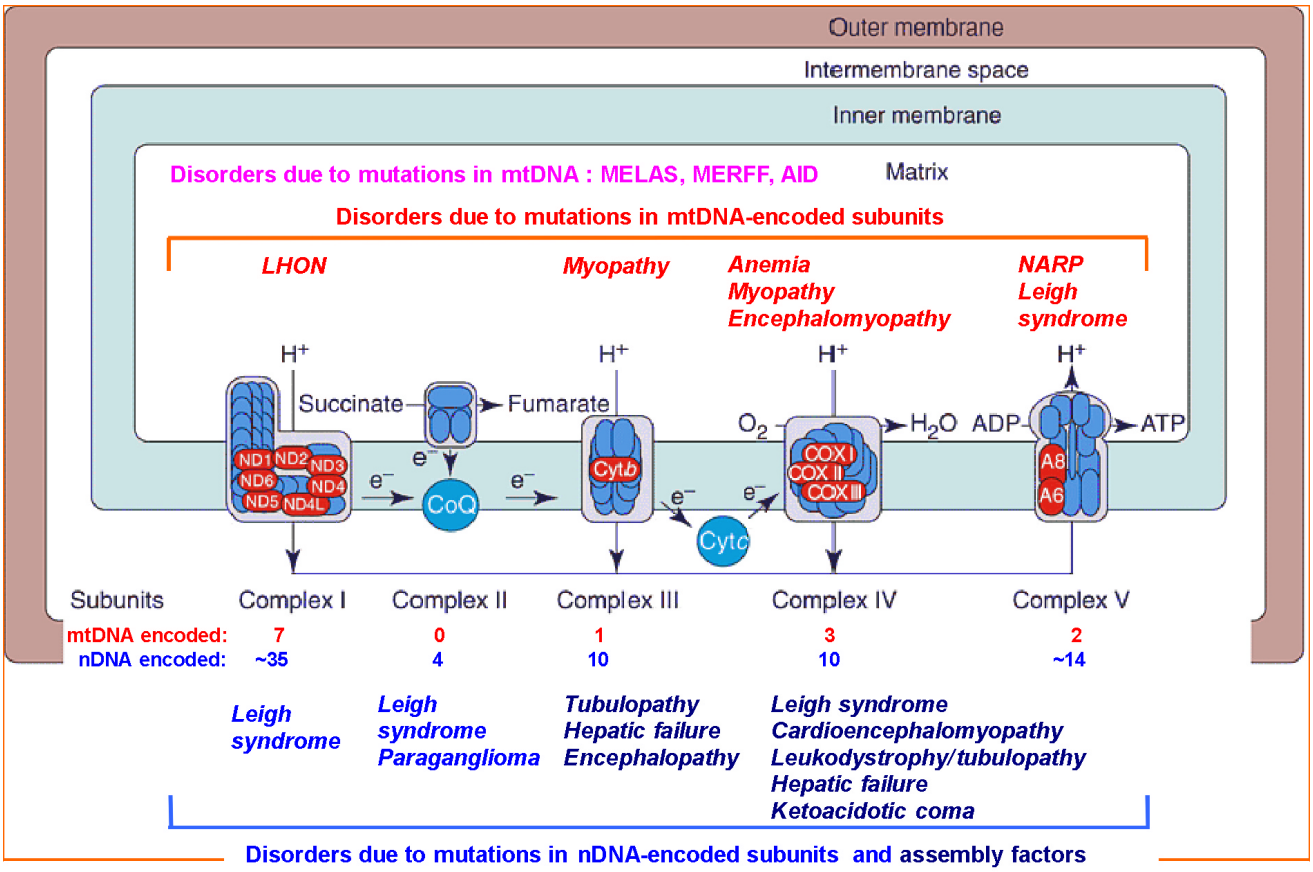

Fig. 1. Diseases associated with defects of OXPHOS.
OXPHOS complexes are composed of nDNA-encoded (blue) and mtDNA-encoded subunits (red). The 'vertical' flow of protons (H^+) and the concomitant 'horizontal' flow of electrons (e^-) through the respiratory complexes and the two mobile electron carriers CoQ and cyt *c* result in the synthesis of ATP from ADP at Complex V. Diseases associated with mutations in mt-encoded tRNA, and rRNA are in pink. The diseases associated with specific complexes are indicated: diseases resulting from mutations in mtDNA-encoded subunits are in red, from mutations in nDNA-encoded subunits are in blue and from mutations in assembly factors are in dark blue. Details and abbreviations are given in the text. (In part taken from [3])

1.1.1 The OXPHOS system and diseases

Mitochondria are maternally inherited. After fertilisation of the oocyte, sperm mtDNA is actively degraded [4]. Each mitochondrion may contain ten or more mtDNA molecules. Usually all copies of mtDNA are identical (homoplasmy). Occasionally, however, mtDNA mutations occur and there arise more populations of mtDNA (heteroplasmy). Heteroplasmic mtDNA ought to be relatively common, considering that human mtDNA mutates 10-20 times faster than nDNA as a result of inadequate proof-reading by mtDNA polymerase and limited mtDNA repair capability [5-8]. Moreover mtDNA lacks protective proteins like histones and is physically associated with the inner mt membrane where highly mutagenic oxygen radicals are generated [9]. Mutations may arise frequently and when mutated gene copies accumulate over a certain threshold, the deleterious effect is no longer suppressed by the coexisting wild-type mtDNA and will be expressed phenotypically as a disease. The threshold for biochemical expression may be around 60 % mutant for mtDNA deletions [10] and 85-95 % for tRNA mutations [11, 12]. The degree of organ dysfunction will also depend on a tissue's energy requirement. Brain and muscle are highly dependent on OXPHOS and neurological illness and myopathy are common features of mtDNA mutations. Mt diseases can have a wide variety of inheritance patterns, maternal, Mendelian, and a combination of both. Adding to this complexity is the fact that the same mtDNA mutation can produce quite different phenotypes and different mutations can produce similar phenotypes.

A significant percentage of respiratory chain disorders is caused by mutations of the mtDNA. Dysfunction of OXPHOS has also been associated with mutations in nuclear-encoded OXPHOS subunits. A further group of diseases results from mutations in genes coding non OXPHOS mt proteins and in genes coding non mt proteins.

1.1.1.1 Diseases associated with mtDNA mutations.

Most pathogenic mtDNA mutations affect the heart, in association with a variety of other clinical manifestations that can include skeletal muscle, the central nervous system (including eye), the endocrine system, and the renal system [13]. They include point mutations, rearrangements (deletions and duplications) and depletion.

Mutations in tRNA and rRNA genes typically affect the translation of all 13 mtDNA-encoded polypeptides, resulting in generalised OXPHOS deficiencies. Mutations in the $tRNA^{Leu}$ gene

are associated with the MELAS syndrome (mitochondrial myopathy, encephalopathy, lactic acidosis and stroke-like episodes) [14], mutations in the $tRNA^{Lys}$ gene are associated with the MERRF syndrome (myoclonic epilepsy with ragged-red fibers) [15] and mutations in the 12S rRNA gene are associated with the AID syndrome (antibiotic-associated deafness) [16].

Most mutations in genes coding for complex I subunits are associated with LHON syndrome (Leber's hereditary optic neuropathy), a degeneration of the optic nerve leading to almost complete blindness [17-19].

Pathogenic mutations in the mt encoded subunit of complex III are associated with myopathies [20].

Mutations in the three subunits of complex IV are associated with unrelated disorders including myopathy, encephalomyopathy and anemia [21-28].

Pathogenic mutations of complex V have been associated with the NARP syndrome (neuropathy, ataxia, and retinitis pigmentosa) [29] or the Leigh syndrome, depending on the degree of heteroplasmy [30].

Large scale rearrangements of mtDNA can be either partial mtDNA deletions or more rarely partial duplications. They are found in some 40 % of adult patients with mt diseases [31]. Three phenotypes are associated with these mutations: Kearns-Sayre syndrome (KSS) [32], progressive external ophthalmoplegia (PEO) [33] and Pearson's syndrome [34]. The pathogenicity of mtDNA deletions is due to the loss of tRNA genes, whereas duplicated mtDNAs do not lack any tRNA genes and are probably not pathogenic [35]. Depletion of mtDNA, first described in 1991 [36], is an important cause of mt dysfunction in neonates and infants. Patients show a severe reduction of mtDNA, up to 98 % in the most severe forms.

1.1.1.2 Diseases associated with mutations of nuclear genes encoding OXPHOS proteins.

The observation of familial cases with Mendelian inheritance and severe isolated defects of the respiratory chain complexes not associated with mtDNA lesions suggests the presence of nuclear genes as a source of respiratory chain deficiencies.

Mutations in nuclear-encoded OXPHOS subunits are rare. So far mutations have been identified for complex I, associated with Leigh syndrome and complex II, associated with Leigh syndrome or with a neoplastic transformation called hereditary paraganglioma (PGL), characterised by benign carotid body tumors in the head and the neck [37].

1.1.1.3 Diseases associated with mutations of nuclear genes encoding mt non OXPHOS proteins.

The OXPHOS system is dependent on mt protein transport and assembly systems, and many nuclear-encoded factors are necessary to maintain mtDNA structure and function.

Defects of mt protein import have been described in two patients with Mohr-Tranebjaerg syndrome. They presented a truncated form of a chaperonin (DPPI) [38], homologous to the yeast protein Tim8p, a member of the inner mt membrane transport machinery located in the mt intermembrane space [39].

Mutations in genes coding for assembly factors have been described for *hSURF1*, *hCOX11*, *hSCO1* and *hSCO2*, four genes involved in the assembly and maintenance of complex IV (see below). Recently a mutation in *hBCS1L*, a gene coding for an assembly factor for complex III, was described in patients suffering from tubulopathy, encephalopathy and liver failure [40].

Defect in frataxin, a protein involved in intramitochondrial iron handling, is associated with Friedreich's ataxia (FRDA), characterised by progressive ataxia, neuropathy, skeletal abnormalities and cardiomyopathy [41]. The causative mutation is an abnormally expanded GAA triplet repeat in intron 1 of the gene [42]. This defect causes decreased frataxin expression [43], with increased iron deposition in the heart and deficiencies in complex I-III and aconitase, which contain iron-sulphur clusters [44].

Mutations in the gene coding for paraplegin, a mt protein with high degree of homology to AAA proteins (ATPases associated with diverse cellular activities) are associated with hereditary spastic paraplegia (HSP) [45]. Mitochondrial AAA proteins are ATP-dependent metalloproteases and have chaperone-like activities, for example, they can activate the assembly of respiratory chain complexes and can participate in protein quality control by binding unfolded peptides and ensuring specificity of proteolysis [46]. The mt dysfunction in HSP patients could result from impaired protein quality control, causing an accumulation of misfolded proteins within the mt matrix.

Defect in copper homeostasis in the Wilson's disease is associated with mutations in a copper transporter P-type ATPase, called WND [47]. The WND protein exists in two isoforms, a 160 kDa form which localises to the trans-Golgi network and a 140 kDa form which localises to mitochondria [48]. This isoform may play a role in the copper-dependent functions of mt enzymes.

1.1.1.4 Diseases associated with mutations of nuclear genes encoding non mitochondrial proteins.

Huntington's disease (HD) is caused by an expansion of a CAG repeat within the huntingtin gene on chromosome 4 [49]. Mutant forms of huntingtin protein accumulate in the nucleus of affected neurons [50]. Defects of complex II, III and aconitase have been described in HD brain [51], but the mechanisms through which huntingtin with expanded polyglutamine repeats cause mt dysfunction is unknown.

Mutations of the human cytosolic Cu/Zn superoxide dismutase 1 (hSod1p) are associated with Amyotrophic Lateral Sclerosis (ALS) [52], a devastating paralytic disorder caused by motor neurons degeneration. Because hSod1p reduces the potentially harmful superoxide radicals, ALS could be a consequence of disturbed free radical homeostasis and resulting oxidative stress. Mouse models show, besides the morphological alteration in motor neurons, massive mt degeneration [53] and abnormal respiration chain functions [54]. Mutated hSod1p forms show no loss of activity and a toxic gain-of-function has been postulated [55].

OXPHOS defects have also been reported in patients suffering from progressive supranuclear palsy (PSP), a disorder characterised by rigidity, slowed movement, tremor and abnormal eyes movement. The *tau* locus on chromosome 21 has been identified as a potential risk factor to develop this disease [56]. Tau is a phosphoprotein that belongs to a family of microtubule-associated proteins. In the adult human brain there are six tau isoforms, generated by alternative splicing of exons 2, 3 and 10, which contain either three or four microtubule binding domains [57]. In the PSP brain, there is a selective enrichment of tau isoforms containing four microtubule binding domains (4-repeat tau), particularly the 64 and 69 kDa isoforms that result from the splicing-in of exon 10 [58]. These two isoforms are hyperphosphorylated [59]. One hypothesis to explain the hyperphosphorylation of tau is that free radical-induced oxidative stress makes tau resistent to dephosphorylation [60].

1.2 The cytochrome *c* oxidase

Complex IV or cytochrome *c* oxidase (COX) is a member of a superfamily of heme-copper containing terminal oxidases. These oxidases contain either a heme O or a heme A moiety at their active site. Both hemes differ from proto-heme having a farnesyl group instead of a vinyl group on position 2 of the porphyrin ring. In addition, in heme A, the methyl group on position 8 of the porphyrin ring is replaced by a formyl group [61]. The nature of the electron input site reflects a division in the cytochrome oxidase in two groups. In cytochrome *c* oxidase, reducing equivalents are delivered from the soluble protein ferrocytochrome *c*. The quinol oxidases, in prokaryotes, receive electrons from a lipid-soluble quinol.

Recently, crystal structures at a resolution of 2.8 Å have been reported for COX from bovine heart [62]. The crystal structure shows that the mammalian oxidase contains 13 polypeptides in equimolar amount and is present as a dimer in the membrane with limited contact between the monomers. Each monomer contains two iron centres, heme *a* and heme a_3 (also referred to as cytochromes *a* and a_3), two copper centres, Cu_A and Cu_B, a magnesium centre and a zinc centre. From the 13 protein components, Cox1p Cox2p and Cox3p are encoded from mtDNA and represent the catalytic core of the enzyme, while the remaining ten subunits (Cox4, 5a, 5b, 6a, 6b, 6c, 7a, 7b, 7c and 8) are nuclear-encoded. The subunits 6a, 7a and 8 have heart (H)- and liver (L)-specific isoforms so that heart and skeletal muscle express the heart form whereas the L isoform is ubiquitously expressed [63-65]. Fetal heart and skeletal muscle mainly express the L isoform, switching to the heart-type after birth [66]. Cox1p, Cox2p and Cox3p are considered to be crucial for the catalytic function of the enzyme because they contain the redox active prosthetic groups and are homologous to COX subunits found in proteobacteria such as *Paracoccus denitrificans* and *Rhodobacter sphaeroides* [61]. Cox1p has 12 transmembrane helices and contains, in the membrane space, heme *a* and the oxygen-binding site, composed of heme a_3 and Cu_B. Cox2p has two transmembrane helices and contains, in the extra-membranous domain exposed to the intermembrane space, the binuclear Cu_A centre. The metal binding motif CxxxC (single letter amino acid code where x is any amino acid) provides 3 of the 6 ligands for the formation of the Cu_A site. Cox2p receives the electrons from cyt *c* and transfers them to heme *a* and finally to heme a_3-Cu_B centre. Cox3p contains seven transmembrane helices and has no metal centres, but it is essential for preserving the structure integrity of the active site during turnover [67]. On the interface between Cox1p and Cox2p, the Mg^{2+} binding site is located, whose function is still unknown. The nuclear encoded

subunits are important for assembly or stability of the complex [68] or for optimal activity of the oxidase [69-72].

1.2.1 Assembly of COX

Many bacterial oxidases have little more than the three core subunits to constitute a fully functional complex. However, both mammalian and yeast systems have difficulty assembling a functional complex unless the additional nuclear subunits are present. The structure of COX from the yeast *Saccharomyces cerevisiae* closely resembles that of its mammalian counterpart [73]. Genetic studies in yeast have identified many nuclear genes that are involved in the correct assembly of the structural components. Many of these factors have human homologues. Some of these factors act in a general manner and also affect the biogenesis of other mt respiratory complexes. Among these are proteins involved in the mt protein import or sorting, like heath shock proteins [74], chaperones, like the AAA family of ATPases, involved in the clearing of unassembled and improperly folded polypeptides [75], proteins like prohibitins, that stabilise or protect unassembled protein subunits [76], and Mba1p [77] and Oxa1p [78] which are required for the insertion of proteins into the inner membrane from the matrix site. Some of the other nuclear genes encode proteins that are specific for the assembly of COX. These include factors involved in heme farnesylation (Cox10p) [79, 80], in the insertion of Cox1p and Cox2p (yShy1p/hSurf1p) [81-83], and in the copper recruitment (Cox17p, Sco1p, Sco2p and Cox11p) [84-87]. In addition to the above genes there are at least eight others that have been proposed to function as assembly facilitators. Proteins required in the assembly of COX are listed in Table 1. The assembly of the multi subunits oxidase apparently occurs in an ordered sequence, but most of the details remain to be resolved. Two dimensional gel electrophoresis performed on mt fractions from cultured human cells provides evidence for four steps (S1-S4) [88] (Fig. 2). The first subunit to assemble is Cox1p. It is inserted into the membrane from the matrix side probably with the aid of Oxa1p and forms a subcomplex with Cox4p. hSurf1p is possibly involved in the insertion of Cox1p. Metabolic labelling experiments have indicated that Cox1p assembles with Cox2p and Cox3p only after a lag period of 1,5 h [89]. It was postulated [90] that during this time Cox1p is folded into the inner membrane and that concurrently the heme a is buried inside the protein. Synthesis of heme A from protoheme requires Cox10p, a 7 transmembrane helix protein of the inner mt membrane, and could be take place before or after the insertion of heme A in Cox1p. Heme A promotes

the binding of Cox1p with Cox2p [91]. In the next step the Cu_B-heme a_3 centre is formed and simultaneously Cox2p associates with Cox1p to stabilise the active site. It was postulated that the insertion of Cu_A occurs during this phase [90]. The insertion of Cu_B could be generated at a later stage [87]. Sco1p, Sco2p and Cox17p are probably involved in the copper transport to the Cu_A site [84, 86, 92], but they might also facilitate copper transfer to the Cu_B site in concert with Cox11p [87]. A larger complex is then formed by association with Cox3p and most of the nuclear-encoded subunits lacking only Cox6ap and Cox7ap which are peripheral polypeptides and are incorporated late.

Yeast protein	**Function**	**Human homologues**	**Associated disease**	**Reference**
yPet100p	Incorporation of nuclear-encoded subunits	Unknown	Unknown	[93]
yShy1p	Insertion of Cox1p and Cox2p	hSurf1p	Leigh syndrome	[82, 83, 94-99]
ySco1p	Incorporation of copper	hSco1p hSco2p	Hepatic failure Encephalomyopathy	[84, 85, 92, 100-108]
ySco2p	Incorporation of copper	hSco1p hSco2p	Hepatic failure Encephalomyopathy	[84, 92, 95, 109-111]
yCox17p	Incorporation of copper	hCox17p	Unknown	[84, 86, 112-117]
yCox10p	Farnesylation of protoheme	hCox10p	Tubulopathy	[79, 80, 118-120]
yCox11p	Incorporation of Cu_B	hCox11p	Unknown	[87, 105]
yCox14p	Function in the late step of assembly	Unknown	Unknown	[121]
yCox15p	Hydroxylation of heme O	hCox15p	Unknown	[122]
yCox18p	Stabilises Cox2p and might assist in its binding to Cox1p	Unknown	Unknown	[123]
yCox20p	Processes the exported precursor of Cox2p	Unknown	Unknown	[124]
yPet117p	Unknown	Unknown	Unknown	[125]
yPet191p	Unknown	Unknown	Unknown	[125]

Table 1. Proteins required for the assembly of COX.
Yeast proteins and their human counterparts specifically involved in the assembly of COX are listed. Diseases associated with mutations in the assembly factors are indicated.

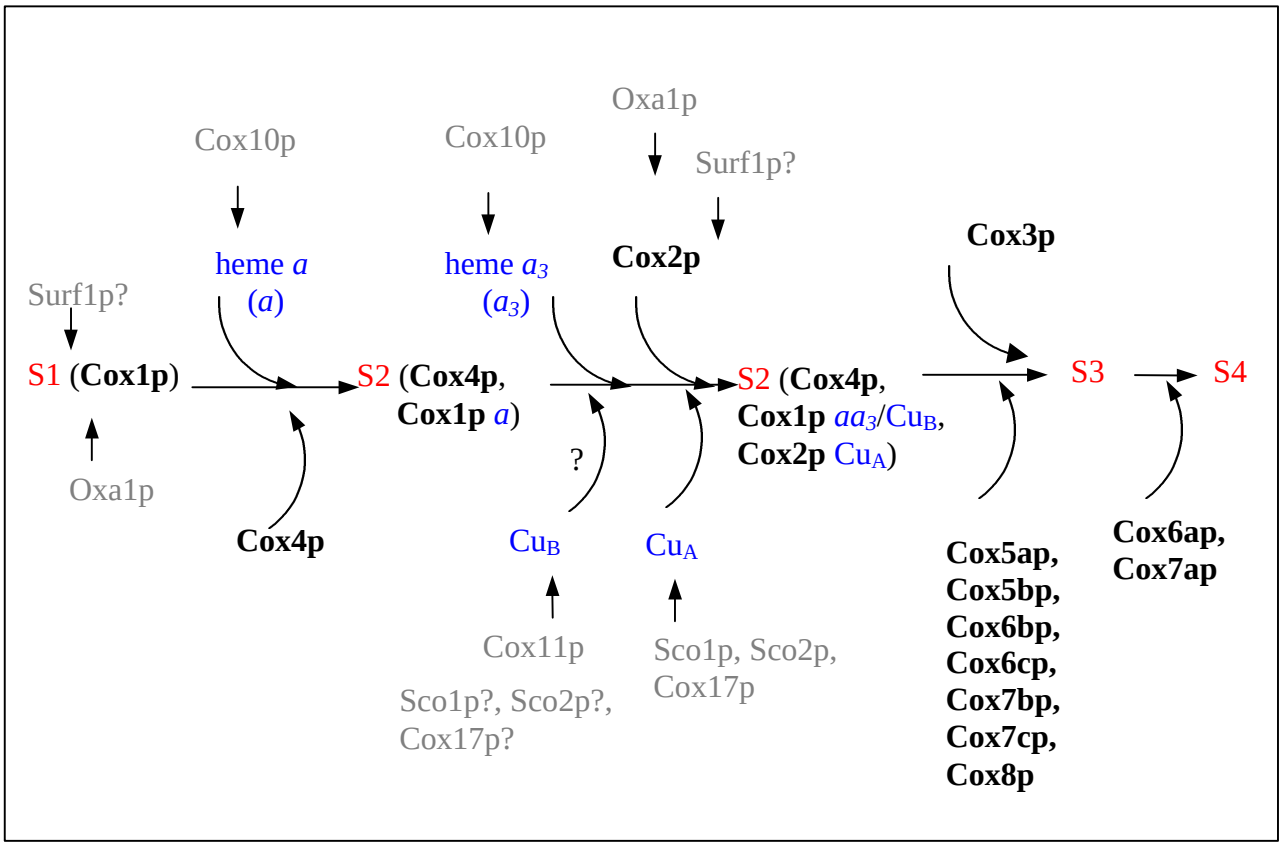

Fig. 2. Model of COX assembly.
Bold letters denote subunits of COX. Red letters indicate the steps of the assembly pathway (S1-S4). Prosthetic groups are indicated in blue and assembly factors are indicated in grey. See text for details.

1.2.2 The thioredoxin system in the COX assembly.

Thioredoxin is a small and ubiquitously expressed protein conserved from prokaryotes to higher eukaryotes (for review see [126]). Thioredoxin is characterised by a CxxC active site [127] and by a conserved fold consisting of four β-sheet and three flanking α-helices [128]. When thioredoxin is in a reduced state, the two active-site cysteines form a dithiol group that is able to catalyse the reduction of disulfides in a number of proteins. Oxidised thioredoxin can be reduced by NADPH through the catalytic action of the thioredoxin reductase. The other major factor generally responsible for maintaining proteins in the reduced state *in vivo* is glutathione and the glutaredoxin system. Thiol-disulfide reductases that belong to the thioredoxin superfamily can have either reducing properties or oxidising properties. In bacterial systems the electron transport of OXPHOS is localised to the cytoplasm membrane and protons are pumped in the periplasm. A broad variety of periplasmic thiol-disulfide oxidoreductases have been identified in recent years (for review see [129]). Like the

cytoplasmic thioredoxins and glutaredoxins, these periplasmic thiol-disulfide oxidoreductases contain the conserved CxxC motif in their active site. Most of them have a domain that displays the thioredoxin-like fold. In contrast to the cytoplasmic system, which consists exclusively of reducing proteins, the periplasmic oxidoreductases have either an oxidising, a reducing or an isomerisation activity. The periplasm of bacterial cells is an oxidising environment and contains an apparatus for catalysing the formation of disulfide bonds, involving in *Escherichia coli* two proteins, DsbA and DsbB [130]. Since the oxidising conditions of the periplasmic compartment may be deleterious for certain proteins, periplasmically oriented redox proteins exist which keep cysteines reduced during protein biogenesis. Unlike other cytochromes, *c*-type cytochromes have two covalent bonds formed between the two vinyl groups of heme and two cysteines of the protein. DipZ and CcsX are required in *Bordetella pertussis* for the periplasmic reduction of the cysteines of apocytochromes *c* before ligation [131]. In *Bradyrhizobium japonicum*, TlpA is essential for the biogenesis of a functional cytochrome aa_3 [132] which contains a binuclear Cu_A ligated by two cysteine thiols, one methionine and two histidines [133]. The two cysteines must be in the reduced state to act as ligands. TlpA could keep these cysteines in the reduced state during aa_3 biogenesis [134]. Thioredoxins have also been identified in yeast mitochondria [135] and mammalian mitochondria [136], and a role in protection against oxidative stress was proposed in both cases. So far no data are available on an involvement of the thioredoxin system in the COX assembly in eukaryotes.

1.2.3 Copper delivery to COX: the role of copper chaperones

The transport of copper is a controlled process. In excess, copper ions are highly toxic, because they catalyse the formation of hydroxyl radicals with subsequent damage of lipids, proteins and DNA [137]. Thus, proper correct trafficking is essential for cell vitality. *In vitro* most copper enzymes easily acquire copper without auxiliary proteins. *In vivo*, free copper is not available, being less than one atom of free copper per cell [138], and metallochaperones are needed to transport copper to the site of utilisation (see Fig. 3). In blood copper is bound to albumin and histidine. The predominant copper-containing protein in mammalian serum is ceruloplasmin [139], a ferroxidase critical for iron metabolism. A candidate for copper uptake in mammal cells is hCtr1p [140], which shows high similarity to the yeast high-affinity Cu-transport proteins yCtr1p and yCtr3p [141, 142]. A putative low affinity mammalian Cu

transporter, hCtr2p has also been identified [143]. Following entry, detoxification mechanisms found across species include the binding of copper to specific proteins, e.g. metallothioneins [144], and the transfer of copper into isolated cell compartments.

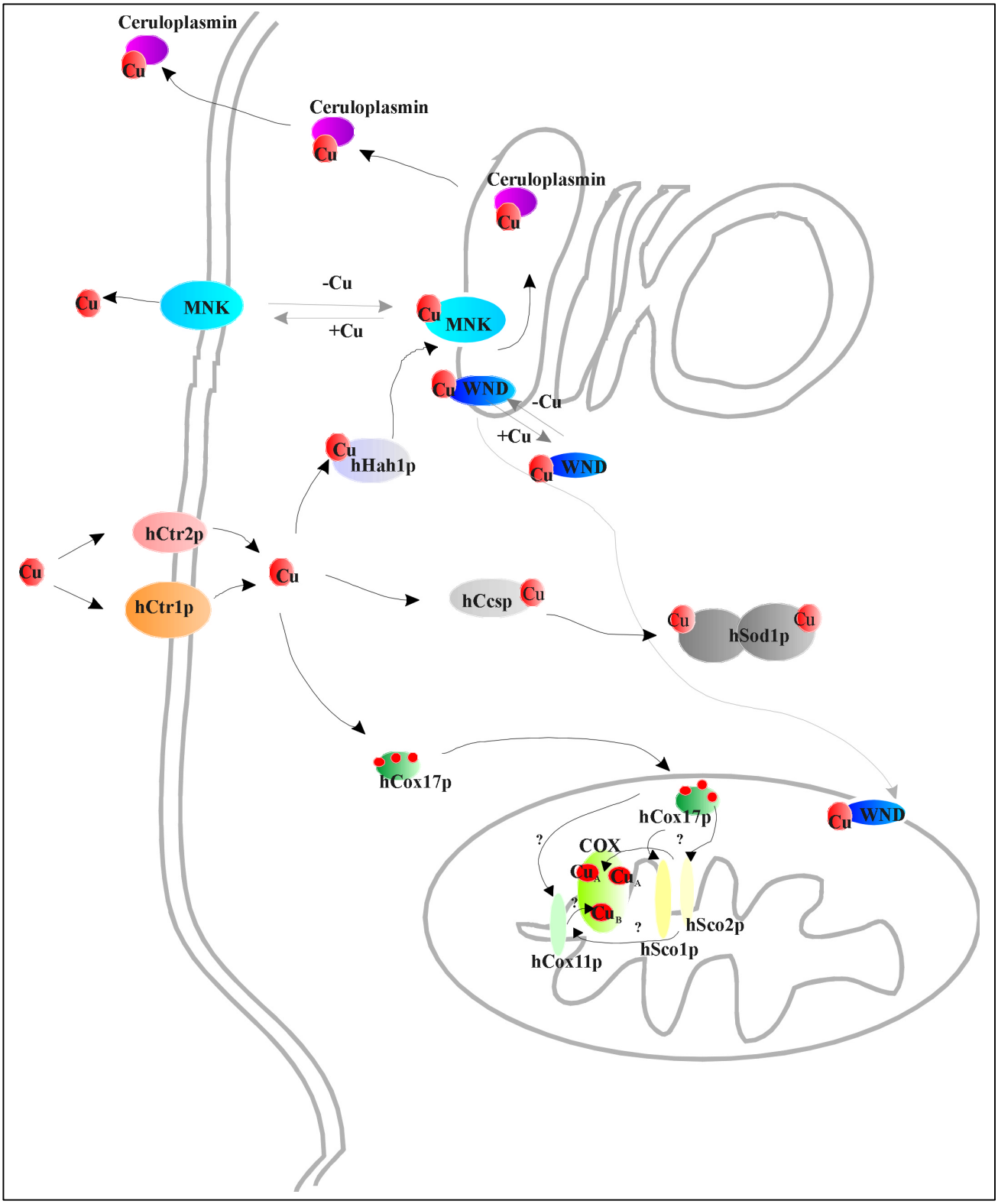

Fig. 3. Copper transport pathways in human cells.
Copper uptake is mediated by hCtr1p and hCtr2p. Cu chaperones (hCox17p, hCcsp, hHah1p) distribute Cu to specific cellular compartments for incorporation in copper requiring enzymes. See text for details.

The transport of copper to mitochondria involves hCox17p [112]. The role of Cox17p as metallochaperone was deduced from the ability of high levels of exogenous copper to complement a *ycox17* disruption mutant [86]. yCox17p is localised in the cytosol and in the intermembrane space [113], acting as a shuttle between the two compartments. yCox17p binds three copper ions per monomer in a polycopper cluster [115]. yCox17p forms oligomers and the oligomeric state is important for its function [115]. The human homologue, *hCOX17*, can complement the *ycox17* disruption mutant [112]. The transfer of copper from Cox17p to COX involves at least three proteins, Sco1p, Sco2p [84, 92] and Cox11p [87], but no data have been so far published about an interaction between these proteins and Cox17p. The pathways for assembly of Cu_A and Cu_B are probably distinct since cytochrome *c* oxidase containing Cu_A but lacking Cu_B can be assembled in a *cox11* null mutant in *Rhodobacter sphaeroides* [87]. yCox11p and its human homologue [105] show a conserved CFCF motif which is possibly involved in the Cu_B insertion.

Two further copper pathways, to the secretion system and to the Cu/Zn superoxide dismutase (Sod1p), have been described. Disruption of these copper pathways is involved in different human diseases.

hHah1p [145] transfers copper to two proteins located in the Golgi network, the Menkes and Wilson's disease proteins (WND and MNK) [146, 147] which transport copper to the secretory pathway for incorporation into copper containing enzymes like ceruloplasmin [139]. Elevated Cu levels stimulate the trafficking of MNK to the plasma membrane where it may be involved in copper efflux [148], and the traffic of WND to an unknown cytosolic vesicular compartment [149]. A cleaved form of WND was reported to localise to mitochondria where it is suggested to play a role in the mt copper homeostasis [48]. Both proteins are P-type ATPase [150], and mutations in the respective genes lead to genetic disorders of copper metabolism. WND is expressed in most tissues but predominantly in the liver and MNK is expressed in all tissues except the liver. In the Wilson's disease, toxic amounts of copper accumulate in liver and brain resulting in cirrhosis and neuronal degeneration. Menkes disease is a neurodegenerative disease caused by copper deficiency in a number of tissues. hHah1p interacts with its partners in a copper-dependent fashion [151, 152]. Yeast homologues are known for WND and MNK (Ccc2p) [153] and for hHah1p (Atx1p) [154]. Copper is bound by the conserved MxCxxC motif present one time in hHah1p [155] and six times in the target ATPases [156, 157].

Sod1p is a cytosolic homodimeric copper and zinc-binding enzyme which protects the cells against oxidative damage by catalysing the conversion of superoxide radicals to hydrogen

peroxide and oxygen [158]. Recent evidences suggest that Sod1p is incapable of acquiring Cu ions *in vivo* in the absence of its chaperone, Ccsp [138]. yCcsp [159] and hCcsp [160] are composed of a three-domain structure [161-163]. Domain I contains a conserved MxCccC domain, domain II has high sequence homology to Sod1p, domain III contains a CxC motif. Domain I and II bind copper and can interact via a cysteine-bridged dicopper cluster [164]. The high degree of homology of domain II to Sod1p was postulated to be important in the target recognition of Sod1p [165]. hCcsp can form homodimers [163] and the metal insertion into ySod1p by yCcsp is accomplished by the formation of a heterodimer between the two proteins [166]. This interaction is not copper dependent [165].

Copper delivery by chaperones appears to be a specific process. One chaperone cannot substitute for the absence of another chaperone. A transitory interaction between the chaperone and its target has been proposed and the docking between the two proteins presumably involves electrostatic interactions [167]. The mechanism of copper transfer between the chaperones and their target proteins are not clear but a ligand attack of the recipient protein on the Cu ion of the chaperone is plausible, implicating a competitive exchange process [154].

1.2.4 COX deficiency

Isolated COX deficiency is the most frequent cause of respiratory chain defects primarily affecting those organs with high energy demand, such as the brain, skeletal muscle, heart and kidney and resulting in a variety of clinical manifestations including Leigh syndrome [82], hepatic failure [168] and encephalomyopathy [169]. COX deficiency has been associated with mutations in the three mt-encoded subunits, Cox1p, Cox2p and Cox3p [21-28], with large scale deletions of the mtDNA [170] and with point mutations in mt tRNA genes [14] (MELAS and MERRF syndrome). No mutations have been reported in any of the nuclear genes encoding COX subunits, however, mutations in nuclear encoded proteins required for the assembly of the COX complex have been identified in human diseases. In patients suffering from Leigh syndrome mutations in the *hSURF1* gene have been detected [82, 96, 97], and *hCOX10* mutations have been found to be the cause of tubulopathy and leukodystrophy [80]. Mutations in *hSCO2* were described in infants who suffered from a fatal disorder with hypertrophic cardiomyopathy as the predominant symptom [95, 109, 110]. Recently a first report on mutations in the *hSCO1* gene was published [108]. The key symptoms of the infant patients were hepatic failure and ketoacidotic coma.

1.2.4.1 hSurf1p

hSurf1p is an integral inner membrane protein. [99]. To date, 30 different mutations have been reported in 40 unrelated patients [96]. The concentration of all COX-subunits except for Cox5ap and Cox5bp is strongly reduced [98, 99]. The transcription [171] and translation [172] of COX genes is normal, implicating a defective assembly or instability of the assembled complex. Northern blot analyses have shown that *hSURF1* mRNA is ubiquitously expressed but expression in the brain appears to be low compared with other highly aerobic tissues like heart, skeletal muscle and kidney [99]. As Leigh syndrome is primarily a central nervous system disorder, it is clear that the protein, despite its low expression in the brain, plays a crucial role in this tissue. Most of the identified mutations in *hSURF1* patients predict truncated proteins. The loss-of-function of this mutants is associated with the absence of hSurf1p due to either mRNA instability, rapid protein degradation or both [173]. Recently, missense mutations have been identified, which do not alter *hSURF1* mRNA expression but are able to prevent its function [97]. Blue native two-dimensional electrophoresis indicates that the absence of hSurf1p causes the accumulation of early intermediates of COX assembly (Cox1p and Cox1p associated with Cox4p) [173], suggesting that it is involved in the incorporation of Cox2p. This crucial step is believed to produce the rapid „cascade-like“ assembly of the other COX subunits. Detection of residual amounts of fully assembled complexes suggests a certain degree of redundancy of hSurf1p in COX assembly [173]. Defect of COX activity in *hSURF1* patients is widespread in all tissues of the body, including skin fibroblasts and it is quite severe, although a residual activity ranging from 5 to 20 % [97] can usually be found.

1.2.4.2 hCox10p

The y*COX10* gene encodes an heme A:farnesyltransferase [120]. The human homologue encodes a protein predicted to contain seven to nine transmembrane domains localised in the mt inner membrane [118]. The protein structure is conserved from bacteria to human, with the amino acid sequence of transmembrane segments II to V being highly conserved [174]. Mutations in the *hCOX10* gene have a major effect on the level of Cox2p, the steady-state levels of the other subunits, including Cox1p, are relatively normal [80]. This is remarkable because Cox1p in these patients cannot associate with heme aa_3 prosthetic groups. This suggests that the heme groups are not necessary to stabilise Cox1p and that assembled enzyme complex may be present, protecting the subunits from proteolytic degradation by mt proteases

[175]. *hCOX10* is expressed in multiple tissues with highest expression observed in heart, skeletal muscle, and testis [119].

1.2.4.3 The Sco proteins

Yeast was the first organism in which a member of the *SCO* gene family was identified and characterised [106]. Mutants lacking the y*SCO1* gene are respiratory deficient due to a COX deficiency. This phenotype results from an incorrect COX-subunits assembly which leads to proteolytic degradation of unassembled COX subunits, especially of Cox1p and Cox2p [102, 106]. ySco1p, which is anchored in the inner mt membrane [100], is thought to be required for transfer of copper ions to Cox1p and/or Cox2p because over-expression of ySco1p can suppress the respiratory deficiency of strains lacking yCox17p [84]. The presence in ySco1p of a CxxxC motif, which is similar to the copper binding site of Cox2p, suggests that ySco1p might be directly involved in copper binding. In line with this suggestion is the finding that the mutational alteration of either one or both of the two cysteine residues of the motif affects the function of the protein [85]. Alternatively, it was proposed that ySco1p could mediate the insertion of copper without direct copper-binding, e.g. as a thioredoxin, which is required for the formation of a binding-competent 3D-structure of the COX-subunits [176]. Chinenov (2000) [176] reported the similarity of proteins of the Sco family to thiol-disulfide oxidoreductases. The overall similarity is low, but cysteine residues and hydrophobic amino acids in the active centre are conserved and the predicted secondary structure of ySco1p display the thioredoxin-like fold. Moreover, a conserved histidine was proposed to activate a sulfhydryl group of the active centre. Indeed, yeast Sco1p carrying a mutation of this histidine was shown to be inactive [104].

Sequence analysis of the yeast genome revealed y*SCO2*, a gene with a high degree of identity to y*SCO1* [177]. The function of ySco2p is unclear: like in the case of ySco1p, over-expression of this mt protein can suppress the lack of the mt copper-shuttle protein yCox17p in the presence of enhanced copper concentrations, suggesting that it might be involved in mt copper metabolism [84]. However, neither there is an obvious mutant phenotype after deletion of the y*SCO2* gene nor the over-expression of y*SCO2* is capable to suppress the respiratory deficiency of y*sco1* null mutants [84]. A partially overlapping function of ySco1p and ySco2p is suggested by the demonstration that chimeras of both proteins can substitue for ySco1p [85].

Sco proteins are conserved among prokaryotes and eukaryotes. All homologues present the CxxxC motif. The best characterised homologues are SenC from *Rhodobacter capsulatus*

[178], YpmQ from *Bacillus subtilis* [179], and PrrC from *Rhodobacter sphaeroides* [180]. *B. subtilis* has two cytochrome oxidases, a cytochrome *c* oxidase, which contains cytochrome *a*, a_3, Cu_A and Cu_B, and a menaquinol oxidase which lacks the Cu_A centre [181]. Deletion of YpmQ disrupts the expression of the cytochrome *c* oxidase but not of menaquinol oxidase, suggesting that YpmQ is involved specifically in the assembly of Cu_A. SenC is required for an optimal COX activity in *Rhodobacter capsulatus,* a photosynthetic bacterium [178]. The cytochrome *c* oxidase of *Rhodobacter capsulatus* has no a Cu_A centre [182] and it was shown that SenC has an additional role in regulating photosynthesis gene expression [178]. A similar role was proposed for the homologous PrrC in *Rhodobacter sphaeroides* [180].

In the human genome two genes with a high degree of identity to *ySCO1* have been identified, *hSCO1* located on chromosome 17p12-13 and *hSCO*2 located on chromosome 22q13.

The essential role of hSco proteins for mt function is evident by the recent finding of mutations associated with fatal infantile COX deficiency. An overview of the so far known mutations is shown in Fig. 4.

Fig. 4. Alignment of hSco1p and hSco2p sequences.
Identical residues are in blue. The putative copper binding site is boxed, the known point mutations and stop mutations (X) are in red.

Mutations in *hSCO2* are associated with muscular hypotonia, hypertrophic cardiomyopathy and encephalopathy. Each patient is heterozygous for a single mutation. Mutations in *hSCO2* have now been described in a total of 9 unrelated patients, each carrying a particular ("common") mutation at position 140 (E140K) with a stop or a missense mutation on the other allele in 6 cases [95, 109] and 3 being homozygous for the E140K mutation [110]. A R20P mutation was identified in patients and in healthy controls suggesting that it is a common polymorphism. The E140K mutation, found in all patients, is near the predicted CxxxC copper binding motif and changes a highly conserved negatively charged glutamate to a positively charged lysine. It was postulated that this mutation could interfere with the copper binding of the protein [95]. The S225F mutation is located next to the highly conserved His 224 and converts an uncharged polar to an hydrophobic residue. His 224 was discussed as potential ligand for copper [179], or as activator of the catalytic function in the case of the thioredoxin model [176]. The R171W mutation converts a positive charged arginine to a polar tryptophan. The known stop mutations occur at position 53 and 90, respectively, and truncate the protein upstream the CxxxC motif. A proof for the causal role of *hSCO2* mutations in COX deficiency has not been obtained in human cells so far, however the transfer of a normal chromosome 22 into COX-deficient fibroblasts of a patient carrying the E140K and the R171W mutations resulted in a rescue of COX activity [109]. Northern blot analysis shows *hSCO2* transcripts in all human tissues, with stronger signals present in heart, skeletal muscle, brain, liver and kidney [95]. Biochemical measurements in biopsy samples show that heart and skeletal muscle have a strong reduction in COX activity (0-18 % rest activity) whereas liver and fibroblasts have mild COX deficiency (16-50 %) [95, 109]. Immunohistochemistry of skeletal muscle shows severe reduction of Cox1p and Cox2p, and a small reduction of Cox4 and Cox5a [95]. Western blot analysis of fibroblasts shows a very small reduction in the steady-state levels of either mtDNA- or nuclearly-encoded subunits [109]. Tissue-specific reduction of COX activity has also been described in a distinct form of Leigh syndrome in the French Canadian population. These patients show very low COX activity in liver and brain and relatively high activity in muscle and fibroblasts [183]. In this case the gene defect is still unknown. A genotype/phenotype correlation was observed: the progress of the disease was more severe in patients carrying an additional stop mutation than in those with an additional point mutation and again lesser in homozygous patients (E140K/E140K). Jaksch *et al.* discuss that this observation could hint at the formation of dimers or higher order oligomers [110]. Most probably, two stop mutations in *hSCO2* would cause early prenatal deleterious effects. Patients

with the E140K homozygous mutation show a less progressive clinical course, with an initial typical Leigh syndrome, a progressive decline of the COX activity (30 % in the final state) and the fatal hypertrophic cardiomyopathy occurring late. In these patients a predominant involvement of the peripheral nervous system was observed and it was hypothesised that the progressive cardiomyopathy in *hSCO2* patients is not necessarily an early symptom of this disorder, but it is indicative of a specific aerobic energy supply threshold for cardiac function [110]. Again, fibroblasts show a relatively high residual COX activity. Interestingly, copper uptake of cultured fibroblasts from a homozygous patient was significantly increased, indicating an involvement of hSco2p in the copper metabolism. Engineered in the y*SCO1* gene of haploid yeast, the common mutation did not result in a measurable phenotype while the S225F mutation caused a loss of respiratory competence resulting from a partial but incorrect assembly of COX [92]. The assembled COX in this mutant specifically lacks Cox2p while Δ*ysco*1 mutant lacks Cox1p, too. The yeast strain carrying the S240F mutation in *ySCO1* (corresponding to the S225F mutation in the human gene) is the first example of a yeast COX assembly mutant that can produce a partially assembled COX complex without undergoing the proteolytic pathway [184]. The specific lack of Cox2p strongly suggests the involvement of Sco proteins in the addition of copper to the Cu_A-site after Cox2p has been incorporated in the assembling enzyme and a stabilising influence of Sco proteins on the assembling enzyme.

Recently a first report on mutations in the *hSCO1* gene was published [108]. The key symptoms of the two infant patients were hepatic failure and ketoacidotic coma. Sequence analysis revealed compound heterozygosity for the *hSCO1* gene. One of the *hSCO1* alleles harboured a -2 bp frame shift mutation resulting in a premature stop codon. The mutated mRNA was highly unstable. The other allele showed a missense mutation, resulting in a substitution of a proline at position 174, immediately adjacent to the CxxxC motif, by a leucine (P174L). Prolines are known to bend proteins and it was proposed that this substitution can modify the tertiary structure of the copper binding motif. This finding suggests that the P174L mutation interferes with the function of the *hSCO1* gene product, however, direct experimental proof for the pathogenicity of this mutation is lacking. COX deficiency was found in liver (10 % residual activity), in muscle (0,5 % residual activity), in lymphocytes and skeletal muscle. COX deficiency was observed, too, in chorionic villi and amniotic cell fluid in two male fetuses of the same family [108]. Northern blot analysis shows *hSCO1* transcripts in all human tissues, with the stronger signals present in heart, skeletal muscle, brain, liver and kidney, like

hSCO2. The steady-state level of *hSCO1* transcripts in these tissues was higher than that of *hSCO2* transcripts [95].

Despite the similar expression patterns and the predicted similar function, the consequences of *hSCO1* mutations are markedly different from those caused by *hSCO2* mutations. So far no data are available to explain the clinical discrepancies .

2 MATERIALS AND METHODS

2.1 Materials

2.1.1 Instruments

LI-COR DNA sequencer (model 4000/4200;)	MWG-BIOTECH
SenSys Digital CCD camera	INVITRO SYSTEM
Atom emission spectroscope: PGS2	ZEISS, Jena
Atom absorption spectroscope: SpectrAA 10 GTA-96	VARIAN, Darmstadt
FPLC system	AMERSHAM PHARMACIA BIOTECH
French Press	SLM-AMINCO
Swing-out centrifuge	HETTICH
CO2 incubator	WTB BINDER
Dounce homogeniser	BRAUN

2.1.2 Materials

5´ IRD800-labelled primers	MWG-BIOTECH
Acrylamide/Bisacrylamide	ROTH
Coomassie® Brilliant blue G250	MERCK
Copper Standards	FLUKA
Cytochrome *c*	SIGMA
Dithiothreitol	SIGMA
DMEM 4500 mg/l D-glucose, with non essential amino acids, without L-glutamine and sodium pyruvate	GIBCO-BRL
dNTP's	GIBCO-BRL
ECL^{plus}-System^{TM}	AMERSHAM PHARMACIA BIOTECH
FCS	GIBCO-BRL
Gel Blotting Paper	SCHLEICHER & SCHUELL
Geneticin	GIBCO-BRL
Glutamine	GIBCO-BRL
GSH-Sepharose 4B	AMERSHAM PHARMACIA BIOTECH
Human thioredoxin	IMCO, STOCKHOLM
Human thioredoxinreductase	IMCO, STOCKHOLM
Immobilon^{TM}-P PVDF-Membrane	MILLIPORE
Insulin	SIGMA
IPTG	SIGMA
MitoTracker® Red CMXRos	MOLECULAR PROBES
NADPH	SIGMA
NP-40	SIGMA

PBS without calcium and magnesium	GIBCO-BRL
Placenta cDNA bank	CLONTECH
PMSF	SIGMA
Precision Protein Standards™	BIO-RAD
Primers	MWG-BIOTECH
Protein G-Agarose	SANTA CRUZ BIOTECHNOLOGY
Proteinase inhibitors	BOEHRINGER MANNHEIM
PVDF (Immobilon™, 0,45 µm)	MILLIPORE
Pwo-Polymerase	BOEHRINGER MANNHEIM
Restriction enzymes	GIBCO-BRL
Spectral plates	B + G BANSE UND GROHMAN
T4-DNA-Ligase	PROMEGA
TEMED	GIBCO-BRL
Tfx™-20 liposome reagent	PROMEGA
Thioredoxin	IMCO
Thrombin	SIGMA
Tissue culture flasks	SARSTEDT
Trypsin (0,05 % Trypsin, 0,02 % EDTA)	GIBCO-BRL
Tween 20	MERCK
X-ray films	AMERSHAM PHARMACIA BIOTECH

2.1.3 Kits

Jetquick PCR Purification Spin Kit	GENOMED
Jetquick Gel Extraction Spin Kit	GENOMED
Jetquick Plasmid Miniprep Spin Kit	GENOMED
DC-Protein Assay	BIO-RAD
Thermo-Sequenase fluorescent labeled primer cycle sequencing kit with 7-deaza-dGTP	AMERSHAM PHARMACIA BIOTECH

2.1.4 Antibodies

	Dilution in 1x TBS-T with 5 % (w/v) skimmed milk powder
Mouse-Anti-yCox1p (MOLECULAR PROBES)	1:400
Mouse-Anti-yCox2p (MOLECULAR PROBES)	1:250
Mouse-Anti-hCox2p (MOLECULAR PROBES)	1:250
Mouse-Anti-Porin (MOLECULAR PROBES)	1:1000
Rabbit-Anti-ySco1p (Buchwald *et al*., 1991)	1:3000
Mouse-Anti-EGFP (ROCHE)	1:1000
Rabbit-Anti-EGFP (SANTA CRUZ)	1:500
Sheep-Anti-mouse IgG-HRP (AMERSHAM PHARMACIA BIOTECH)	1:5000
Donkey-Anti-rabbit IgG-HRP (AMERSHAM PHARMACIA BIOTECH)	1:5000

2.1.5 Strains

2.1.5.1 *Escherichia coli* (*E. coli*)

Strain	Genotype	Reference
DH5a	Φ80d*lacZ*ΔM15, *recA*1, *endA*1, *gyrA*96, *thi*-1, *hsdR*17 (r_K^-, m_K^+), *supE*44, *relA*1, *deoR*, Δ(*lacZYA-argF*)U169	[185]
BL21	F-[*dcm*], *ompT*, [*lon*], *hsdS*(rB^-mB^-) *gal*	[186]

2.1.5.2 *Saccharomyces cerevisiae* (*S. cerevisiae*)

Strain	Genotype	Reference
GR20	*MATa, ura3-251, ura3-379, ura3-228, leu2-3, leu2-112, his3-11, his3-15, SCO1::URA3, [rho$^+$]*	[106]

2.1.5.3 Human cells

Strain	Reference
HeLa	[187]
HeLa 17A3	This work

2.1.6 Media

2.1.6.1 *E. coli*-media

LB	1,0 % (w/v) Tryptone 0,5 % (w/v) Yeast extract 0,5 % (w/v) NaCl 2,0 % (w/v) Agar (for LB-Plates)
Marker selection	100 µg/ml Ampicillin 30 µg/ml Kanamycin

2.1.6.2 *S. cerevisiae*-media

YPD	1,0 % (w/v) Yeast extract 2,0 % (w/v) Peptone 2,0 % (w/v) Glucose 2,0 % (w/v) Agar (for YP-Plates)
YPGal	1,0 % (w/v) Yeast extract 2,0 % (w/v) Peptone

	2,0 % (w/v) Galactose 2,0 % (w/v) Agar (forYP-Plates)
YPGly	1,0 % (w/v) Yeast extract 2,0 % (w/v) Peptone 3,0 % (v/v) Glycerol 2,0 % (w/v) Agar (for YP-Plates)
WO	1,7 g/l Yeast nitrogen base 5,0 g/l Ammonium sulphate 2,0 % (w/v) Agar (for MM-Plates) 2,0 % (w/v) Glucose for selection with YEp351 in GR20 add 3,0 g/l L-Histidine
WO-Gal	1,7 g/l Yeast nitrogen base 5,0 g/l Ammonium sulphate 2,0 % (w/v) Agar (for MM-Plates) 2,0 % (w/v) Galactose for selection with YEp351 in GR20 add 3,0 g/l L-Histidine

2.1.6.3 Human cells media

Complete medium	DMEM 10 % (v/v) FCS 2 mM Glutamine
Incomplete medium	DMEM 2 mM Glutamine
Freezing solution (10 ml)	DMEM 20 % DMSO 20 % FCS

2.1.6.4 Buffers

TBE	90 mM Tris 90 mM Boric acid 2,5 mM EDTA
TBS	137 mM NaCl 20 mM Tris-HCl (pH 7,4)
TBS-T	1 x TBS 0,1 % (v/v) Tween 20
PBS	140 mM NaCl 2,7 mM KCl

	10,1 mM Na_2HPO_4 1,8 mM KH_2PO_4
PBS-DTT	140 mM NaCl 2,7 mM KCl 10,1 mM Na_2HPO_4 1,8 mM KH_2PO_4 1 mM DTT (freshly added)
MTE	1,8 mM KH_2PO_4, pH 7,3 0,65 M Mannitol 20 mM Tris-HCl, pH 7,1 1 mM EDTA 1 mM PMSF (freshly added)
Homogenisation buffer	20 mM Hepes-KOH, pH 7.5 250 mM Sucrose 1 mM EDTA 10 mM $MgCl_2$ 0,1 mM PMSF 10 mM KCl 1 mM DTT (freshly added)
WM	250 mM Sucrose 10 mM Tris-HCl, pH 7,8 2 mM EDTA
Lysis buffer	150 mM NaCl 50 mM Tris, pH 8 1 % (v/v) NP-40 1 mM DTT (freshly added) add 1X Proteinase inhibitors before use
Proteinase inhibitors stock solution (1000X) in DMSO	5 mg/ml Chymostatin 5 mg/ml Antipain 5 mg/ml Leupeptin 5 mg/ml Pepstatin 5 mg/ml Aprotinin

2.1.6.5 Solutions for SDS-PAGE

Running gel (12 %)	375 mM Tris-HCl, pH 8,8 12 % (w/v) Acrylamide 0,32 % (w/v) Bisacrylamide 0,1 % (w/v) SDS 0,1 % (w/v) Ammonium persulfate 0,1 % (v/v) TEMED

Stacking gel	125 mM Tris-HCl, pH 6,8 4 % (w/v) Acrylamide 0,1 % (w/v) Bisacrylamide 0,1 % (w/v) SDS 0,1 % (w/v) Ammonium persulfate 0,1 % (v/v) TEMED
Running buffer	25 mM Tris 192 mM Glycine 0,1 % (w/v) SDS
6 x loading buffer	300 mM Tris-HCl, pH 6,8 30 % (w/v) Glycerol 10 % (w/v) SDS 0,1 % (w/v) Bromphenol blue 600 mM DTT or 5 % ß-mercaptoethanol (freshly added)
Coomassie blue staining	42 % (v/v) Methanol 17 % (v/v) Acetic acid 0,1 % (w/v) Coomassie brilliant blue G250
Destaining solution	30 % (v/v) Methanol 7 % (v/v) Acetic acid

2.1.6.6 Solutions for Western blot

Transfer buffer	192 mM Glycine 25 mM Tris 5,0 % (v/v) Methanol 0,1 % (w/v) SDS
Ponceau S staining	0,5 % (w/v) Ponceau S 1 % (v/v) Acetic acid
Blocking solution	TBS-T 5 % (w/v) skimmed milk powder

2.1.6.7 Solutions for the Bradford assay

Bradford solution	0,01 % (w/v) Coomassie brilliant blue G250 5 % (v/v) Ethanol 10 % (v/v) H_3PO_4

2.1.7 Vectors

Vector	Genetic marker	Reference
YEp351	Amp^r, *LEU2*, 2 μ, *lacZ'*	[188]
p415 ADH	Amp^r, *LEU2*, *CEN-ARS*, *ADH*-promoter	[189]
pGEX-4T-3	Amp^r, *Taq*-promoter/*GST*-ORF/ MCS, *lacI^q*-ORF	AMERSHAM PHARMACIA BIOTECH
pEGFP-N1	Kan^r/Neo^r, *CMV*-promoter, MCS, *EGFP*-ORF,	CLONTECH

2.1.8 Primers

primer	**Sequence (5' ® 3')**	**enzyme site**
1	TATA*GGATCC*AT**ATGCTGCTGCTGACTCGGAGCCC**	*Bam*HI
2	TATA*GGATCCGTCGAC***TCAAGACAGGACACTGCGG**	*Bam*HI, *Sal*I
3	TATATA*GGATCC***ATGGCGATGCTGGTCCTAGTACCC**	*Bam*HI,
4	TATATATA*GTCGAC***CTAGCTCTTTTTTCTGTATGGCCT**	*Sal*I
5	GTCCTC*GAGCTC***CCAATTGAAACTAAATTG**	*Sac*I
6	AGGGAGAAA/**GAGAGGCTG**CAGCAGCAAAAG	
7	CAGCCTCTC/**TTTCTCCCT**GTTGAAGAAATA	
8	CTGGATAAG/**CTGGTGCAG**GTGGTGCGGCAG	
9	CTGCACCAG/**CTTATCCAG**TTCATCAGGACA	
10	CAGCCATTA/**TTCATCACT**GTGGACCCCGAGCGG	
11	AGTGATGAA/**TAATGGCTG**CAGAGTAATACCATA	
12	CCAGCAAGA/**GACGACGTT**GAAGCCATGGCCCGC	
13	AACGTCGTC/**TCTTGCTGG**ATCACAAGTTATAAA	
14	AGAGTATAC/**TACAATGCC**GGCCCCAAGGATGAG	
15	GGCATTGTA/**GTATACTCT**GTACTTCTTGCATGC	
16	CGTAGAAAA/**GTACACGCG**GTAACTGTGACTAGC	
17	CGCGTGTAC/**TTTTCTACG**CCTCCAAACGTCAAA	
18	TATATAT*GTCGAC***CTTCCCACGTTCACATAG**	*Sal*I
19	AGGGAGAAG/**AAGGAAAAG**GCAGAGAAGTTAGAGAAG	
20	CTTTTCCTT/**CTTCTCCCT**GTTGAAGAAATAAGAAAG	
21	CTGGACAAG/**ATGATCCAA**GTCGTGGATGAAATAGATAGC	
22	TTGGATCAT/**CTTGTCCAG**TTCATCAGGACAGAT	
23	AGTATA*AAGCTT***ATGCTGCTGCTGACTCGGAGCCCC**	*Hind*III
24	AGTATA*CCGCGG***AGACAGGACACTGCGGAAAGCCGC**	*Sac*II
25	TATATA*AAGCTT***ATGGCGATGCTGGTCCTAGTACCC**	*Hind*III
26	TATATATA*CCGCGG***GCTCTTTTTTCTGTATGGCCTCAT**	*Sac*II
27	AAGAACCTT/**TTGGGTCAG**TGGTTATTGATTTATTTTGGC	
28	CTGACCCAA/**AAGGTTCTT**CTCCGTAAACTCATT	
29	CTTGGGGGA/**CCGTTTTCC**CTCACAACTCATAC	
30	GGAAAACGG/**TCCCCCAAG**TGAAGGTTTACCGTA	
31	**CCTGATGTCTGTCTAGAAGAACTAG**	
32	**CTAGTTCTTCTAGACAGACATCAGG**	

33	**TGCCCAGACAAGCTGGAGAAGCTGGTG**	
34	**CTCCAGCTTGTCTG GGCAGATGTCAGGG**	
35	**GTGGACCACTTCATTGCCATCTACCTG**	
36	**GGCAATGAAGTGGT CCACGATGTAGTC**	
37	**GATGTCAGG/GGCGTGAGTGAAGCC**	
38	**ACTCACGCC/CCTGACATCGCCCCAGACGAGCTGG**	
39	**GACATCAGGGGCATGAGTGAAGCC**	
40	**ACTCATGCCCCTGATGTCGCCCCAGAAGAACTA**	
41	TATATA*AAGCTT***ATGCCGGGTCTGGTTGACTC**	*Hind*III
42	TATATA*CCGCGG***TATTTTAAATCCTAGGGCTCTCATGC**	*Sac*II
43	TATATA*GGATCC***AAGCACGTCAAGAAAGAAAAGGCA**	*Bam*HI
44	TATATA*GGATCC*AGGGCTGAGAAGGAGAGGCTG	*Bam*HI
45	TATATATA*GCGGCCGC*TTACTACTTCAGGTAAAAGTCGGT*C*	*Not*I,
	*CGCGG***AGACAGGACACTGCGGAAAGCCGC**	*Sac*II
uni-21*	**TGTAAAACGACGGCCAGT**	
rev-29*	**CAGGAAACAGCTATGACC**	
GST-for*	**GGGCTGGCAAGCCACGTTTG**	
GST-rev*	**CCGGGAGCTGCATGTGTCAG**	
hSco2-int-rev*	**AAACCAGGCTCTGCTTCCAG**	
hSco2-int-vor*	**GTGCAGCCTGTCTTCATCAC**	
hSco1-int-rev*	**AAGTAAAGGCTTGCCGATGT**	
EGFP-vor*	**CTGGTTTAGTGAACCGTCAG**	
EGFP-rev*	**ACGCTGAACTTGTGGCCGTT**	
EGFP-rev2*	**TTATGTTTCAGGTTCAGGGG**	

Table 2. Primers used for the plasmids construction and for sequencing.
The enzyme recognition sites are indicated in italic. The primer annealing regions are in bold, overlapping sequences are underlined, (/) indicates the switch between two genes, the introduced mutations are in red, (*) indicates 5' IRD800 labelled sequencing primers.

2.1.9 Plasmids

Plasmid	primers	over-lapping primers	template	protein
p415 ADH-hSco1p	3, 4		*hSCO1* cDNA	hSco1p
p415 ADH-hSco2p	1, 2		*hSCO2* cDNA	hSco2p
YEp351-ySco1p(1-95)/ hSco1p(117-301)	5, 4	19, 20	p415 ADH-hSco1p, YEp351-ySco1p	ySco1p(1-95)/ hSco1p(117-301)
YEp351-ySco1p(1-158)/ hSco1p(180-301)	5, 4	21, 22	p415 ADH-hSco1p, YEp351-ySco1p	ySco1p(1-158)/ hSco1p(180-301)
YEp351-ySco1p(1-95)/ hSco2p(83-266)	5, 2	6, 7	p415 ADH-hSco2p, YEp351-ySco1p	ySco1p(1-95)/ hSco2p(83-266)
YEp351-ySco1p(1-158)/hSco2p(144-266)	5, 2	8, 9	p415 ADH-hSco2p, YEp351-ySco1	ySco1p(1-158)/ hSco2p(144-266)
YEp351-ySco1p(1-177)/ hSco2p(164-266)	5, 2	10, 11	p415 ADH-hSco2p, YEp351-ySco1p	ySco1p(1-177)/ hSco2p(164-266)
YEp351-ySco1p(1-185)/	5, 2	12, 13	p415 ADH-hSco2p,	ySco1p(1-185)/

hSco2p(172-266)			YEp351-ySco1p	hSco2p(172-266)
YEp351-ySco1p(1-222)/ hSco2p(209-266)	5, 2	14, 15	p415 ADH-hSco2p, YEp351-ySco1p	ySco1p(1-222)/ hSco2p(209-266)
YEp351-ySco1p(1-158)/ hSco2p(144-208)/ ySco1p(223-295)	5, 18	16, 17	YEp351-ySco1p (1-158)/hSco2p (144-266), YEp351-ySco1p	ySco1p(1-158)/ hSco2p(144-208)/ ySco1p(223-295)
YEp351-ySco1p(1-134)/ hSco1p(156-301)	5, 4	27, 28	p415 ADH-hSco1p, YEp351-ySco1p	K1
YEp351-ySco1p(1-117)/ hSco1p(139-301)	5, 4	29, 30	p415 ADH-hSco1p, YEp351-ySco1p	K2
YEp351-ySco1p(1-134)/ hSco1p(156-301)(P174L)	5, 4	31, 32	YEp351-ySco1p (1-134)/hSco1p (156-301)	K1L
YEp351-ySco1p(1-117)/ hSco1p(139-301)(P174L)	5, 4	31, 32	YEp351-ySco1p(1-117)/hSco1p(139-301)	K2L
pEGFP-hSco1p	25, 26		p415 ADH-hSco1p	hSco1p-EGFP
pEGFP-hSco2p	23, 24		p415 ADH-hSco2p	hSco2p-EGFP
pEGFP-hSco2p(E140K)	23, 24	33, 34	pEGFP-hSco2p	hSco2p(E140K)-EGFP
pEGFP-hSco2p(S225F)	23, 24	35, 36	pEGFP-hSco2p	hSco2p(S225F)-EGFP
pEGFP-hSco1pΔcys	25, 26	37, 38	pEGFP-hSco1p	hSco1pΔcys-EGFP
pEGFP-hSco2pΔcys	23, 24	39, 40	pEGFP-hSco2p	hSco2pΔcys-EGFP
pEGFP-hCox17p	41, 42		cDNA	hCox17p-EGFP
pGEX-4T-3-hSco1p(C)	43, 4		pEGFP-hSco1p	hSco1p(C)
pGEX-4T-3-hSco2p(C)	44, 2		pEGFP-hSco2p	hSco2p(C)
pGEX-4T-3-hSco2p(C)(E140K)	44, 2		pEGFP-hSco2p(E140K)	hSco2p(C)(E140K)
pGEX-4T-3-hSco2p(C)(S225F)	44, 2		pEGFP-hSco2p(S225F)	hSco2p(C)(S225F)
pGEX-4T-3-hSco2p(C)Δcys	44, 2		pEGFP-hSco2pΔcys	hSco2p(C)Δcys
pGEX-4T-3-hSco1p(C)Δcys	43,.4		pEGFP-hSco1pΔcys	hSco1p(C)Δcys
pAU5-hSco1p	25, 45		pEGFP-hSco1p	hSco1p-AU5

Table 3. List of the plasmids constructed in this work.
The name of the plasmids are indicated on the left and the resulting protein on the right, the numbers in brackets indicate amino acids position. The primers and the templates used in the PCR are indicated.

2.2 Methods

2.2.1 Plasmids

The oligonucleotide primers used for PCRs are listed in Table 2. The combination of primers and the created constructs are listed in Table 3. The annealing temperature (Ta) of the primers was calculated according to the following formula (MWG-BIOTECH):

Ta = 69,4°C +0,41 x (GC-Percent) – 650/Primer length – 6°C

The following mix was used:

	Final concentration
Template	1 ng/µl
Upstream primer (100 pmol/µl)	1 pmol/µl
Downstream primer (100 pmol/µl)	1 pmol/µl
dNTP mix (each dNTP 10 mM)	each dNTP 200µM
PCR puffer (10X)	1X
Pwo Polymerase (5 units/µl)	2 units
Total volume	100 µl

The following PCR programs were used:

General PCR

5 min 95°C addition of Polymerase (“hot start”)	Initial denaturation	1X
1 min 94°C 1 min Ta 2 min 72°C	Denaturation Annealing Elongation	20X
5 min 72°C	Final elongation	1X

Overlay PCR

5 min 95°C addition of Polymerase (“hot start”)	Initial denaturation	1X
1 min 94°C 1 min Ta 2 min 72°C	Denaturation Annealing Elongation	10X
1 min 94°C 1 min Ta + 5°C 2 min 72°C	Denaturation Annealing Elongation	20X
5 min 72°C	Final elongation	1X

Standard techniques were used for restriction endonuclease analysis of DNA, ligation of DNA fragments, transformations and recovery of plasmid DNA from *E. coli* [190]. Purification of PCR products and plasmids was carried out with the kits listed in section 2.1.3.

The construct YEp351-ySco1p comprises the promoter, the coding region and the terminator of *ySCO1* [85]. A cDNA clone containing the *hSCO2* gene was obtained from Luc Smink (Sanger Centre, Hinxton, GB) and a cDNA clone containing the *hSCO1* gene was provided by Professor Massimo Zeviani (National Neurological Institute “C. Besta”, Milano, Italy). Constructs p415 ADH-hSco1p and p415 ADH-hSco2p, in which the human genes are under control of the *ADH* promoter, were obtained by cloning a PCR product in the vector p415 ADH.

Chimeras under the control of the y*SCO1* promoter were created by overlap extension PCR [191] and cloned into the vector YEp351. The mutant chimeras K1L and K2L, in which the proline at position 174 of the original human wild type protein was substituted by leucine, were obtained with overlap extension PCR and cloned in the YEp351 vector.

Plasmids pEGFP-hSco1p and pEGFP-hSco2p, in which the human genes are fused C-terminally to the *EGFP* gene, were obtained by cloning a PCR product into the pEGFP-N1 vector.

Mutant genes coding for hSco2p(E140K), in which the aspartic acid at position 140 is changed into a lysine and hSco2p(S225F), in which serine at position 225 is changed to phenylalanine, were obtained by overlap extension PCR. The PCR products were cloned into the vector pEGFP-N1 to create pEGFP-hSco2p(E140K) and pEGFP-hSco2p(S225F).

Mutant gene coding for hSco2pΔcys, in which the cysteine residues at positions 133 and 137 are substituted through alanines, and mutant gene coding for hSco1pΔcys, in which the cysteine residues at positions 169 and 173 are changed to alanines, were obtained by overlap extension PCR. The PCR products were cloned into the vector pEGFP-N1 to create pEGFP-hSco1pΔcys and pEGFP-hSco2pΔcys.

The C-terminal portion of hSco1p and hSco1pΔcys was generated by amplification of the gene region coding for Aa 113-301 of hSco1p and hSco1pΔcys respectively. The PCR products were cloned into the GST-fusion expression vector pGEX-4T-3 to obtain pGEX-4T-3-hSco1p(C) and pGEX-4T-3-hSco1p(C)Δcys in which the *hSCO1* genes are fused N-terminally to *GST* gene. The C-terminal portions of hSco2p, hSco2p(E140K), hSco2p(S225F) and hSco1pΔcys were obtained by amplification of the gene region coding for Aa 79-266 of the respective constructs. The PCR products were cloned into the vector pGEX-4T-3 to create pGEX-4T-3-hSco2p(C), pGEX-4T-3-hSco2p(C)(E140K), pGEX-4T-3-hSco2p(C)(S225F) pGEX-4T-3-hSco2p(C)Δcys and pGEX-4T-3-hSco1p(C)Δcys in which the *hSCO2* genes are fused N-terminally to *GST* gene.

The vector pAU5-hSco1p was constructed from the pEGFP-N1 vector by removing the *EGFP* gene with the enzymes *Bam*H1 and *No*t1 and by cloning a PCR product carrying the sequence coding for hSco1p fused C-terminally with the sequence coding for the AU5 tag [192].

The *hCOX*17 gene was amplified from a placenta cDNA bank (CLONTECH) by PCR and cloned into the plasmid pEGFP-N1 to create pEGFP-hCox17p.

2.2.2 Sequencing

DNA sequences were determined by the dideoxy chain termination method of Sanger [193] using 5´ IRD800-labelled primers and the Thermo Sequenase fluorescent labelled primer cycle sequencing kit with 7-deaza-dGTP as described by the manufacturer and the LI-COR DNA sequencer. Primers used for sequencing are listed in Table 2. The annealing temperature of the primers was calculated according the following formula (MWG-BIOTECH):

Ta = 69,4°C +0,41 x (GC-Percent) – 650/Primer length + 3°C

2.2.3 Human cell methods

2.2.3.1 Cell Culture

HeLa cells were grown routinely in 75 cm^2 flask in Dulbecco's modified Eagle medium (DMEM) containing 10 % fetal calf serum and 2 mM glutamine (complete medium). Cultures were maintained at 37°C in a humidified atmosphere containing 5 % (v/v) CO_2. Cultures were splitted every three days by detaching the cells from the surface of the flask with the protease trypsin. Before trypsin treatment, complete medium was removed and the adherent cells were washed with 2 x 10 ml Ca^{2+}- and Mg^{2+}-free PBS. 1 ml trypsin was added and cells were incubated at 37°C for 3 minutes. 10 ml complete medium were added to inactivate the trypsin and the cells were pelleted by centrifugation for 5 min at 800 x g with a swing-out rotor at room temperature. After removing the supernatant, cells were resuspend in 10 ml complete medium and 10 µl of this suspension were used for determining the cell amount in a Neubauer-counting chamber. $5x10^5$ cells were transferred to a new flask.

For long-term storage, $1X10^7$ cells were detached from the flask with trypsin, washed with 2 x 10 ml Ca^{2+}- and Mg^{2+}-free PBS and resuspend in 800 µl complete medium. 800 µl ice cold freezing solution were then added drop by drop. The cells suspension was transferred to a freezing vial and was stored for one year at –80°. For longer storage, cells were frozen overnight at –80°C and then transferred to liquid nitrogen. To recover the frozen cells, the vial was kept in a 37°C water bath. When the cells were thawed, the cells suspension was transferred to a centrifuge tube. 1,8 ml complete medium (at room temperature) were added and the cells were incubated for 5 minutes in a 37°C water bath. 3,6 ml complete medium were added and the cells were again incubated for 5 minutes in a 37°C water bath. 1 ml complete medium was finally added and the cells were centrifuged for 5 min at 800 x g at room temperature. The medium was removed and 10 ml complete medium were added. The cells were transferred to a tissue culture flask.

2.2.3.2 Transfection of HeLa cells

For transient expression cells were cultured in one-well TC chamber slides and transformed using liposome-mediated transfection (Tfx™-20) as described by the manufacturer. Cells were seeded 1 day prior to transfection at 40-70 % confluence. For transfection of about 3 x 10^5 cells, 1 µg of plasmid DNA and 2 µl of liposome-solution (1 mM stock solution) in 1 ml incomplete medium were used. Cells were washed with 2 x 10 ml Ca^{2+}- and Mg^{2+}-free PBS

and the DNA/liposome mixture was added. After 2 h incubation in the CO_2 incubator at 37°, 2 ml complete medium were added and the cells were incubated for further 14 hours. Transfection efficiency was routinely high (approximately 50 %). Transfections in 100-mm plates ($3X10^6$ cells) were performed with 20 µl DNA and 40 µl of liposome reagent in 10 ml incomplete medium.

For stable transfection, cells were put under geneticin™ selection (final concentration: 500 µg/ml) 48 h after transfection. To improve selection, cells were successively replated to eliminate untransfected cells. Geneticin-resistant clones were picked by ring cloning, regrown in multiwell plates, and subsequently tested for the presence of an expressed transgene by Western blot analysis and fluorescence microscopy.

2.2.3.3 Isolation of human mitochondria

Cells were detached from the flask as described in 2.2.3.1. and the cell pellet was washed twice with PBS. The pellet was resuspend by gentle pipetting in 2 volumes of ice-cold homogenisation buffer, kept on ice for 5 min and then homogenised in a dounce homogeniser with 20 strokes. Disruption of the cells was monitored by microscopy. Nuclei and cell debris were pelleted by two sequential centrifugations at 1200 x g for 3 min at 4°C. Mitochondria from the post-nuclear supernatants were recovered by centrifugation at 12000 x g for 10 min at 4 °C. Mitochondrial pellet was washed once with 1 ml ice-cold wash-buffer (WM) and either directly processed or frozen at -80 °C. 800 µg mitochondria were obtained from $2x10^7$ cells.

2.2.3.4 Preparation of HeLa cells mitochondrial lysate and whole lysate

Mitochondrial and whole cell lysate were prepared by lysing mitochondria (prepared as described in section 2.2.3.3) or cells in lysis buffer for 1 h on ice. For $1x10^7$ cells or 1 mg mitochondria, 1 ml lysis puffer was used. Cells debris was removed by centrifugation at 3000 x g for 10 min at 4°C. Supernatant was collected after centrifugation at 13000 x g at 4° for 15 min.

2.2.3.5 Fluorescence microscopy

HeLa cells were subcultured in TC chamber slides and transfected as described above. For staining of mitochondria cells were incubated for 30 min in the presence of 50 nM MitoTracker® Red CMXRos. Cells were visualized with a Jena Lumar fluorescence microscope 14 hours after transfection. EGFP has a fluorescence excitation maximum at 408

nm and a fluorescence emission maximum at 507 nm. MitoTracker has a fluorescence excitation maximum at 579 nm and a fluorescence emission maximum at 599 nm. Pictures were taken with the SenSys Digital CCD camera and edited with the MetaView software (INVITRO SYSTEM).

2.2.4 Yeast cells methods

2.2.4.1 Transformation

Yeast cells were transformed using the LiAc procedure [194].

2.2.4.2 Isolation of yeast mitochondria

Yeast transformants were grown to stationary phase in WO-Gal medium. Cells were harvested by centrifugation at 3000 x g for 5 minutes. After washing with 1 ml ice-cold water, cells were resuspended in 1 ml ice-cold MTE. Cells were lysed by vortexing vigorously for 5 min in the presence of 500 µl glass beads (∅ 0,45 mm). Supernatants were collected to new tubes and glass beads were washed once with 500 µl ice-cold MTE. The supernatant of the washing step was added to the previous supernatants. Unbroken cells and the cell debris were removed by centrifugation at 3000 x g for 3 min at 4°C. Mitochondria were pelleted by centrifugation at 13000 x g for 15 min at 4°C.

2.2.4.3 Determination of COX-activity

COX activity was determined as described by Tzagoloff *et al*. [195]. 50 µg of mitochondria were solubilized in assay-buffer (50 mM potassium phosphate, pH 7,2; 0,5 % (v/v) Tween 80). The enzyme reaction was started by addition of 50 µM reduced ferrocytochrome *c* and the initial rate of oxidation was determined at room temperature by following the decrease in absorbance at 550 nm.

2.2.5 Affinity purification of recombinant proteins

BL21 transformants harbouring plasmid pGEX-4T-3 or pGEX-4T-3 carrying the coding region for the genes of interest were inoculated 1:100 from an overnight culture and grown at 30°C in LB broth with 2 % (w/v) glucose and 100 µg/ml ampicillin until an absorbance of 0,8 at 600 nm was reached. The culture was induced with 100 µM IPTG. For isolation of proteins for

atomic absorption spectroscopy 0,5 mM $CuSO_4$ was added at the time of induction. After 30 minutes cells were harvested, washed twice in PBS-DTT and resuspended in PBS-DTT with 10 % (v/v) glycerol, 1 mM PMSF. Cells were lysed using a French press at 1000 psi 2 times and cell debris was removed by centrifugation at 20000 x g at 4°C for 1 h. The supernatant was incubated for 1 h at 4°C with 50 % (w/v) Glutathione (GSH)-Sepharose 4B suspension equilibrated three times with 20 volumes PBS-DTT. GSH-Sepharose 4B was pelleted by centrifugation and washed with PBS-DTT. Bound fusion protein was cleaved on the matrix with thrombin in PBS-DTT at room temperature to eliminate the GST moiety. Proteins were analysed by SDS-PAGE and stained with Coomassie Blue G-250.

2.2.6 *In vitro* interaction assay

20 µg of GST fusion proteins or GST alone were immobilized on GSH-Sepharose beads and allowed to interact for 2 h at 4°C with cell lysate of $2x10^6$ HeLa cells or with 800 µg mitochondrial lysate (prepared as described in section 2.2.3.4). In some experiments immobilised fusion proteins were loaded with copper by incubation with 200 µM $CuSO_4$ and 1 mM DTT in TBS for 2 h at 4°C. Excess copper was removed by washing with 30 volumes TBS. Following binding, the beads were washed extensively with 1x PBS-DTT containing 0,3 % (v/v) NP-40 and protein complexes were released by the addition of sample buffer with β-mercaptoethanol and heating at 100° for 5 min. Samples were analysed in Western blot with antibody against Cox2p or EGFP. In some experiments lysis puffer and wash solution without DTT were used.

2.2.7 Immunoprecipitation

Immunoprecipitation of mitochondrial proteins were performed with anti-AU5 or anti-EGFP antibodies. 1 mg mitochondria were lysed as described in section 2.2.3.4 and the supernatant was incubated with 10 µl anti-AU5 antibody or anti-EGFP antibody for 3 h at 4°C on an orbital shaker. 30 µl protein G-Sepharose were added and the samples were incubated for further 2 h at 4°C. The beads were washed four times with 1 ml lysis buffer. Immunoprecipitates were examined with Western blot analysis.

2.2.8 Determination of the protein concentration

The protein concentration was determined using the DC protein-assay as described by the supplier or using the Bradford method [196].

2.2.9 Western blot analysis

Proteins were separated on a 12 % polyacrylamide gel in the presence of SDS. Proteins were transferred to a PVDF membrane using the semi-dry method for 1 h at RT at 1,5 mA/cm^2. Membranes were blocked over night at 4° C or 1 hour at room temperature with 5 % (w/v) non-fat dry milk in TBS-T. Membranes were probed with polyclonal or monoclonal antisera for 1 hour at room temperature and then washed three times for 10 minutes in TBS-T. Horseradish peroxidase-conjugated anti-rabbit or anti-mouse antibodies were used as secondary antibodies. The secondary antibody was added to the membranes for 30 minutes at room temperature and the membranes were then again washed three times for 10 minutes in TBS-T. Antigen-antibody complexes were visualised by enhanced chemiluminescence (ECL plus).

2.2.10 FPLC analysis

Proteins were separated on a Superdex 75 HR 10/30 gel filtration column. Column was equilibrated with two column volumes of PBS-DTT. 500 µg of affinity purified proteins were loaded and separation was performed at a flow rate of 0,5 ml/min at RT. Calibration of the column for estimation of the molecular weights was performed using BSA and carbonic anhydrase.

2.2.11 Thioredoxin assay

The reaction mixture contained 500 μM NADPH, 55 μM insulin, 15 μM of a purified human Sco protein or 5 μM human thioredoxin in 100 mM potassium phosphate, 2 mM EDTA, pH 7.4 [197]. The reaction was started by adding 80 nM human thioredoxin reductase. The increase in turbidity as a result of the formation of the insoluble insulin B chain was followed at 595 nm. The schema of the reaction is shown in Fig. 5.

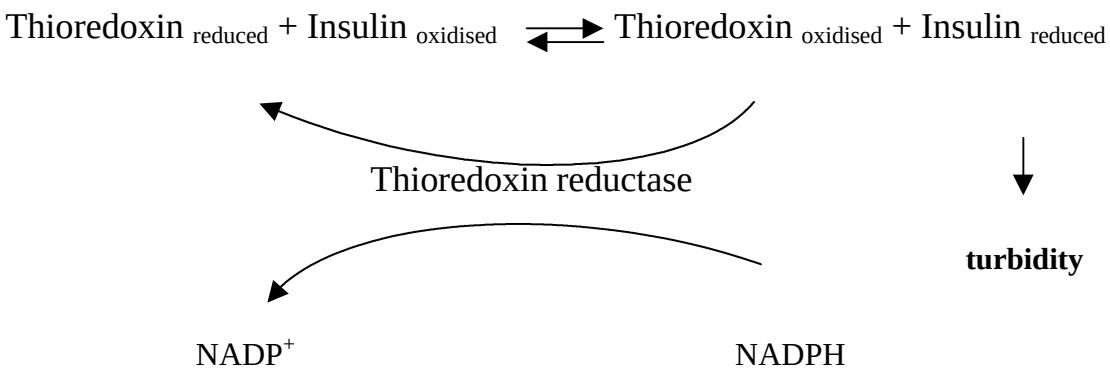

Fig. 5. Reactions involved in the thioredoxin assay.
Thioredoxin, in its reduced state, reduce the disulfides of insulin and the free insulin B chain precipitates. Oxidised thioredoxin is converted back to the reduced form by thioredoxin reductase with the use of the electrons from NADPH.

2.2.12 Atomic emission spectroscopy

Atomic emission spectroscopy of affinity purified proteins (60 μg in PBS-DTT) was performed with the plangrating spectrograph PGS2 using the arc method with carbon electrodes. Spectral lines were recorded on a photo plate. Copper-specific lines at 324,75 nm and 327,40 nm were identified with the spectral lines of iron as a reference. The principle of the method is illustrated in Fig. 6.

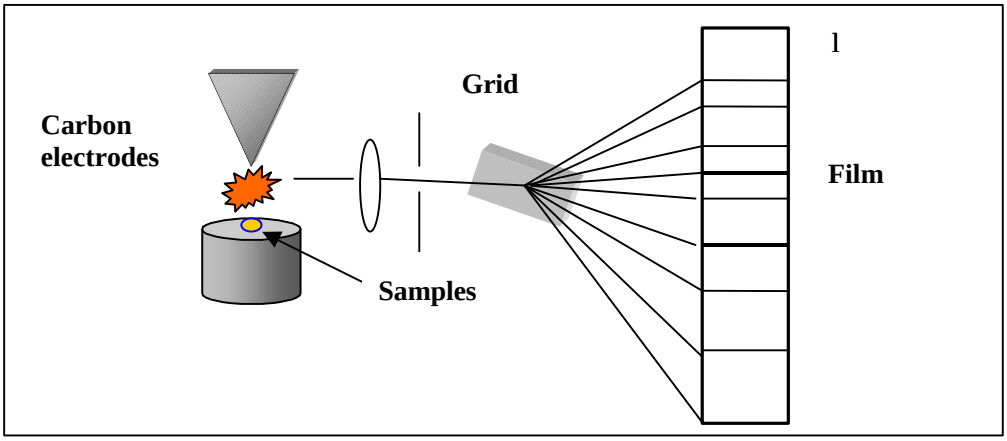

Fig. 6. Scheme of functioning of the atom emission spectroscopy.
The sample is submitted to a arc between two carbon electrodes. The radiation emitted from the sample is separated by a grid in its wavelengths (λ) and recovered on a film.

2.2.13 Atomic absorption spectroscopy (AAS)

Atomic absorption spectroscopy of affinity purified proteins in PBS-DTT isolated from *E. coli* cells grown in the presence of 0,5 mM $CuSO_4$, was performed with the SpectrAA 10 GTA-96. The principle of functioning of the AAS is given in Fig. 7.

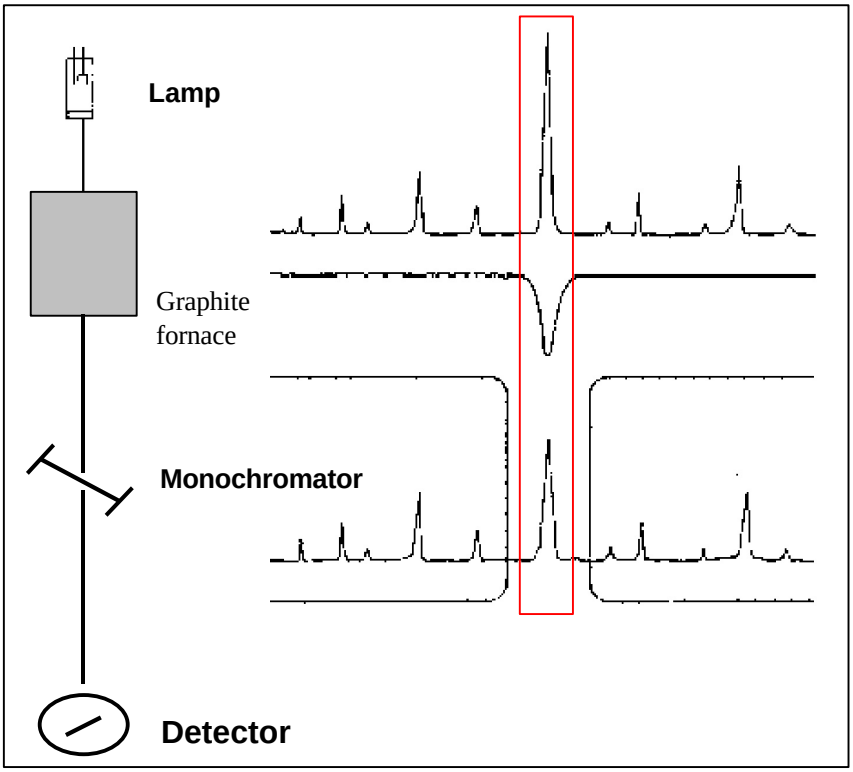

Fig. 7. Scheme of atom absorption spectroscopy for copper analysis.
A copper cavity cathode lamp emits the radiation which is directed to the graphite furnace. In the graphite furnace the sample is atomised and absorbs part of the radiation. The monochromator separates the analytic line (λ = 324,75, in red), the intensity of which is measured by the detector. The Lambert-Beer law fixes a relation between the decrease in the intensity of the initial radiation and the concentration of the sample.

3 RESULTS

3.1 Structural analysis of hSco proteins

The *ySCO1* human homologous gene on chromosome 22 (*hSCO2*) [Sequence ID: AL021683] was detected in the course of the systematic sequencing project of the human genome by Luc Smink at the Sanger Centre. The homologue on chromosome 17 (*hSCO1*) [Sequence ID: AF026852] was identified by the group of Massimo Zeviani [105]. *hSCO1* contains six exons and five introns, *hSCO2* two exons and one intron.

The homologues of ySco1p share a high degree of similarity with respect to the primary sequence and to their overall structure (Fig. 8). The BLAST 2 program [198] predicts 39 % overall identity and 59 % similarity between hSco1p and ySco1p, and 41 % overall identity and 59 % similarity between hSco2p and ySco1p. The overall identity between hSco1p and hSco2p is 43 % and the similarity 63 %. The N-terminal part of ySco1p contains a mitochondrial import sequence and a single predicted TM-region which directs the protein to mitochondria and anchors it in the inner mitochondrial membrane [100]. The N-termini of both hSco proteins are also reminiscent of mitochondrial pre-sequences in that they lack negatively charged amino acids while they contain positively charged and hydroxylated amino acid residues [199]. MitoProtII [200] predicts that hSco1p and hSco2p are very likely to be mitochondrial proteins with a N-terminal import signal of 42 amino acids (Aa) for hSco1p and of 31 Aa for hSco2p. The predicted molecular mass is 34 kDa for hSco1p (30 kDa without the import sequence) and 29 kDa for hSco2p (26 kDa without the import signal). Computer analysis of both human homologues with the MacMolly Tetra® program (Mologen, Berlin) predicts a single transmembranous domain between Aa 95-112 for hSco1p and Aa 61-78 for hSco2p. The region following the transmembranous domain (in this work indicated as C-terminal portion), including Aa 113-301 for hSco1p and 79-266 for hSco2p, shows the highest degree of homology between all known homologues and contains the conserved motif CxxxC which is essential for ySco1p function [85]. This motif is localised at Aa position 169-173 in hSco1p and at Aa position 133-137 in hSco2p. Within the C-terminal portion, the two hSco proteins reach a similarity of 73 %. At the extreme end of the C-terminal domain, the human homologues differ strongly from the yeast proteins. A PSI-BLAST [201] search made by Chinenov [176], revealed a low similarity of Sco proteins to bacterial thiol-disulfide reductases, and a secondary structure predictions using PHD [202] suggests a thioredoxin fold. Otherwise, the CxxxC motif is reminescent of the copper binding domain of Cox2p .

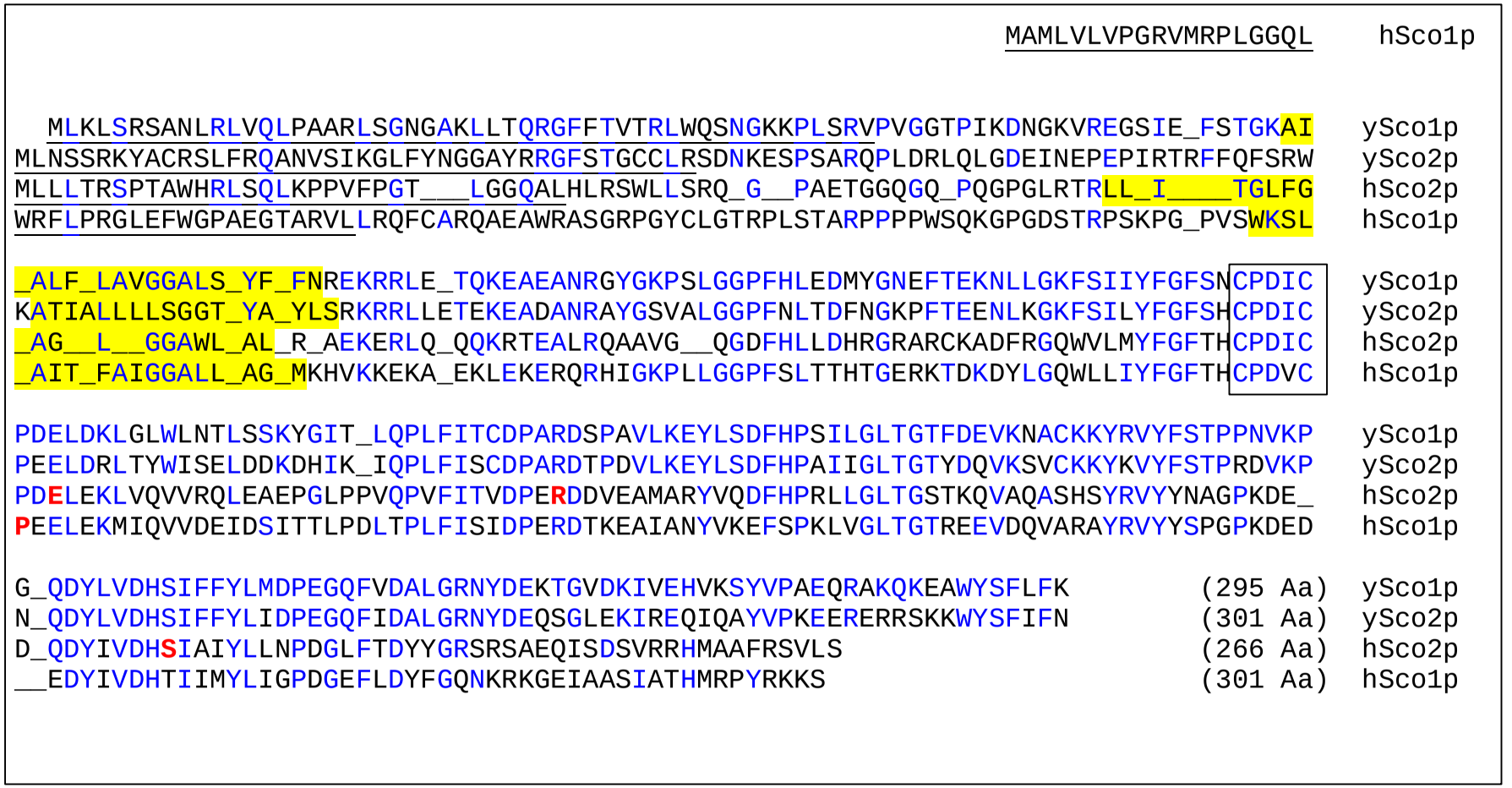

Fig. 8. Multiple alignment of yeast and human Sco proteins.
Identical residues are in blue, putative import signals, as predicted with the MitoProtII program, are underlined, the predicted copper binding motif is boxed, potential transmembrane domains, as predicted with the MacMolly Tetra program, are in yellow, the point mutations involved in lethal COX deficiency are in red.

3.2 Complementation analysis in yeast of hSco1p and hSco2p

hSco1p and hSco2p were tested for their ability to substitute ySco1p. The respective cDNAs of the homologues were cloned behind the strong *S. cerevisiae ADH1* promoter in the p415 *ADH* vector and transformed into strain GR20, which is deleted for *ySCO1*. Both constructs failed to restore respiratory competence (Fig. 9, (5) and (6)), *i.e.* the genes are not *per se* functional homologues of *ySCO1*.

Different chimeric proteins (Fig. 10) were constructed between ySco1p and the human homologues to identify regions of the human genes which are able to substitute for the corresponding yeast parts. The chimeras were cloned in the YEp351 vector behind the *ySCO1* promoter. To exclude the possibility that the import signal and/or the TM-region of the human proteins are not functional in *S. cerevisiae*, chimeras were constructed consisting of the N-terminal 95 amino acids of ySco1p (including import signal and TM region) and the C-terminus of hSco1p (ySco1p(1-95)/hSco1p(117-301)) and hSco2p (ySco1p (1-95)/hSco2p(83-266)), respectively. These constructs, too, proved not to be able to complement the respiratory deficiency of strain GR20.

In a second set of chimeras the N-terminal 158 amino acids of ySco1p up to the CxxxC-motif were fused to the C-termini of hSco2p (ySco1p(1-158)/hSco2p(144-266)) and hSco1p (ySco1p(1-158)/hSco1p(180-301)), respectively. In a control experiment it was shown that the aminoterminal 158 amino acids of ySco1p (ySco1p(1-158)) alone do not restore respiratory competence in the Δ*ysco1* strain GR20 [203]. Interestingly the ySco1p(1-158)/hSco1p(180-301) chimera restored respiratory competence in GR20, while the chimeric protein ySco1p(1-158)/hSco2p(144-266) did not (Fig. 9, (3) and (4)). Transformants bearing ySco1p(1-158)/hSco1p(180-301) show a slight cold sensitive phenotype, *i.e.* a somewhat reduced growth rate at 23°C as compared to wild type (data not shown). The difference in complementation behaviour is not due to a proteolytic sensitivity of ySco1p(1-158)/hSco2p(144-266), as a protein of the expected molecular mass can be detected with ySco1p-antibodies in Western analysis (data not shown). To test whether parts of the C-terminal region of the human chromosome 22 homologue may replace the respective yeast sequences, the C-terminal portion derived from the human homologue was progressively shortened as outlined in Fig. 10: ySco1p(1-177)/hSco2p(164-266), ySco1p(1-185)/hSco2p (172-266) and ySco1p(1-222)/hSco2p(209-266). All constructs were transformed into strain GR20 and tested for their ability to restore respiratory competence. None of the chimeras was able to substitute for ySco1p function.

In yeast a truncated version of ySco1p (ySco1p(1-258)), lacking the C-terminal 35 amino acids, is not functional [203]. Because the extreme C-terminus is one of the most divergent regions between the homologues it was tested whether the authentic ySco1p C-terminus might be necessary for function of a chimeric protein. To this end the chimera ySco1p(1-158)/hSco2p(144-208)/ySco1p(223-295) was constructed. In this protein the aminoterminal 158 amino acids as well as the carboxyterminal 73 amino acids are derived from ySco1p, while the internal segment corresponds to amino acids 144-208 of hSco2p. This construct, too, proved not to be functional in yeast.

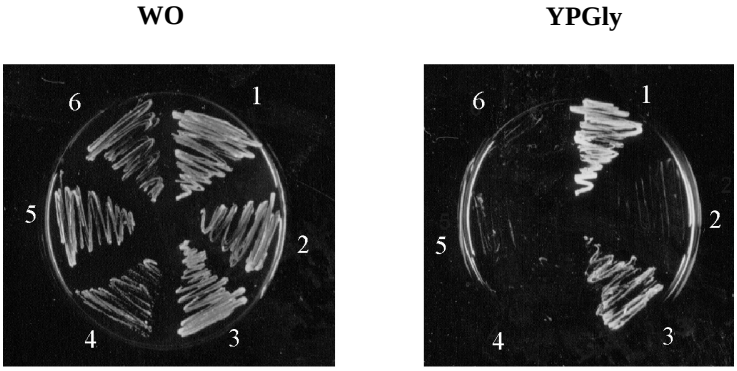

Fig. 9. Complementation behaviour of Sco1p-derivatives in strain GR20.
Δ*ysco1*-strain GR20 was transformed with YEp351 (control (2)) or with plasmids encoding: (1) ySco1p, (3) ySco1p(1-158)/hSco1p(180-301), (4) ySco1p(1-158)/hSco2p(144-266), (5) hSco1p, (6) hSco2p. Growth on minimal medium (WO) and glycerol medium (YPGly) was monitored after 3 days of incubation at 30°C.

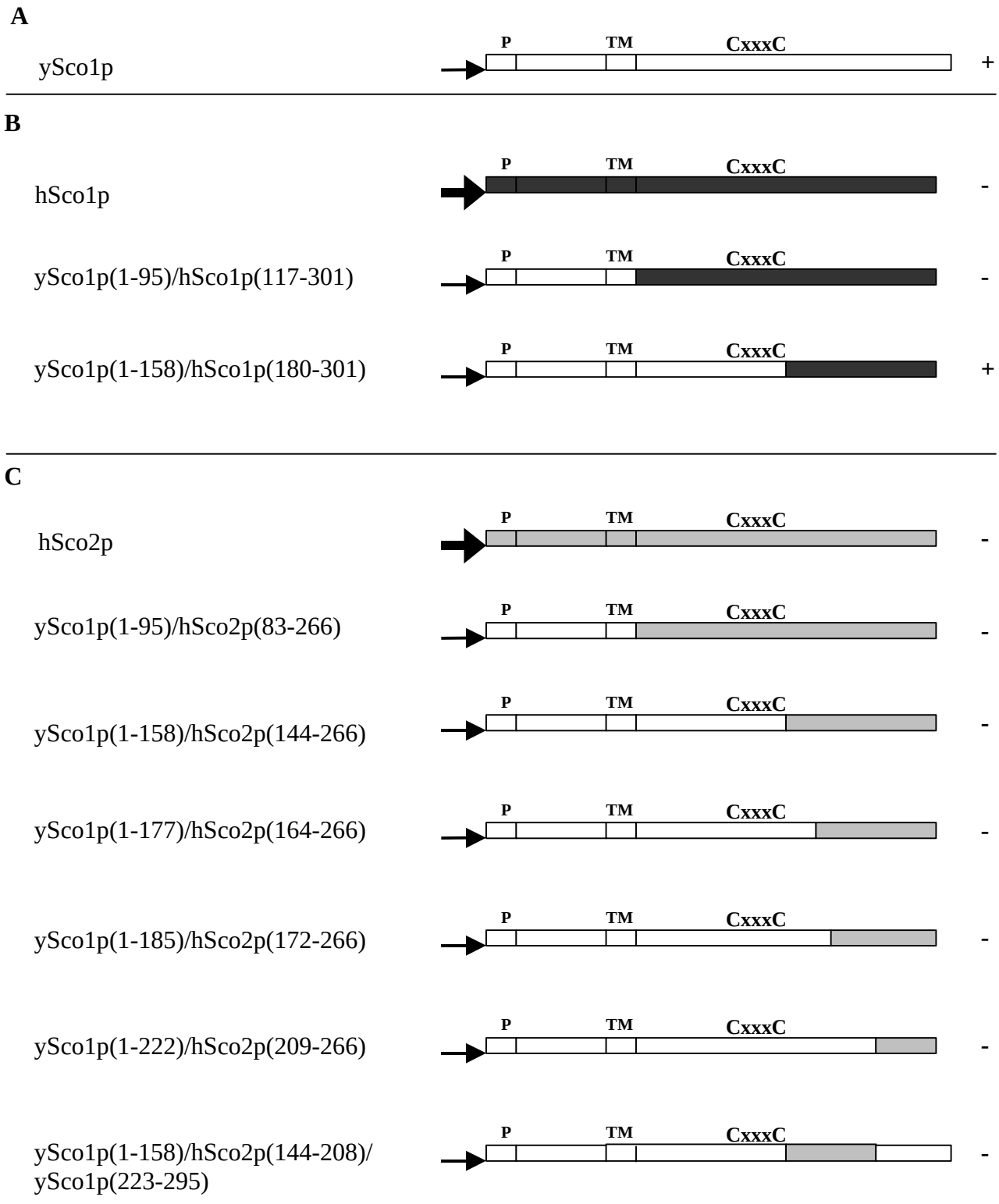

Fig. 10. Overview of constructs tested in the complementation analysis of the D**y*sco1*-strain GR20.**

A. Schematic presentation of ySco1p. **B**. Schematic presentation of hSco1p and ySco1p/hSco1p chimeras. **C**. Schematic presentation of hSco2p and ySco1p/hSco2p chimeras. **P** indicates the putative mitochondrial pre-sequence, **TM** the putative transmembrane domain and **CxxxC** the potential metal-binding site. The thin arrow indicates the *ySCO1* promoter and the fat arrow the *ADH1* promoter. Sequences derived from ySco1p are in white, from hSco1p in dark grey and from hSco2p in light grey. Growth of GR20 transformants on YPGly is indicated on the right side: + = growth; - = no growth.

3.3 Localisation of hSco1p and hSco2p

The finding that both human Sco proteins by themselves fail to substitute ySco1p function in yeast raised the question whether the human homologues are located within mitochondria. To examine the subcellular distribution *in vivo*, the proteins were fused at the C-terminus to the enhanced green fluorescent protein (EGFP) and placed behind the cytomegalovirus (CMV) promoter. The spontaneously fluorescent EGFP protein, an enhanced variant of the GFP protein from the jellyfish *Aequoria victoria*, is widely used to facilitate subcellular localisation of a target protein [204]. When expressed in mammalian cells fluorescence from wild type GFP is typically distributed throughout the cytoplasm and the nucleus, but excluded from the nucleolus and vesicular organelles [204]. However, highly specific intracellular localisation including the nucleus, mitochondria, secretory pathway, plasma membrane and cytoskeleton [205, 206] can be achieved via fusions to individual targeting sequences. EGFP contains two amino acids substitutions in the chromophore and fluoresces 35-fold more intensive than wild type GFP. HeLa cells were transfected, using the liposome method, with the plasmid encoding for EGFP (control), with the plasmid encoding for hSco2p-EGFP and with the plasmid encoding for hSco1p-EGFP, respectively. After 14 h HeLa cells were analysed with a fluorescence microscope. Transfectants expressing the hSco1p-EGFP clearly exhibited staining in punctuated structures (Fig. 11 A). Evidence that these structures represent mitochondria was obtained by staining with the mitochondria-specific dye MitoTracker® Red CMXRos, which resulted in an identical staining pattern (Fig 11 B). The identity of the patterns was confirmed by overlay of both fluorescences (Fig. 11 C). In the case of hSco2p-EGFP an identical staining pattern was observed (Fig. 12). In contrast to hSco1p-EGFP, however, occasionally a slight green fluorescence was also detected in the cytosol, possibly reflecting a higher concentration of the EGFP-fusion protein or a less efficient mitochondrial import. As expected, HeLa cells transfected with the EGFP-bearing control plasmid showed an homogeneous green fluorescence which did not correspond to the labeling pattern with MitoTracker® Red CMXRos (data not shown). These data demonstrate that both chimeric hSco-EGFP proteins are localised in mitochondria and that mitochondrial localisation is mediated by the hSco portions of the fusion proteins.

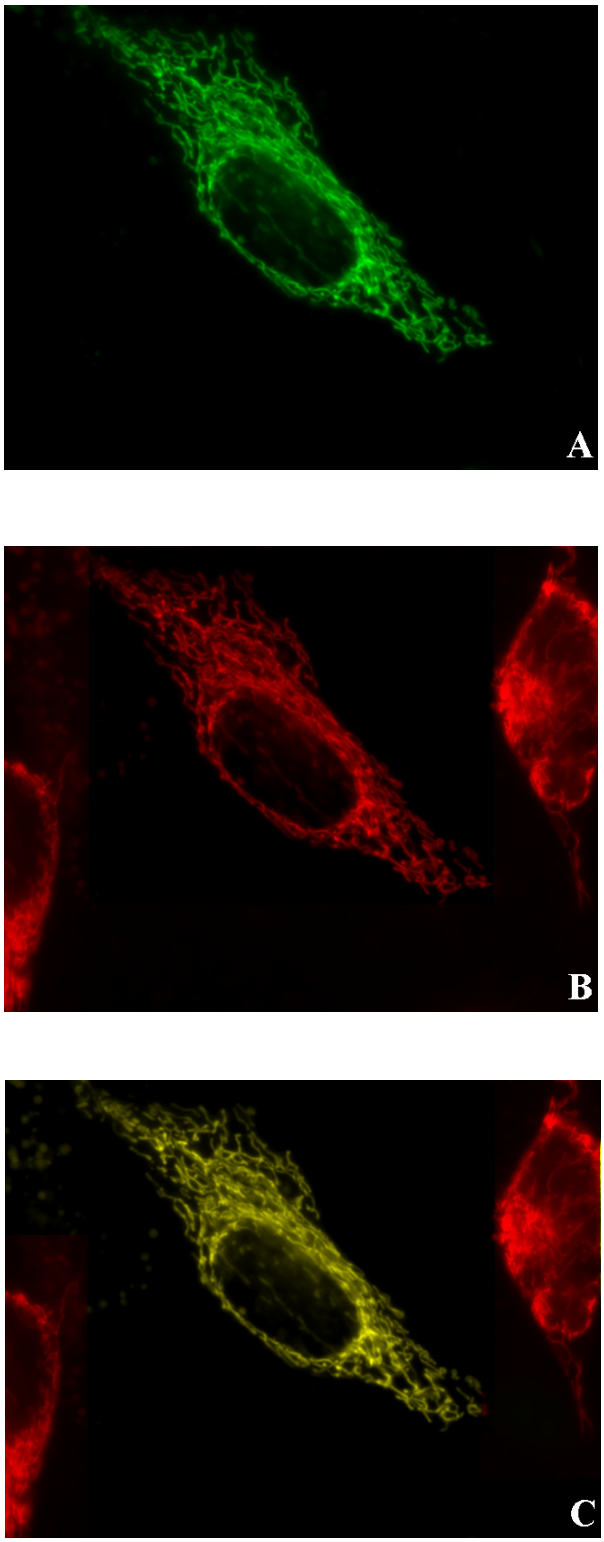

Fig. 11. ***In vivo*** **localisation of hSco1p.**
HeLa cells were transfected with a plasmid encoding for hSco1p-EGFP. After 14 h cells were counterstained with the mitochondria-specific dye MitoTracker® Red CMXRos. **A**. Green fluorescence by EGFP. **B**. Red fluorescence by MitoTracker® Red CMXRos. **C**. Overlay of green and red fluorescence

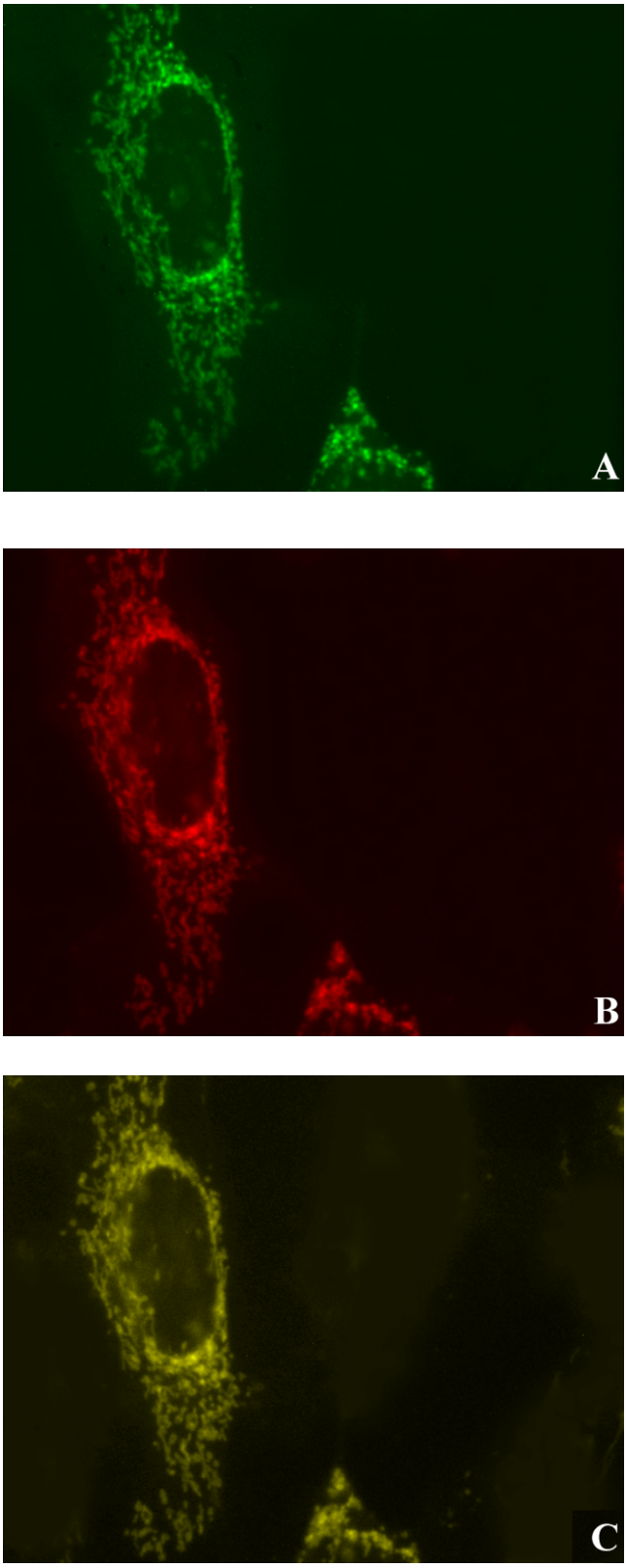

Fig. 12. ***In vivo*** **localisation of hSco2p.**
HeLa cells were transfected with the plasmid encoding for hSco2p-EGFP After 14 h cells were counterstained with the mitochondria-specific dye MitoTracker® Red CMXRos. **A**. Green fluorescence by EGFP. **B**. Red fluorescence by MitoTracker® Red CMXRos. **C**. Overlay of green and red fluorescence.

These results were confirmed by Western blot analysis. Because no antisera against hSco1p and hSco2p were available, C-terminal EGFP-tagged versions of both proteins were used. EGFP can function as a protein tag, as it tolerates N- and C-terminal fusions to a broad variety of proteins many of which have been shown to retain native function [204]. The molecular mass of EGFP is 27 kDa. The expected molecular mass, without the postulated import signal, is approximately 57 kDa for hSco1p-EGFP and 53 kDa for hSco2p-EGFP. HeLa cells were transfected with the plasmids encoding for hSco1p-EGFP and for hSco2p-EGFP, respectively. Mitochondrial and cytosolic fractions were prepared and probed with anti-EGFP antibody. Cox2p was used as a marker for the mitochondrial fraction. Fig. 13 shows that a band of the expected molecular mass is localised only in the mitochondrial fraction of hSco1p-EGFP expressing cells (lane 1) and of hSco2p-EGFP expressing cells (lane 3). The thin bands observed in both cases above the major bands probably represent the precursor forms. Because of the high protein expression induced from the *CMV* promoter, it is possible that not all proteins are processed to the mature form. This finding would confirm the hypothesis that hSco1p and hSco2p have a cleavable import sequence. These data are in agreement with the results of the *in vitro* import of hSco1p [105].

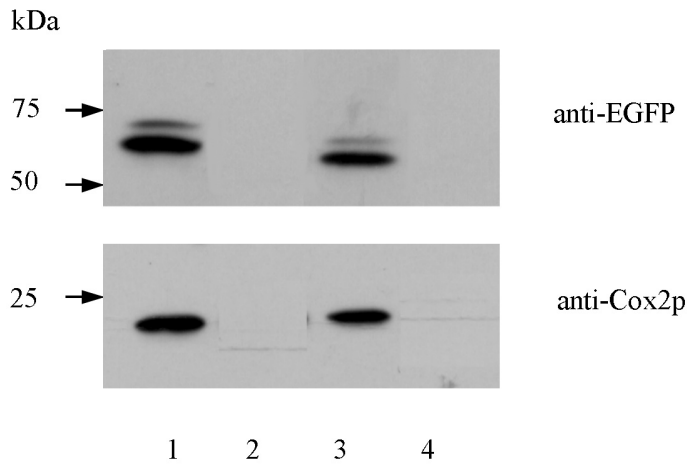

Fig. 13. Localisation of hSco1p and hSco2p.
Mitochondria (lane 1 and 3) and cytoplasm (lane 2 and 4) of HeLa cells expressing hSco1p-EGFP (lane 1 and 2) and hSco2p-EGFP (lane 3 and 4) were prepared. Western blot analysis of the two fractions was done with antibodies against EGFP and Cox2p.

3.4 Creation of cell lines stably expressing hSco1p-EGFP and hSco2p-EGFP

Transient transfection of cells is time-consuming and expensive. To dispose from a permanent source of cells expressing hSco1p-EGFP and hSco2p-EGFP, stable cell lines were created. HeLa cells were transfected with the plasmids encoding for hSco1p-EGFP and hSco2p-EGFP, respectively, and cells were cultivated under Geneticin selection for five weeks. Single Geneticin-resistant clones were isolated and allowed to grow for further four weeks. The resulting cultures were tested for their ability to express the EGFP fusion protein *in vivo* and by Western blot analysis. The selection was successful so far only for transfectants expressing hSco1p-EGFP. One clone, called HeLa 17A3, was isolated which shows a single mitochondrial band of the expected molecular mass of hSco1p-EGFP in Western blot analysis (Fig. 14) and a mitochondrial pattern of the EGFP fluorescence in fluorescence microscopic analysis (Fig. 15). Selection of stable hSco2p-EGFP transfectants was not successful after three months selection and is still in progress.

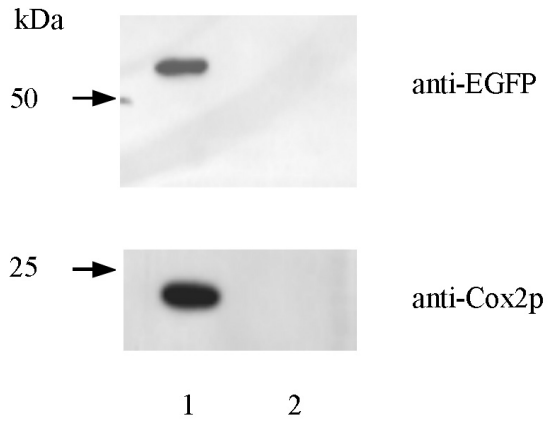

Fig. 14. Western blot analysis of the HeLa 17A3 cell line.
HeLa cells were stably transfected with the plasmid encoding for hSco1p-EGFP. Mitochondria (lane 1) and cytoplasm (lane 2) were probed with the anti-EGFP and the anti-Cox2p antibodies.

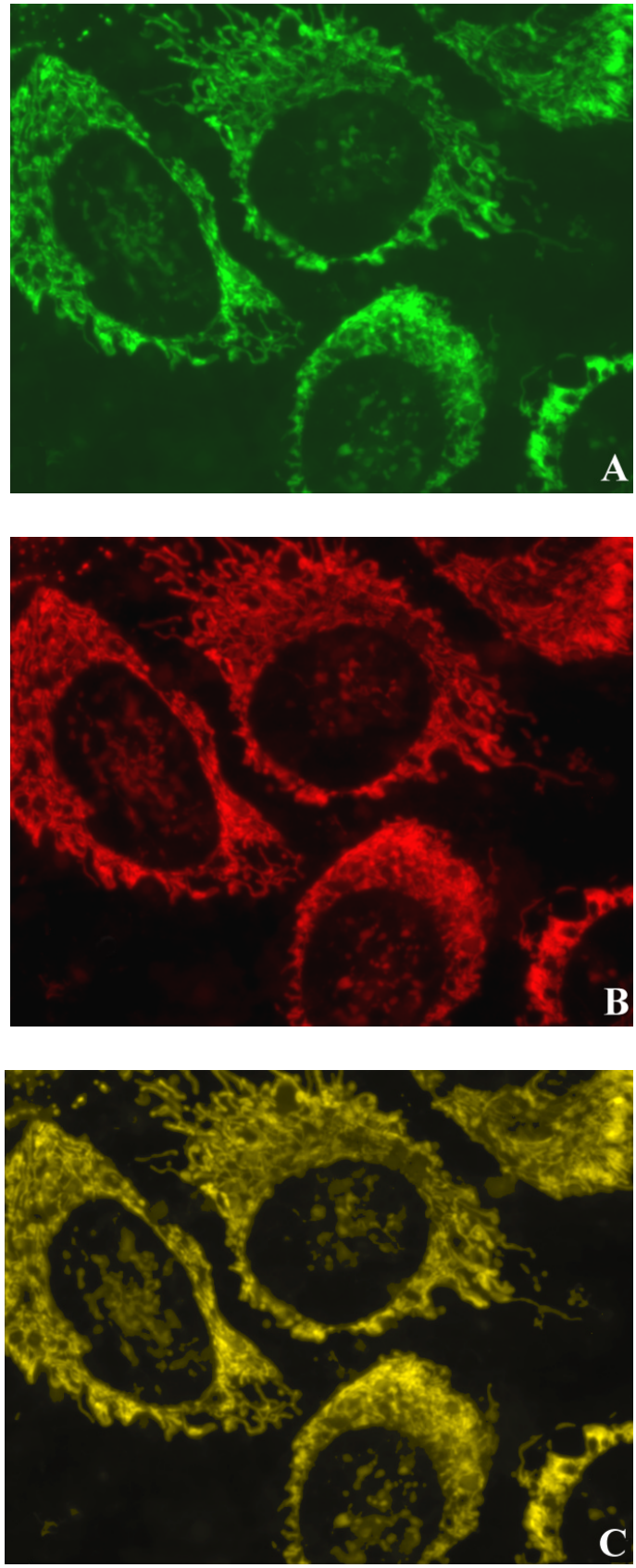

Fig. 15. Fluorescence microscopic analysis of the HeLa 17A3 cell line.
HeLa cells were stably transfected with the plasmid coding for hSco1p-EGFP. Cells were counterstained with the mitochondria-specific dye MitoTracker® Red CMXRos. **A.** Green fluorescence by EGFP. **B.** Red fluorescence by MitoTracker® Red CMXRos. **C.** Overlay of green and red fluorescence.

3.5 Functional analysis of hSco1p and hSco2p

All known eukaryotic members of the Sco-protein family possess a single transmembrane segment, which divides the proteins into a smaller N-terminal segment and a larger C-terminal segment which bears the essential motif CxxxC. As outlined in the introduction, the CxxxC motif could be involved in the copper delivery to COX. Sco proteins could mediate this transfer by direct copper binding or as a thioredoxin which is required for the formation of a binding-competent 3D-structure of the COX-subunits. To discriminate between the two models, the C-terminus (Aa 113-301) of hSco1p (hSco1p(C)) and the C-terminus (Aa 79-266) of hSco2p (hSco2p(C)) were purified and tested for their ability to reduce insulin, a classical thioredoxin test, and to bind copper. Because the CxxxC motif is essential for the protein function [85], mutant forms in which both cysteines were replaced by alanines (hSco1pΔcys and hSco2pΔcys) were constructed by directed mutagenesis. The C-terminal portions of the two mutant proteins (hSco1p(C)Δcys and hSco2p(C)Δcys) were then purified for functional analysis. Because of the difficulty to obtain a membrane protein in its native form, the full-length proteins have not been purified. Moreover, reductase activity as well as copper binding have been often proved using only a protein segment bearing the putative functional motif [156, 157, 207]. The recombinant proteins were isolated from *E. coli* using affinity chromatography. Although the folding process is different between the bacterial and the eukaryotic system, human proteins purified from *E. coli* often retain their functionality. Reductase activity was shown for a bacterial-purified mammalian thioredoxin [136] and copper binding properties have been analysed in bacterial-purified Wilson's and Menkes disease proteins [157].

3.5.1 Affinity purification of the C-terminal portions of hSco1p, hSco2p and of the mutant hSco forms

The coding regions for hSco2p(C) hSco2p(C)Δcys, hSco1p(C) and hSco1p(C)Δcys were cloned into plasmid pGEX-4T-3. In the resulting constructs the reading frames of the Sco proteins are fused in frame to the 3´-end of the *GST* gene, separated by a sequence which encodes a thrombin cleavage site. Expression of the fusion proteins under the control of the *tac* promoter was induced in *E. coli* transformants by the addition of IPTG. Steady state concentrations of the chimeric proteins were monitored at various time points after induction by SDS-PAGE of cell lysates containing GST-hSco1p and GST-hSco2p and subsequent Coomassie Blue staining of the gels. Fig. 16 shows the appearance of a band of the expected molecular weight (48 kDa for both proteins) only after induction with IPTG. Cells were lysed and insoluble material was removed by centrifugation. Several conditions were tested to increase the solubility of the recombinant proteins. The solubility increased by lowering the growth temperature and by induction for a shorter period of time. Moreover several lysis methods were tested: sonication, freeze/thaw, and french press [190]. The highest protein yields (1-2 mg protein pro litre culture) were obtained with the latter technique. Lysates of cells grown at 30° and induced for 30 minutes were used for affinity binding to GSH-Sepharose. For copper binding analysis, 0,5 mM copper sulphate was added at the beginning of the induction period. This copper concentration does not affect the growth rate and it was used in a similar experiment to determine the copper stoichiometry of MNK and WND [157]. Purified fusion proteins bound to GSH-Sepharose were incubated with thrombin to remove the GST segments. The released hSco2(C) proteins show a molecular mass of 22 kDa, as expected (Fig. 17). No difference was observed between hSco2p(C) (A) and the mutant form hSco2p(C)Δcys (B). The recombinant hSco1p(C) and hSco1p(C)Δcys have a molecular mass of 25 kDa (Fig. 17, C and D), contrary to the expected molecular mass of 22 kDa. To confirm that the 25 kDa purified segment was not a GST contamination (GST has a molecular mass of 25 kDa after thrombin cleavage), Western blot analysis was performed with anti-GST antibody. The purified 25 kDa segment was not recognised by the anti-GST antibody (data not shown). The recombinant hSco1p(C) obviously migrates with an apparent size of 25 kDa on SDS-polyacrylamide gels. The purity grade of the recombinant proteins were high as deduced from the Coomassie Blue staining of the gels. This observation was confirmed by gel filtration analysis (see section 3.6.5).

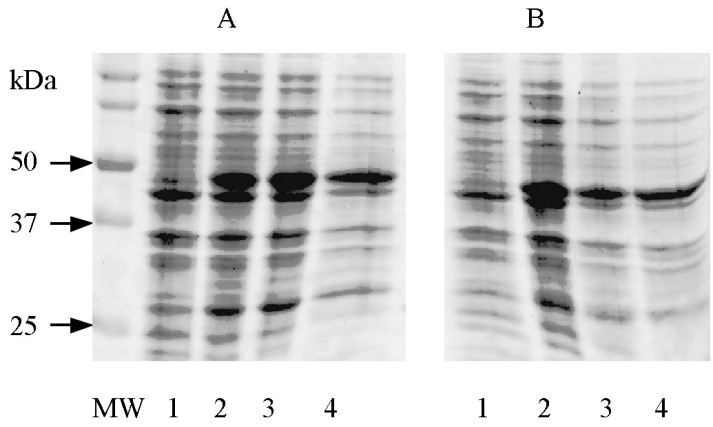

Fig. 16. Expression analysis of the C-terminal portions of hSco1p and hSco2p.
BL21 transformants harbouring plasmid pGEX-4T-3 carrying the coding region for Aa 113-301 of hSco1p (**A**) and for Aa 79-266 of hSco2p (**B**) were grown at 30°. The level of protein expression, before the induction (lane 1), and 30 minutes (lane 2), one hour (lane 3) and two hours (lane 4) after induction with IPTG, was monitored by SDS-PAGE of cell lysates and subsequent Coomassie Blue staining of the gels.

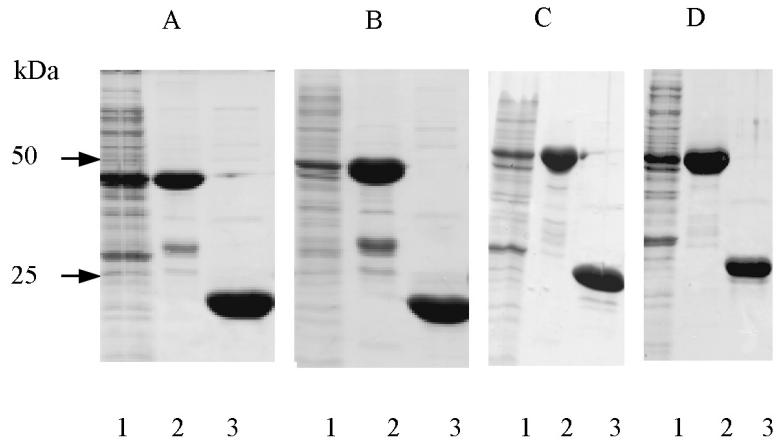

Fig. 17. Purification of the C-terminal portions of wild type and mutant forms of hSco2p.
The C-terminal portions of hSco2p (**A**), hSco2pΔCys (**B**), hSco1p (**C**) and of hSco1pΔCys (**D**) were expressed in BL21 and purified by affinity chromatography. Lane 1, supernatant after cell lysis prior to incubation with GSH. Lane 2, GSH-bound GST-fusion protein. Lane 3, purified protein after cleavage with thrombin.

3.5.2 hSco1p(C) and hSco2p(C) have no thioredoxin activity

Thioredoxins catalyse the formation and the reduction of disulfide bonds in proteins. The putative active sites of hSco1p and hSco2p does not perfectly match those of classical thioredoxins and other related proteins. However, a predicted thioredoxin fold and the similarity to thiol-disulfide oxidoreductases, led to the suggestion that Sco proteins could have a catalytic function [176]. To test whether hSco1p and hSco2p act as a thioredoxin, recombinant hSco2p(C) and hSco1p(C) were assayed for their ability to reduce disulfide bridges in insulin in the presence of NADPH and thioredoxin reductase. In this assay, disulfide reductase activity is monitored by increase in the turbidity of the reaction mixture due to the formation of fine precipitates of dissociated insulin B chains. In the control, human thioredoxin was used to reduce insulin. Fig. 18 shows that hSco1p(C) and hSco2p(C) are not active as a disulfide reductase.

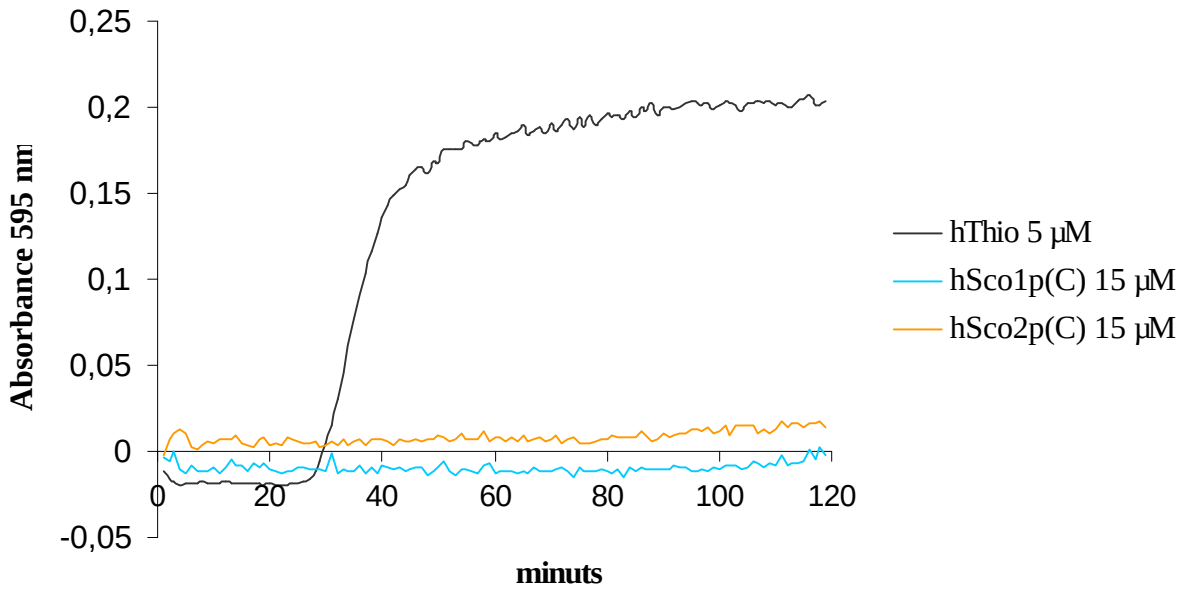

Fig. 18. Thioredoxin activity of hSco1p(C) and hSco2p(C).
Human thioredoxin (hThio), hSco1p(C) and hSco2p(C) were tested for their ability to reduce insulin. Formation of insoluble insulin B chain was followed at 595 nm for 120 minutes.

3.5.3 Qualitative analysis of copper binding properties of hSco1p(C) and hSco2p(C): atomic emission analysis

Atomic emission spectroscopy allows the analysis of the metal's content of a sample. To test if hSco1p and hSco2p bind copper *in vivo*, the C-terminal portion of hSco2p and hSco1p was purified from *E. coli* grown in medium containing 0,5 mM $CuSO_4$. 60 µg of the purified protein in PBS-DTT were analysed by atomic emission spectroscopy. Copper-specific absorption lines at 324,75 nm and 327,40 nm are clearly visible (Fig. 19). Copper lines from hSco2p(C) are more intensive than from hSco1p(C). However because this method was not performed in a quantitative manner, the question remains open if the two human homologues bind copper with different affinities or different stoichiometries. No other metal-specific lines were present. The absorption lines were less intensive when the protein was isolated from cells grown in a medium without added $CuSO_4$ (data not shown). This observation suggests that under normal growth conditions the copper concentration may be too low to load all hSco proteins with the metal. As negative control PBS-DTT alone and purified GST-Sepharose were analysed. No copper absorption lines were detected.

To test the requirement of the CxxxC motif for copper-binding, hSco1p(C)Δcys and hSco2p(C)Δcys were purified as described previously and 60 µg of the protein were analysed by atomic emission spectroscopy. The two copper-specific signals are detected for hSco2p(C), however their intensities are dramatically lower as compared to the wild type protein. Copper-specific signals are detected for hSco1p(C)Δcys, too, if more protein was analysed (data not shown). This results show that the cysteine residues are involved in copper-binding. The residual copper binding may indicate the involvement of additional amino acids in the binding of copper. Copper can require 3 or 4 ligands, and histidine residues in the C-terminal portion of both proteins could accomplish this function.

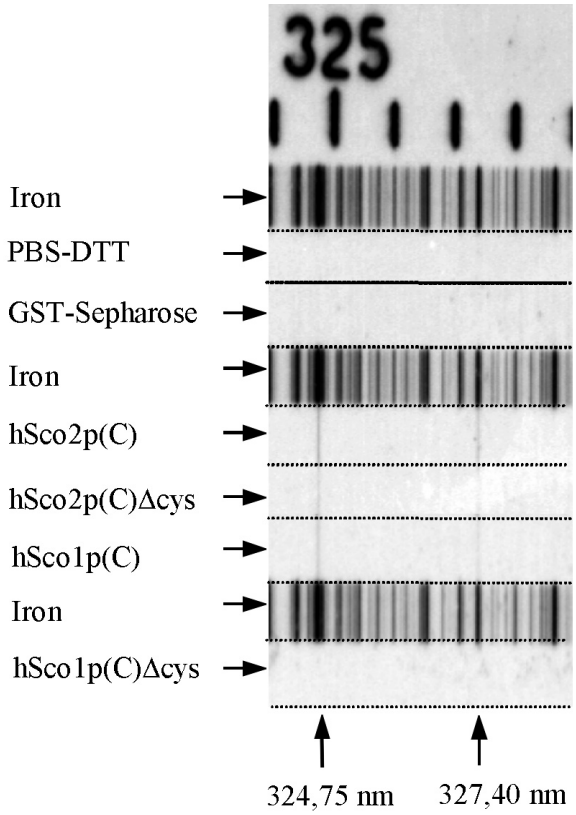

Fig. 19. Atomic emission spectra of wild type and mutant C-terminal portions of hSco1p and hSco2p.

60 µg of purified C-terminal portions of wild type hSco2p, hSco2pΔcys, hSco1p and of hSco1pΔcys were analysed by atomic emission spectroscopy. The spectrum of iron was used as reference and PBS-DTT and GST-Sepharose were used as negative controls. Wavelengths of the copper-specific lines are indicated.

3.5.4 Quantitative analysis of copper binding of hSco1p(C) and hSco2p(C): atomic absorption analysis

To determine the stoichiometry of bound copper in hSco1p and hSco2p *in vivo*, the C-terminal portions of hSco1p, hSco2p and hSco2pΔcys were purified from *E. coli* grown in a medium containing 0,5 mM $CuSO_4$. Bound copper was quantified using atomic absorption spectroscopy. The graphite furnace atomic absorption was used because it is a very sensible method which requires only a small amount of sample for the analysis. In the graphite furnace, the sample is subjected to three heating processes: drying, incineration and atomisation. The duration and the temperature of these processes have been optimised to obtain the best signal/noise ratio. The appropriate temperature programme allowed to analyse the native proteins and to obtain a very good calibration curve in PBS-DTT (Fig. 20). The concentration of the protein was determined using the Bradford method. This method was preferred to the

Lowry method because it is not copper-dependent. Protein calibration was performed with BSA. The protein concentration was calculated from three independent measurements. The stoichiometry of copper binding was shown to be 1 ± 0,2 µmol of copper per µmol of protein for hSco2p(C) and 0,2 ± 0,05 µmol of copper per µmol of protein for hSco2p(C)Δcys in three independent experiments. This result was confirmed by a coupled plasma mass spectrometry (ICP-MS) analysis performed by Dr. H. Hartel (Department of Chemistry, LMU Munich). The purified hSco1p(C) contained 0,6 µmol of copper per µmol of protein as determined in a single experiment. The lower binding capacity of hSco1p(C) compared to hSco2p(C) can reflect a different copper binding stoichiometry, a different affinity of the two proteins to copper or a misfolded recombinant hSco1p(C) protein (see Discussion). Recently it was shown that the C-terminal portion of ySco1p binds copper with a stoichiometry of 1 ± 0,1 µmol copper per µmol of protein, while the C-terminal portion of ySco1pΔcys binds copper with a stoichiometry of 0,15 ± 0,01 µmol copper per µmol of protein [208]. Because a ySco1p/hSco1p chimeric construct, in which the CxxxC motif was derived from the human protein, can complement the Δ*ysco1* strain GR20 (see section 3.7.2.1), it can be expected that hSco1p, too, binds copper with a 1:1 stoichiometry.

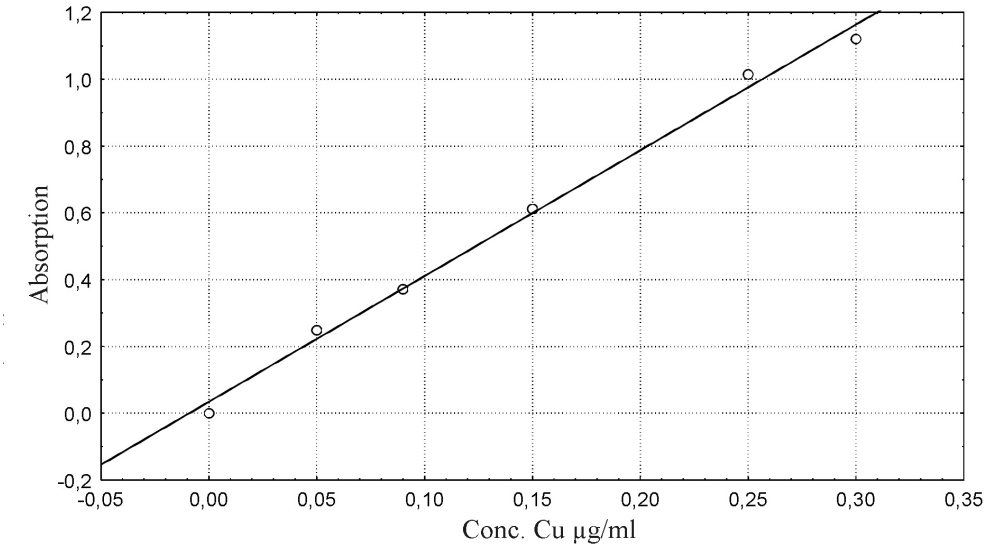

Fig. 20. Calibration curve for the atomic absorption analysis.
Calibration was performed using 0,8 µM, 1,4 µM, 2,4 µM, 4 µM and 4,8 µM copper nitrate in PBS-DTT. Each standard was measured once. Three independent calibration curves were performed.

3.6 Interaction analysis of hSco1p and hSco2p

The functional analysis suggests that Sco proteins are mitochondrial copper chaperones. In the model proposed for yeast, copper is delivered from Cox17p to the Sco proteins in the mitochondrial intermembrane space. Sco proteins then incorporate the copper into Cox2p [84]. According to this model, an interaction between hSco1p and/or hSco2p with hCox17p and Cox2p can be postulated. Moreover, dimerisation of copper transporter has been reported for yCcs [162] and hCcsp [163], and yCox17p forms oligomer complexes [115]. The striking homology between hSco1p and hSco2p suggests that these two proteins may form an heteromeric complex, like Sod1p and its chaperone Ccsp [165, 166]. These interactions were analysed *in vitro* by affinity chromatography and in some cases *in vivo* by coimmunoprecipitation. In the *in vitro* analysis, one of the proteins is expressed as a GST-fusion protein, immobilised on GSH-Sepharose and incubated with cell lysate containing the partner proteins. In the *in vivo* analysis, one protein is immunoprecipitated from a cell lysate containing both partner proteins. In the case of an interaction, the partner protein will be found in the immunoprecipitate. If not specified, both analyses were performed in the presence of 1 mM DTT to avoid unspecific cross-linking by disulfide-bridges. For the analysis of the dimerisation, gel filtration chromatography was also used. Because no antibodies were available against hSco1p, hSco2p and hCox17p, epitope-tagged variants were used in both assays. As epitope tags, EGFP (see section 3.3) and AU5 were used. AU5 is a 6 Aa peptide from the bovine papillomavirus type 1 (BPV-1) [192]. Both tags were placed at the C-terminus of the investigated proteins.

3.6.1 Interaction between hSco proteins and hCox17p

The interaction with hCox17p was tested by affinity chromatography. A C-terminal EGFP-tagged hCox17p was used in the test. The expected molecular mass for hCox17p-EGFP is 34 kDa. GST-hSco2p(C) (Fig. 21 A), GST-hSco1p(C) (Fig. 21 B) and GST (Fig. 21 C) were coupled to GSH-Sepharose and incubated with lysate of HeLa-cells expressing hCox17p-EGFP in the absence of DTT. Sepharose-bound proteins were separated on a 12 % SDS-PAGE, transferred to PVDF membrane and probed with anti-EGFP antibody. As shown in lanes 1, hCox17p-EGFP is bound by GST-hSco1p(C) and GST-hSco2p(C), but only a small amount is bound by GST. The interaction between copper chaperones can be copper-dependent [151, 154]. To test this eventuality, the GST fusion proteins were loaded with

copper before incubation with the cell lysate containing hCox17p-EGFP. Lanes 2 show that hCox17p-EGFP is bound in a copper-dependent manner. If the interaction was performed in the presence of DTT, almost no interaction could be detected (lanes 3).

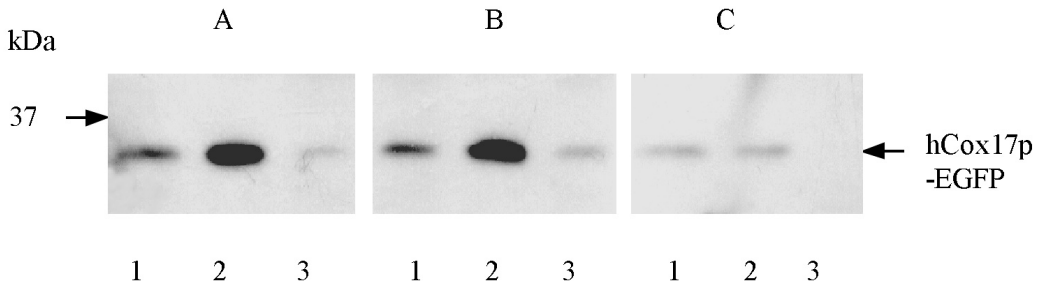

Fig. 21. *In vitro* interaction with hCox17p.
GST-hSco1p(C) (**A**), GST-hSco2p(C) (**B**), and GST (**C**) were bound to GSH-Sepharose and incubated with cells lysate from HeLa cells expressing hCox17-EGFP. Lane 1: Sepharose-bound proteins were not loaded with copper. Lane 2: Sepharose bound proteins were loaded with copper. Lane 3: Sepharose bound proteins were loaded with copper and the interaction was performed in the presence of 1 mM DTT. Western blot analysis of the precipitates was done with anti-EGFP antibody.

3.6.2 Interaction between hSco proteins and Cox2p

In accordance with the proposed function of Sco proteins as chaperones for the assembly of Cox2p, an interaction between Sco1p and/or Sco2p with Cox2p can be postulated. This interaction has been reported for ySco1p [104] and ySco2p [203]. To test this possibility, affinity chromatography was performed. GST-hSco1p(C) (Fig.22 A, lane 1), GST-hSco2p(C) (Fig.22 B, lane 1) and GST alone (Fig.22 A, B, lane 2) were coupled to GSH-Sepharose and incubated with mitochondrial lysate of HeLa cells. Bound material was analysed by Western blot with anti-Cox2p antibody. No interaction was detected. To test if the interaction is copper-dependent, GST-hSco1p(C) and GST-hSco2p(C) were loaded with copper before the incubation with mitochondrial lysate (lanes 3). Again no interaction was detected.

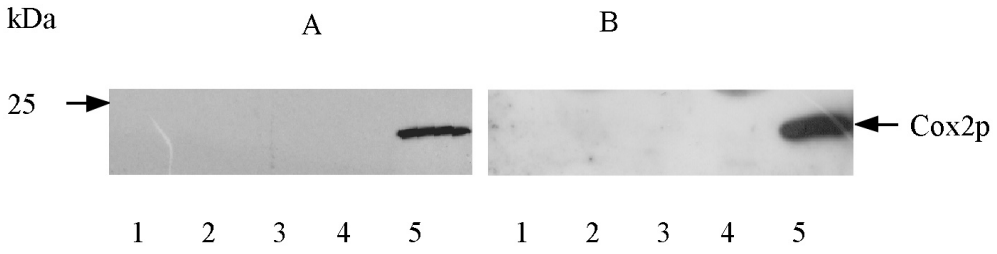

Fig. 22. *In vitro* interaction between hSco1p and Cox2p and between hSco2p and Cox2p.
A. GST-hSco1p(C) (lane 1) or GST-hSco1p(C) loaded with copper (lane3) were bound to GSH-Sepharose and incubated with mitochondrial lysate of HeLa cells (lane 5). As control GST (lane 2) or GST loaded with copper (lane 4) were incubated with mitochondrial lysate. **B**. GST-hSco2p(C) (lane 1) or GST-hSco2p(C) loaded with copper (lane 3) were bound to GSH-Sepharose and incubated with mitochondrial lysate (lane 5). As control GST (lane 2) or GST loaded with copper (lane 4) were incubated with mitochondrial lysate. Western blot analysis was performed with anti-Cox2p antibody.

The interaction with Cox2p was tested also with coimmunoprecipitation. hSco1p-EGFP and hSco2p-EGFP were immunoprecipitated with anti-EGFP antibody from lysate of HeLa cells expressing the two EGFP fusion constructs, respectively. As a negative control, immunoprecipitation with anti-EGFP antibody was performed from lysate of HeLa cells expressing EGFP alone. Immunoprecipitates were analysed with anti-Cox2p antibody. Fig. 23 shows that a weak Cox2p band was detected only in the precipitate of hSco1p-EGFP-expressing cells (lane 2) but not in hSco2p-EGFP-expressing cells (lane 3) or in the control (lane 4)

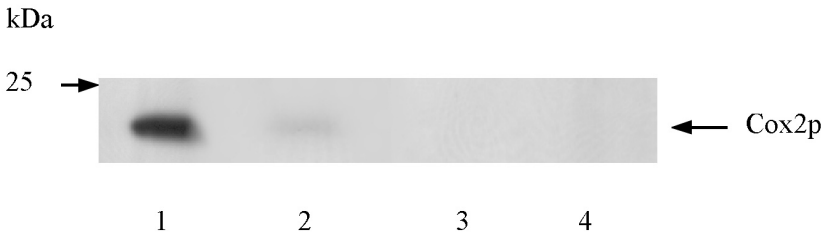

Fig. 23. Coimmunoprecipitation of hSco1p, hSco2p and Cox2p.
Mitochondrial lysate from HeLa cells expressing hSco1p-EGFP (lane 2), hSco2p-EGFP (lane 3) or EGFP (lane 4) was immunoprecipitated with anti-EGFP antibody. In lane 1 mitochondrial lysate of untransfected HeLa cells was loaded. Western blot analysis of the precipitates was done with anti-Cox2p antibody.

3.6.3 Homomerisation of hSco1p and hSco2p

The ability of the C-terminal segment of hSco1p and hSco2p to form homomeric complexes was tested by affinity chromatography. hSco2p(C) fused to GST was coupled to GSH-Sepharose and incubated with cell lysate of HeLa transformants expressing a hSco2p-EGFP fusion protein. Sepharose-bound material was analyzed in Western blot with antibody against EGFP. Fig. 24 A shows that hSco2p-EGFP is bound to GST-hSco2p(C)-Sepharose (lane 1), but not to GST-Sepharose (lane 3). In a further control, Sepharose-bound GST-hSco2p(C) was incubated with cell lysates containing EGFP. Again no binding was observed (data not shown). Similar results were obtained if GST-hSco1p(C) was incubated with lysate of Hela cells expressing hSco1p-EGFP (Fig. 24 B). hSco1p-EGFP is bound by GST-hSco1p(C) (lane 1), but not by GST alone (lane 3).

To test whether the CxxxC motif is required for homomerisation, GST-hSco1p(C) and GST-hSco2p(C) were bound to Sepharose and incubated with hSco1pΔcys-EGFP (Fig. 24 A, lane 2) and hSco2pΔcys-EGFP, respectively (Fig. 24 B, lane 2). The results show that the interaction does not depend on the CxxxC motif.

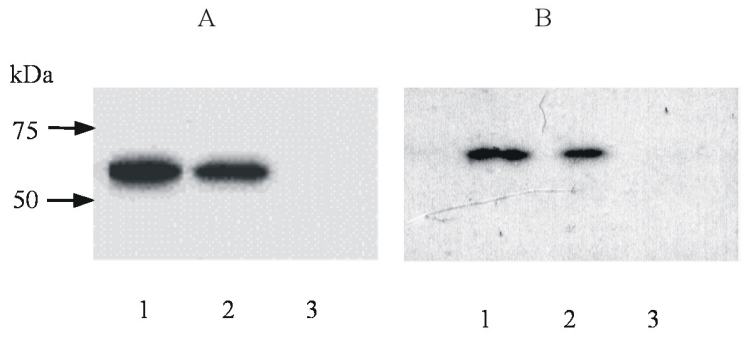

Fig. 24. Homomerisation of hSco2p and hSco1p.
A. GST-hSco2p(C) was bound to GSH-Sepharose and incubated with lysate of HeLa cells expressing hSco2p-EGFP (lane 1) or hSco2pΔcys-EGFP (lane 2). In lane 3, GST was bound to GSH-Sepharose and incubated with lysate of HeLa cells expressing hSco2p-EGFP. **B**. GST-hSco1p(C) was bound to GSH-Sepharose and incubated with lysate of HeLa cells expressing hSco1p-EGFP (lane 1) or hSco1pΔcys-EGFP (lane 2). In lane 3, GST was bound to GSH-Sepharose and incubated with lysate of HeLa cells expressing hSco1p-EGFP. Western blot analysis of the precipitates was done with anti-EGFP antibody.

3.6.4 Heterodimerisation between hSco1p and hSco2p

The interaction between hSco1p and hSco2p was tested by affinity chromatography and by immunoprecipitation. In the first test, GST-hSco2p(C) was coupled to GSH-Sepharose and incubated with lysate of HeLa cells expressing hSco1p-EGFP (Fig. 25, lane 1). In a parallel experiment, GST-hSco1p(C) was coupled to GSH-Sepharose and incubated with lysate of cells expressing hSco2p-EGFP (Fig. 25, lane 2). Sepharose-bound proteins were analysed by immunoblotting with anti-EGFP antibody. The results show that hSco1p and hSco2p are able to interact *in vitro*.

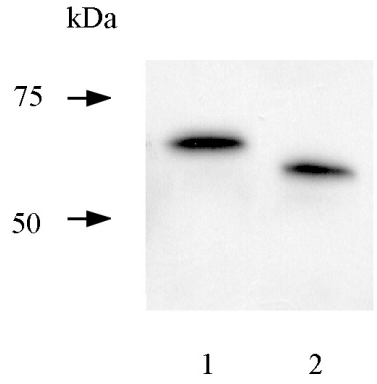

Fig. 25. Interaction between hSco1p and hSco2p.
hSco2p-GST was coupled to GSH-Sepharose and incubated with lysate of HeLa cells expressing hSco1p-EGFP (lane 1). hSco1p-GST was coupled to GSH-Sepharose and incubated with lysate of cells expressing hSco2p-EGFP (lane 2). Western blot analysis of the precipitates was performed with anti-EGFP antibody.

This result was confirmed by coimmunoprecipitation. hSco1p-AU5 was immunoprecipitated with anti-AU5 antibody from lysate of HeLa cells expressing hSco1p-AU5 and hSco2p-EGFP. As negative control, immunoprecipitation with anti-AU5 antibody was performed from HeLa cells lysate containing only hSco2p-EGFP. Immunoprecipitate was analysed with antibody against EGFP produced in rabbit to avoid the detection of the light and heavy chain of the AU5 antibody. Fig. 26 shows that the hSco2p-EGFP band was detected in the precipitate of hSco1p-AU5 expressing cells (lane 1), but not in the control (lane 2).

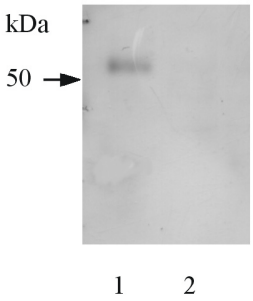

Fig. 26. Coimmunoprecipitation of hSco1p and hSco2p.
Cell lysate containing hSco1p-AU5 and hSco2p-EGFP (lane 1) or hSco2p-EGFP (lane 2) was immunoprecipitated with anti-AU5 antibody. Western blot analysis of the precipitates was done with anti-EGFP antibody.

.

3.6.5 FPLC analysis of hSco1p(C) and hSco2p(C)

The ability of the C-terminal portion of hSco1p(C) and hSco2p(C) to form dimers was also tested with analytical gel filtration. hSco1p(C) and hSco2p(C) were affinity-purified as described in section 3.5.1 and 500 µg purified proteins were loaded on a Sephadex 75 HR 10/30 column. Proteins were eluted in PBS-DTT at room temperature. The most part of hSco2p(C) elutes as a monomer, hSco1p(C) elutes as a 1:1 mixture of the monomeric and dimeric form (Fig. 27). No other proteins peaks have been detected, confirming the high purity of the affinity-purified proteins. As molecular mass marker, carbonic anhydrase (29 kDa) and BSA (66 kDa) were used.

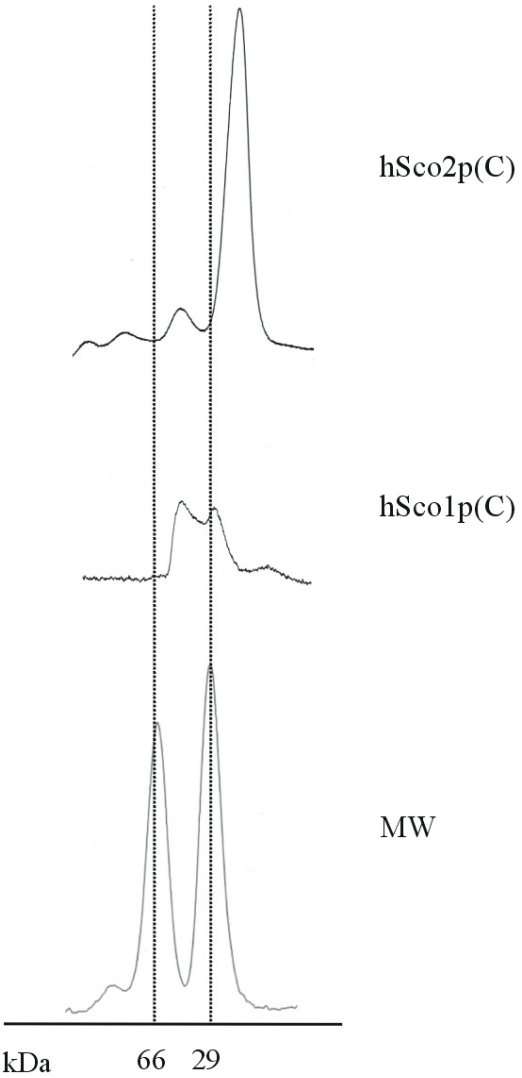

Fig. 27. Elution profile of hSco1p(C) and hSco2p(C) on gel filtration column.
hSco2p(C) and hSco1p(C) were chromatographed in PBS-DTT under the same conditions. The column was calibrated with molecular weight standards (MW) of 66 kDa and 29 kDa.

3.7 Characterisation of pathogenic mutant proteins

The yeast system offers a wide spectrum of molecular genetic manipulation and has been repeatedly used for analysing human mutations [40, 80, 81, 92]. Because the *hSCO2* gene can not substitute for the *ySCO1* gene and the deletion of the *ySCO2* gene does not result in a phenotype, information about the role of the hSco2p mutations can be deduced only indirectly from the yeast model for example by introducing the mutations in ySco1p [92]. To characterise the role of the hSco2p mutations, analyses in HeLa cells and with the purified mutant proteins were performed. hSco1p can substitute ySco1p in chimeras and the yeast model was used to test the effect of the reported mutation on COX assembly.

3.7.1 Characterisation of pathogenic hSco2 mutant proteins

Compound heterozygotes for mutations in *hSCO2* suffer from a fatal form of cardioencephalomyopathy [95, 109, 110]. Three point mutations have been identified so far. In this work, attention was focused on the E140K mutation and on the S225F mutation. In the yeast system only one of the two missense mutations (S225F), introduced in ySco1p, had a strong effect on COX-activity and COX-assembly, while the other (E140K) did not impair COX-activity [92]. To elucidate the mechanisms, by which the two mutations affect the function of hSco2p, the intracellular localisation, the copper binding and the homomerisation were analysed. The mutations were introduced into *hSCO2* by site-directed mutagenesis. C-terminal-EGFP tagged versions of the two mutant proteins were created. The C-terminal portions (Aa 79-266) of hSco2p(E140K) (hSco2p(C)(E140K)) and hSco2p(S225F) (hSco2p(C)(S225F)) were purified as described for the wild type hSco2p(C). Fig. 28 shows that a fragment of the expected molecular mass of 22 kDa was obtained, like the wild type hSco2p(C) (see section 3.5.1). The amount of purified hSco2p(C)(E140K) was somewhat reduced (Fig. 28 A). This can hint at an effect of the mutation on the stability of the protein.

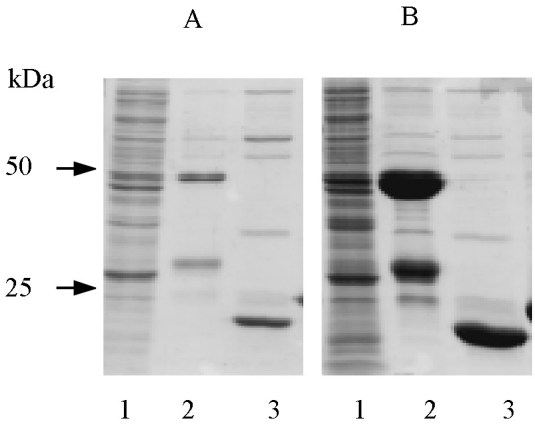

Fig. 28. Purification of the C-terminal portions of mutant hSco2 proteins.
hSco2p(C)(E140K) (**A**) and hSco2p(C)(S225F) (**B**) were expressed in BL21 and purified by affinity chromatography. Lane 1, supernatant after cell lysis prior to incubation with GSH. Lane 2, GSH-Sepharose bound GST-fusion protein. Lane 3, purified protein after cleavage with thrombin.

3.7.1.1 Mutant proteins localise to mitochondria

HeLa cells expressing hSco2p(E140K)-EGFP (Fig. 29) or hSco2p(S225F)-EGFP (Fig. 30) were analysed by fluorescence microscopy. Both mutant proteins are targeted to mitochondria as revealed by counterstaining with the mitochondria-specific stain MitoTracker® Red CMXRos. Therefore, mislocalisation due to the mutations can be excluded. The localisation was confirmed by Western blot analysis. Mitochondrial and cytosolic fractions of HeLa cells expressing hSco2p(E140K)-EGFP or hSco2p(S225F)-EGFP were prepared and probed with anti-EGFP and anti-Cox2p antibodies. A band of the expected molecular mass was observed only in the mitochondrial fraction of both constructs (data not shown).

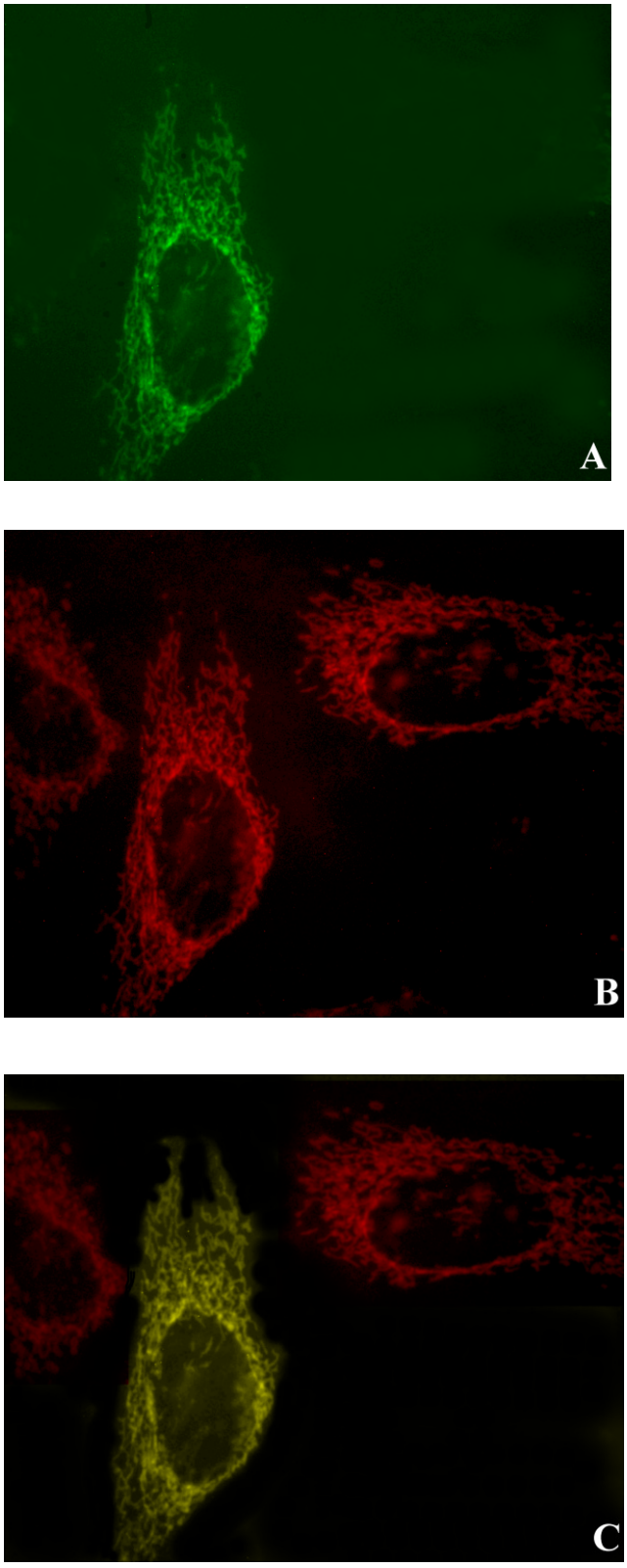

Fig. 29. Intracellular localisation of hSco2p(E140K)-EGFP.
The coding region of hSco2p(E140K) was fused to *EGFP*, the resulting plasmid transfected into HeLa cells, and transfectants were visualised by fluorescence microscopy. Mitochondria were counterstained with MitoTracker® Red CMXRos. **A**. Green fluorescence. **B**. Red fluorescence. **C**. Overlay of green and red fluorescence.

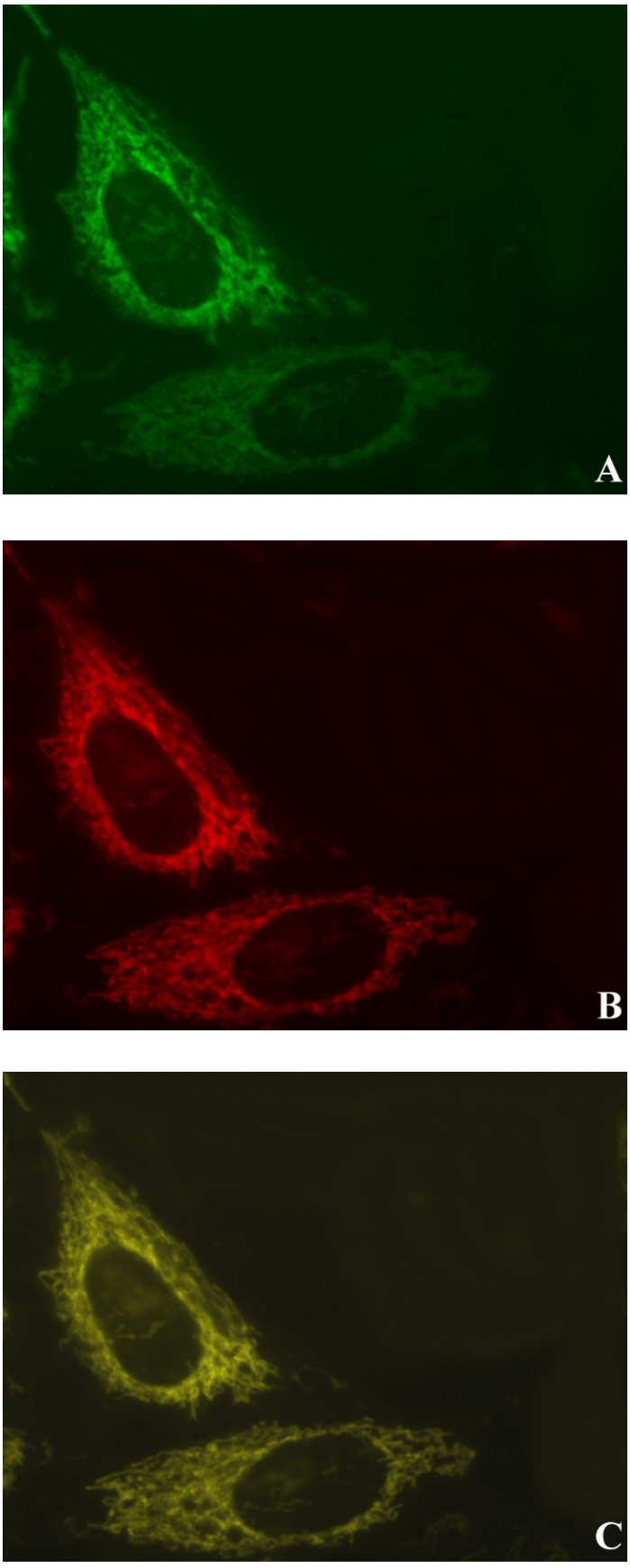

Fig. 30. Intracellular localisation of hSco2p(S225F)-EGFP.
The coding region of hSco2p(S225F), was fused to EGFP, the resulting plasmid transfected into HeLa cells, and tranfectants were visualised by fluorescence microscopy. Mitochondria were counterstained with MitoTracker® Red CMXRos. **A**. Green fluorescence. **B**. Red fluorescence. **C**. Overlay of green and red fluorescence.

3.7.1.2 Copper binding of mutant proteins

One of the mutations, E140K, is located next to the metal-binding motif. The other mutation, S225F, is located next to a conserved histidine which was discussed as copper binding site [179] and which was shown to be essential for the protein function [104, 179]. Purified hSco2p(E140K)(C) and hSco2p(S225F)(C) from *E. coli* grown in 0,5 mM $CuSO_4$ were subjected to atomic emission spectroscopy. Fig. 31 shows that both mutant proteins are still able to bind copper. However the exact stoichiometry of the bound copper has still to be analysed.

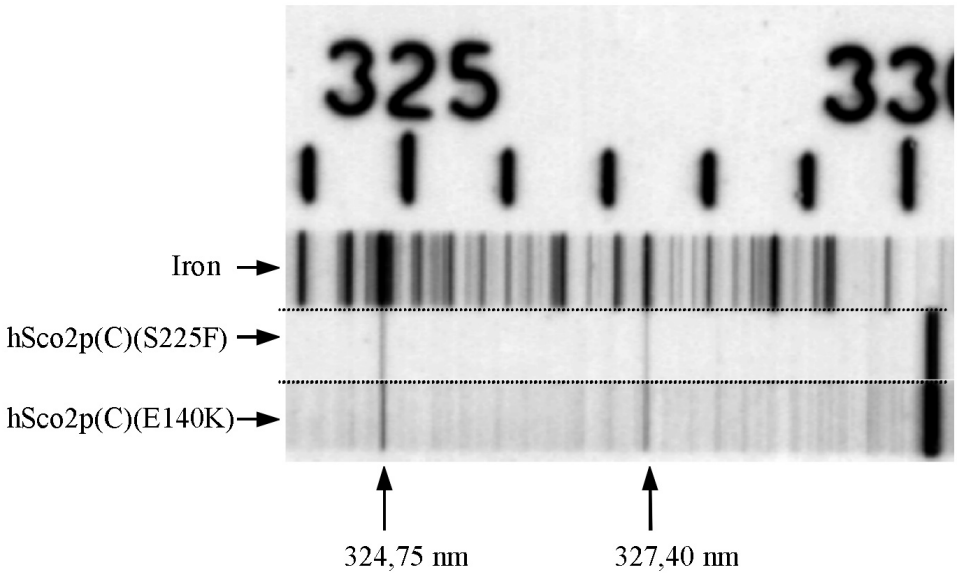

Fig. 31. Atomic emission spectrum of the C-terminal portions of hSco2p mutants.
60 µg of purified C-terminal portions of hSco2p(S225F) and of hSco2p(E140K) were analysed by atomic emission spectroscopy. The spectrum of iron was used as reference. Wavelengths of the copper-specific lines are indicated.

3.7.1.3 Mutant proteins can homomerise

The mutant proteins were also tested for their ability to homomerise. The C-terminal segments of hSco2p(E140K) (Fig 32 A, lane 1) and hSco2p(S225F) (Fig 32 A, lane 2) were bound as GST-fusions to GSH-Sepharose and tested for interaction with hSco2p-EGFP. In a parallel assay wild type hSco2p(C)-GST was coupled to GSH-Sepharose and tested for binding to hSco2p(E140K)-EGFP (Fig 32 B, lane 1) and to hSco2p(S225F)-EGFP (Fig 32 B, lane 2). Both mutant proteins are able to form homomeric complexes. This result shows that the mutations do not affect the homomerisation.

To mimic the situation in patients, who present with two independent *hSCO2* mutant alleles, the interaction between hSco2p(E140K) and hSco2p(S225F) was determined using GST-hSco2p(C)(S225F) and hSco2p(E140K)-EGFP (Fig. 32 B, lane 3). Again the formation of homomeric complexes by the mutant proteins was observed.

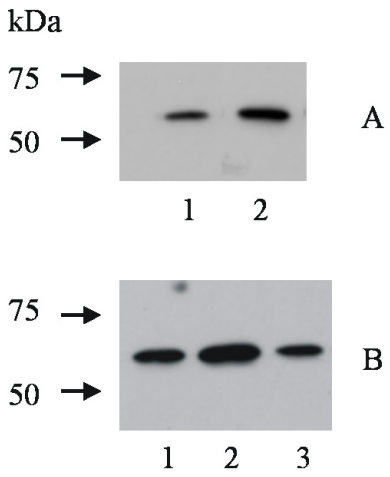

Fig. 32. Homomerisation of hSco2 mutant proteins.
A. GST-hSco2p(C)(E140K) (lane 1) and GST-hSco2p(C)(S225F) (lane 2), were bound to GSH-Sepharose and incubated with lysate of HeLa cells expressing hSco2p-EGFP. **B**. GST-hSco2p(C) was bound to GSH-Sepharose beads and incubated with lysate of HeLa cells expressing hSco2p(E140K)-EGFP (lane 1) and hSco2p(S225F)-EGFP (lane 2). In lane 3, GST-hSco2p(C)(S225F) was bound to GSH-Sepharose and incubated with lysate of HeLa cells expressing hSco2p(E140K)-EGFP.

3.7.2 Characterisation of the pathogenic hSco1p mutant

Recently it was reported that mutations in the *hSCO1* gene may result in COX-deficiency. A substitution of proline at position 174 by leucine (P174L) was detected in compound heterozygous patients suffering from hepatic failure and ketoacidotic coma [108]. However, direct experimental proof for the pathogenicity of this mutation was lacking. Because the authentic human gene is not capable to complement a Δ*ysco1* strain, yeast/human chimeric constructs were used to test the effect of this mutation on mitochondrial function in yeast. To this purpose, two novel chimeric proteins were created. In both proteins the C-terminal portion derived from hSco1p included the CxxxC motif.

3.7.2.1 Complementation of yeast/human Sco1p chimeras K1 and K2

Two novel chimeric *SCO1* genes which differ in the carboxyl-terminal portion derived from the human *hSCO1* gene were constructed and cloned in YEp351 behind the *ySCO1* promoter (Fig. 33). In chimera K1 (ySco1p(1-134)/hSco1p(156-301)) the human portion comprises 145 amino acids, while in chimera K2 (ySco1p(1-117)/hSco1p(139-301)) 162 amino acids stem from the human protein. In both chimeric proteins the conserved CxxxC-motif is derived from hSco1p. Each of the proteins was expressed in the respiratory deficient Δ*ysco1* strain GR20 and the transformants were tested for their ability to grow on the non-fermentable carbon source glycerol at three temperatures (23°C, 30°C, 37°C) (Fig. 34). K2-transformants show a faint cold-sensitive phenotype: at 30°C and 37°C they grow like wild type cells, while their growth is somewhat reduced at 23°C. K1-transformants exhibit a strong temperature-sensitive effect, they grow only at 30°C. Addition of 0.2 % copper sulphate to YPEG plates resulted in a wild type-like growth of all transformants at all temperatures (Fig. 34).

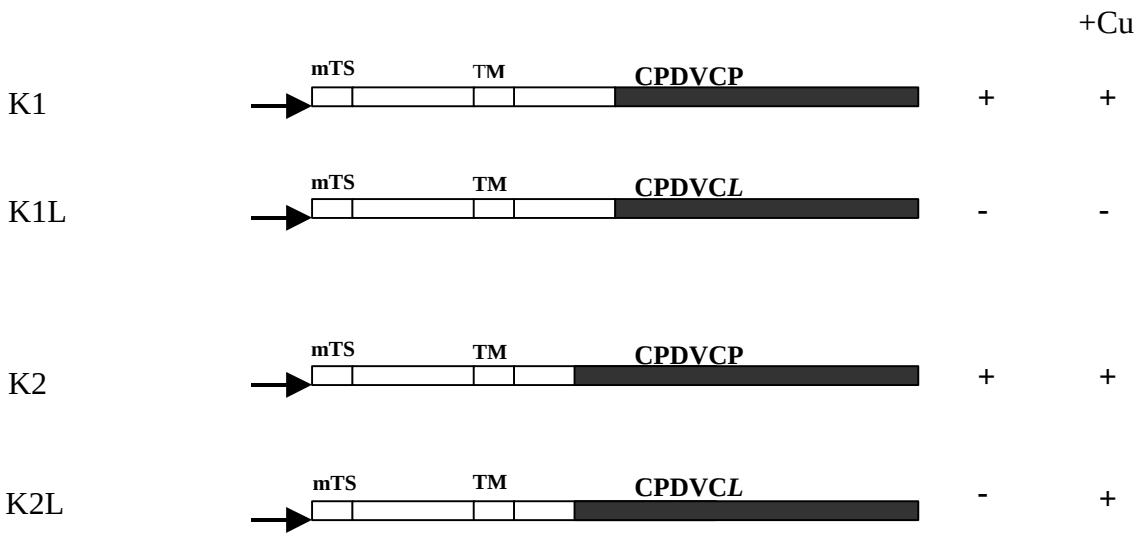

Fig. 33. Yeast/human Sco1p chimeras created to test the effect of the P174L mutation.
The arrow indicates the *ySCO1* promoter, mTS the mitochondrial presequence, TM the transmembrane domain, CPDVC the potential metal-binding site. Mutated amino acids are shown in Italics. Sequences derived from ySco1p are given in white, those from hSco1p in dark. Growth of GR20 transformants on YPGly or YPGly supplemented with 0,2 % $CuSO_4$ (+ Cu) at 30° are indicated on the right: + = growth, - = no growth.

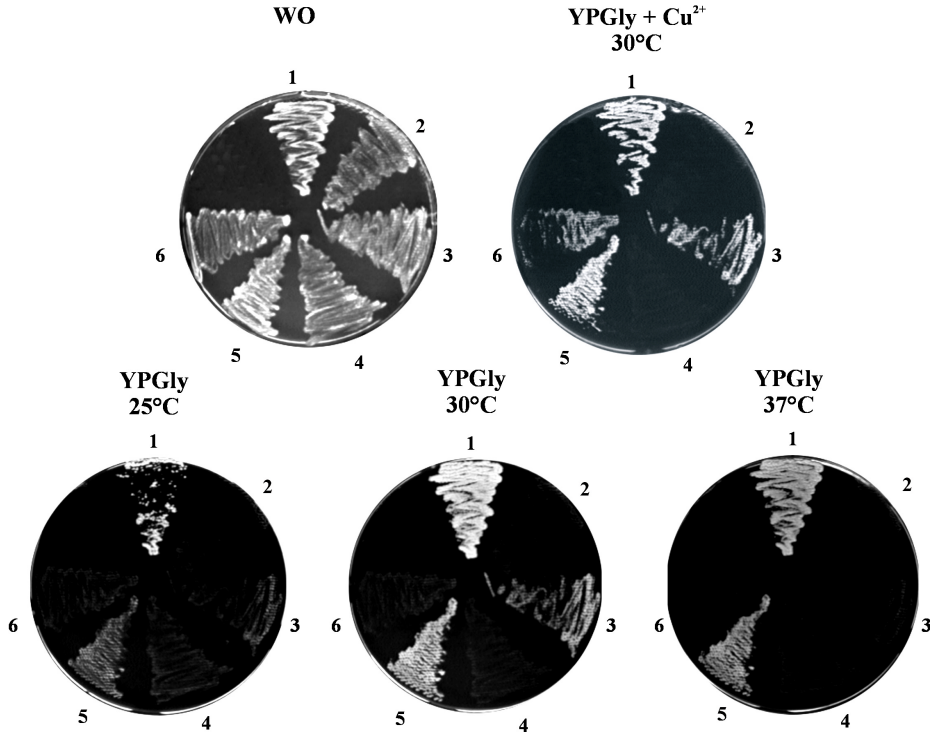

Fig. 34. Effect of the P174L mutation on the complementation behaviour of yeast/human Sco1p constructs in strain GR20.
Δy*sco1* strain GR20 was transformed with YEp351 (2) or with plasmids encoding ySco1p (1), K1 (3), K1L (4), K2 (5) or K2L (6). Growth on minimal medium (WO) and glycerol medium (YPGly) or glycerol medium supplemented with 0,2 % $CuSO_4$ (YPGly + Cu^{2+}) was monitored after 3 days incubation at the indicated temperatures.

3.7.2.2 The P174L mutation impairs the function of the chimeras K1 and K2

The P174L mutation was introduced into chimeras K1 and K2 with directed mutagenesis. The resulting mutant chimeras K1L and K2L, respectively, were expressed in strain GR20 and the transformants were tested for their respiratory competence at 23°C, 30°C and 37°C (Fig. 34, (4) and (6)). All transformants failed to grow on glycerol medium, indicating that the mutant Sco-proteins are non-functional. Addition of copper sulphate to the YPGly plates resulted in a wild-type like growth of K2L-transformants, whereas K1L-transformants still failed to grow. These data show, that the P174L mutation is pathogenic in the yeast model and strongly suggest that this mutational alteration may also be refractive for the function of the human hSco1p.

To test whether the pathogenic nature of the mutation results from an instability of the mutant proteins, mitochondria from the respective transformants were analysed for the presence of the chimeric proteins. As shown in Fig. 35 all chimeric proteins are present in comparable concentrations with the exception of construct K1L, the quantity of which is somewhat reduced (lane 4). It seems unlikely that this reduction in the concentration can account for the complete loss of function. Therefore, the inability of the mutant proteins to complement strain GR20 does not result from instability, but rather from an impaired function.

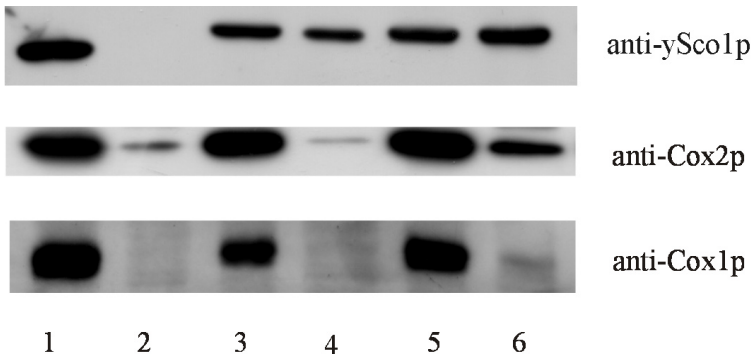

Fig. 35. Influence of the P174L mutation on COX assembly.
10 µg of mitochondrial proteins were separated on a 12 % polyacrylamide gel, transferred to PVDF membrane and probed with antibodies directed against ySco1p, Cox1p and Cox2p. The Δy*sco1* strain GR20 was transformed with the vector YEp351 (lane 2) or with plasmids encoding ySco1p (lane 1), K1 (lane 3), K1L (lane 4), K2 (lane 5) or K2L (lane 6).

3.7.2.3 COX assembly is disturbed in strain GR20 expressing chimeras K1L or K2L

As described in the Introduction, lack of ySco1p results in the preferential degradation of unassembled subunits Cox1p and Cox2p. The concentration of these subunits was determined in GR20 cells, which express chimeras K1L or K2L. Mitochondria obtained from GR20 cells, transformed with K1, K1L, K2, or K2L were analysed with antibodies directed against Cox1p or Cox2p. As shown in Fig. 35, there is a very good correlation between the steady state concentration of Cox1p and Cox2p and the COX activity: in K1- and K2-transformants both subunits are present in concentrations similar to those of wild type cells (lanes 3 and 5). By contrast, the two COX-subunits are almost completely absent in K1L-transformants (lane 4) or only present in trace amounts in K2L-transformants (lane 6).

3.7.2.4 COX activity is affected by the P174L mutation

Mitochondria were prepared from strain GR20, expressing chimeras K1, K1L, K2, or K2L, and assayed for COX activity as described in Material and Methods. Fig. 36 summarises the results. As expected there is almost no COX-activity in the Δ*ysco1* strain GR20 (1,5 % of wild type activity, lane 2). After expression of chimeras K1 or K2, the COX-activities are 55 % (lane 3) and 85 % (lane 5), respectively, of the wild type activity. These data correlate well with the growth characteristics of the transformants on YPGly: growth of K2-transformants on YPGly is almost indistinguishable from that of wild type cells, while growth of K1-transformants is more severely affected. Expression of the chimeric proteins with the P174L mutation results in a dramatic reduction of COX activity to 2,5 % in the case of K1L (lane 4) and to 30 % in the case of K2L (lane 6). Again these data correlate well with the growth phenotype of the transformants on YPGly.

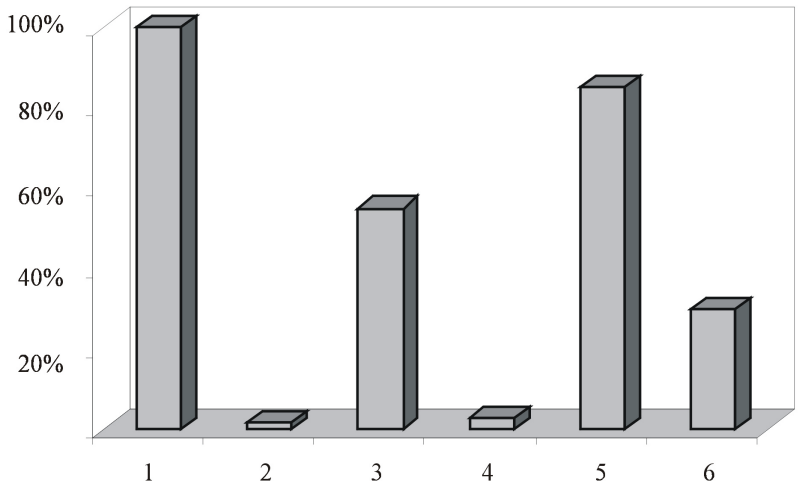

Fig. 36. COX activity in strains expressing wild type ySco1p or ySco1p/hSco1p chimeras.
Mitochondria were isolated and cytochrome *c* oxidase activity was determined. Activities are mean values of several independent experiments and are normalized to the value obtained for the transformant expressing wild type ySco1p (= 200 nmol cytochrome *c* oxidised/min/mg mitochondrial protein). The Δ*ysco1* strain GR20 was transformed with the vector YEp351 (lane 2, negative control) or with plasmids encoding ySco1p (lane 1, positive control), K1 (lane 3), K1L (lane 4), K2 (lane 5) or K2L (lane 6).

4 DISCUSSION

4.1 Structural analysis and localisation of hSco proteins

hSco1p and hSco2p belong to the family of Sco proteins, conserved from prokaryotes to eukaryotes. The best characterised Sco proteins are from the yeast *Saccharomyces cerevisiae*. ySco1p has a tripartite structure with a single transmembrane segment (TM) which anchors the protein in the inner mitochondrial membrane (IM), a minor aminoterminal part, which is oriented to the mitochondrial matrix [103], and a major carboxylterminal part, which is exposed to the mitochondrial intermembrane space (IMS) and which carries the conserved CxxxC motif. The structure of both human proteins is similar to that of the yeast protein. Computer analysis predicts a N-terminal import signal and a transmembrane domain, the CxxxC motif is present. The mitochondrial localisation of both human proteins was demonstrated in this work by two methods. *hSCO1* and *hSCO2* were fused C-terminally with *EGFP* and the localisation of the resulting fusion proteins was observed *in vivo* in HeLa cells with fluorescence microscopy. In both cases the EGFP-fluorescence pattern hints at a mitochondrial localisation, because it is the same as in the cells stained with a mitochondria-specific dye. Western blot analysis of the EGFP-fusion proteins confirms the mitochondrial localisation and hints at the existence of a cleavable import sequence. N-terminal cleavable mitochondrial targeting sequences (MTS) represent the most common form of mitochondrial protein import [209]. Other arrangements, however, have been described recently. The mitochondrial DNA-helicase Hmi1p has a cleavable carboxyl-terminal targeting sequence [210]. Bcs1p does not contain a N-terminal targeting sequence. A positively charged segment of amino acids which is located immediately C-terminal to the transmembrane domain acts as an internal targeting signal. This sequence co-operates with the transmembrane domain to form a tight hairpin loop structure which is translocated across the inner membrane. This mechanism of import and sorting of Bcs1p is proposed to represent a more general mechanism used by a number of inner membrane proteins [211]. Interestingly a similar cluster of positive residues is present in Sco proteins and it was shown that ySco1p without the putative N-terminal MTS is still imported in mitochondria [203]. Moreover, this region was shown to be important for the protein structure [203]. It cannot be excluded that the import of Sco proteins involves the presence of two sorting informations. The cleavable N-terminal presequence therefore would not be essential, but it would enhance the specificity and/or efficiency of import. This

possibility was discussed for the phosphate carrier of mammalian mitochondria [212]. Preliminary experiments using the C-terminal portion of hSco proteins suggest that the human homologues can also be imported in the mitochondria without the N-terminal import signal (data not shown).

The involvement of Sco proteins in the COX deficiency suggests that both proteins are localised in the inner membrane. This localisation was demonstrated so far only for ySco1p [103]. In this case it was also shown that the C-terminal portion of the protein is oriented to the IMS [100]. The importance of the orientation of the protein will be discussed later.

4.2 Complementation analysis in yeast

The ability of hSco proteins to substitute for the yeast homologue was tested in the Δ*ysco1* strain GR20. The human proteins are *per se* not able to complement the GR20 strain. Therefore, either the hSco proteins are not functional homologues or some parts of the yeast protein cannot be replaced from their human counterparts. The N-terminal portion is the most divergent between the Sco homologues. To exclude the possibility that differences in the import machinery between yeast and human led to a mislocalisation of the human constructs in yeast, chimeras were created in which the N-terminal portion and the TM domain were derived from the yeast protein (ySco1p(1-95)/hSco1p(117-301) and ySco1p(1-95)/hSco2p(83-266)). These constructs, too, were not able to complement the GR20 strain. Because the region around the TM was shown to be important for the protein structure [203], further chimeras were created. A construct in which the N-terminal portion, the TM domain, and a part of the C-terminal portion up to the CxxxC motif was derived from ySco1p and the remaining C-terminal portion from hSco1p (ySco1p(1-158)/hSco1p(180-301)) was able to complement. This result suggests that the protein stretch between the TM and the CxxxC motif, encompassing about 60 amino acids, is critical for function in yeast and must - at least in part - be derived from the authentic yeast protein. This idea is supported from studies on ySco1p and ySco2p chimeras [203]. The finding that two novel chimeras, K1 (ySco1p(1-134)/hSco1p(156-301)) and K2 (ySco1p(1-117)/hSco1p(139-301)), in which the C-terminal portion derived from hSco1p was progressively increased, are functional in yeast, allows the restriction of this critical region to a stretch of about 20 amino acids. Possibly this protein part is involved in protein-protein interactions or it is required for the correct steric positioning of functionally important amino acids. Alternatively this part may be involved in protein import as discussed above. Whatever the function of this segment may be, it obviously cannot be provided by the

homologous stretch of hSco1p. Interestingly, chimera K2, in which the hSco1p-derived portion is larger than in chimera K1, seems to be more functional as suggested by the higher COX-activity and the growth characteristic of the respective transformants. This observation may hint at a domain structure of the C-terminal portion of the Sco proteins. Perhaps, formation of a functional three-dimensional structure is favoured, if most or all amino acids of such a domain originate from a single protein. This interpretation is supported by the temperature-sensitive growth phenotype of K1-transformants on YPGly, which may hint at the inability of the protein to correctly fold at 23°C and 37°C, respectively.

Interestingly, in this work no chimeras between ySco1p and hSco2p were found which could suppress the respiratory deficiency of the GR20 strain. Although it cannot be excluded that improper folding of the chimeras interferes with their function in yeast, these data favour the idea that the chromosome 17 homologue, hSco1p, represents the functional ySco1p homologue. The chromosome 22 homologue, hSco2p, could represent the homologue of ySco2p. This result is in agreement with the actual nomenclature proposed by Papadopoulou *et al.* (1999) [95]. Because a Δy*sco2* strain does not show any mutant phenotype [84], it is not possible to test if hSco2p can substitute for ySco2p. Even if hSco2p represents the homologue of ySco2p, it would be expected that a chimera exists which can complement the GR20 strain, as is the case for ySco1p/ySco2p chimeras [203].

Yeast has often been used as a model to analyse human mutations. Yeast provides special advantages for studying mitochondrial proteins because – as a facultative anaerobe - it can grow on fermentable media if the respiratory chain is deficient. Mutations in various mt proteins found by sequencing DNA from patients have been engineered in the corresponding yeast genes to assess the functionality of the mutant proteins. For example, the pathogenic nature of the N204K mutation in Cox10p was confirmed in this way [80]. Yeast strains with mutations in the *hSURF1* homologue *ySHY1* display inadequate electron transfer between COX and other components of the respiratory chain [81]. Recently complementation study in yeast confirmed the deleterious effect of mutations in *hBCS1L*, a nuclear gene involved in the assembly of complex III [40]. Despite the fact that hSco2p is not a functional homologue of ySco1p, the yeast system can be used to obtain valuable information on the effect of mutations detected in patients. Dickinson *et al*. [92] described the effect of the S225F mutation of *hSCO2* on COX-assembly, when introduced into the homologous y*SCO1* gene. In this work, the yeast system was chosen to analyse the effect of a hSco1p mutation. A substitution of proline at position 174 by a leucine was recently detected in compound heterozygous patients suffering

from hepatic failure and ketoacidotic coma [108]. However, direct experimental proof of the pathogenicity of this mutation was lacking. Because the authentic human gene is not capable of complementing the Δ*ysco1* strain, the K1 and K2 yeast/human chimeric constructs, in which the CxxxC motif is provided by the human homologue, were used to test the effect of this mutation on mitochondrial function in yeast. The P174L mutation was introduced into chimeras K1 and K2 with directed mutagenesis. The resulting mutant chimeras K1L and K2L documented that the P174L mutation severely affects the function of the protein in the assembly of COX. A dramatic reduction in the content of subunits Cox1p and Cox2p, which are known to be susceptible to degradation in case of incorrect assembly [102, 106], was observed. Concomitantly the COX-activity was severely reduced. Interestingly, the effect was less pronounced in transformants expressing chimera K2L: their COX-activity was about 30 % of wild-type activity and in line with this observation residual levels of Cox1p and Cox2p could be detected. This suggests that the mutant protein has retained some of its function. The possible role of this mutation will be discussed later.

4.3 Functional analysis of hSco proteins

ySco1p is essential for mitochondrial respiration. A Δ*ysco1* strain is respiration deficient and spectroscopic analysis shows a selective reduction of cytochrome *a* and a_3, [92] which are localised in COX. Western blot analysis of the COX complexes shows a specific reduction of Cox1p and Cox2p while the other subunits are less affected [102]. The ability of the Δ*ysco1* strain to synthesise the mitochondrial encoded subunits of COX and to accumulate the nuclearly encoded subunits suggests that ySco1p is involved in the assembly pathway [100, 107]. Mutations in the two corresponding human genes also cause severe COX deficiencies. Immunohistochemistry shows a specific reduction of Cox1p and Cox2p in *hSCO2* patients [95]. Besides, the data from this work showed that mutations in hSco1p, if engineered in yeast/human chimeras, lead to a reduction of Cox1p and Cox2p. Therefore, it seems likely that assembly of Cox1p and Cox2p is affected.

Both subunits carry the prosthetic groups essential for COX activity. Cox2p carries two copper ions, Cox1p carries heme *a* and a_3 and a copper ion. The assembly of the heme centre requires Cox10p [118] and mutations in this gene have been detected in patients suffering from tubulopathy and leukodystrophy [80]. Sco proteins are probably not involved in the assembly of the heme centre. This can be deduced from the finding that in yeast, a specific *ySCO1*

mutation leads to a partially assembled COX complex lacking only Cox2p, but showing the absorption bands typical of the heme centres [92].

Since Cox1p and Cox2p are synthesised inside the mitochondria, the 3 copper atoms have to be imported from the cytoplasm. As underlined in the introduction, different evidences implicate that Sco proteins are involved in the assembly of copper centre. Overexpression of ySco1p can compensate for the loss of yCox17p, which acts as a copper shuttle between the cytosol and the mitochondrial intermembrane space [84]. Suppression of a *ycox17* deletion by over-expression of *ySCO1* is more efficient in the presence of an elevated concentration of copper ions in the growth medium [84]. Overexpression of *ySCO2* can also complement the Δ*ycox17* strain, but only in the presence of higher amount of copper. Furthermore, it has been shown in this work that the chimeric construct between ySco1p and hSco1p carrying the P174L mutation can be rescued by addition of copper to YPGly plates. Therefore, Sco proteins are possibly involved in the transfer of copper ions to COX, and COX-subunits lacking copper cannot be correctly assembled and are degraded. Importance of copper in the COX assembly is confirmed by the observation of a decrease of COX level in heart mitochondria of copper-deficient rats, due to a diminished content of assembled protein [213].

Sco proteins could act either as copper chaperones by binding copper and transferring it to COX or as thioredoxins, required to maintain the cysteine residues of the copper binding site in a reduced state. This last function can be postulated only for the Cu_A centre: the two copper atoms of the Cu_A centre are coordinated by two His, one Met, a backbone carbonyl oxygen of Glu, and two bridging Cys residues, while Cu_B is bonded by three His and a Tyr. A schematic representation of both models is given in fig 37.

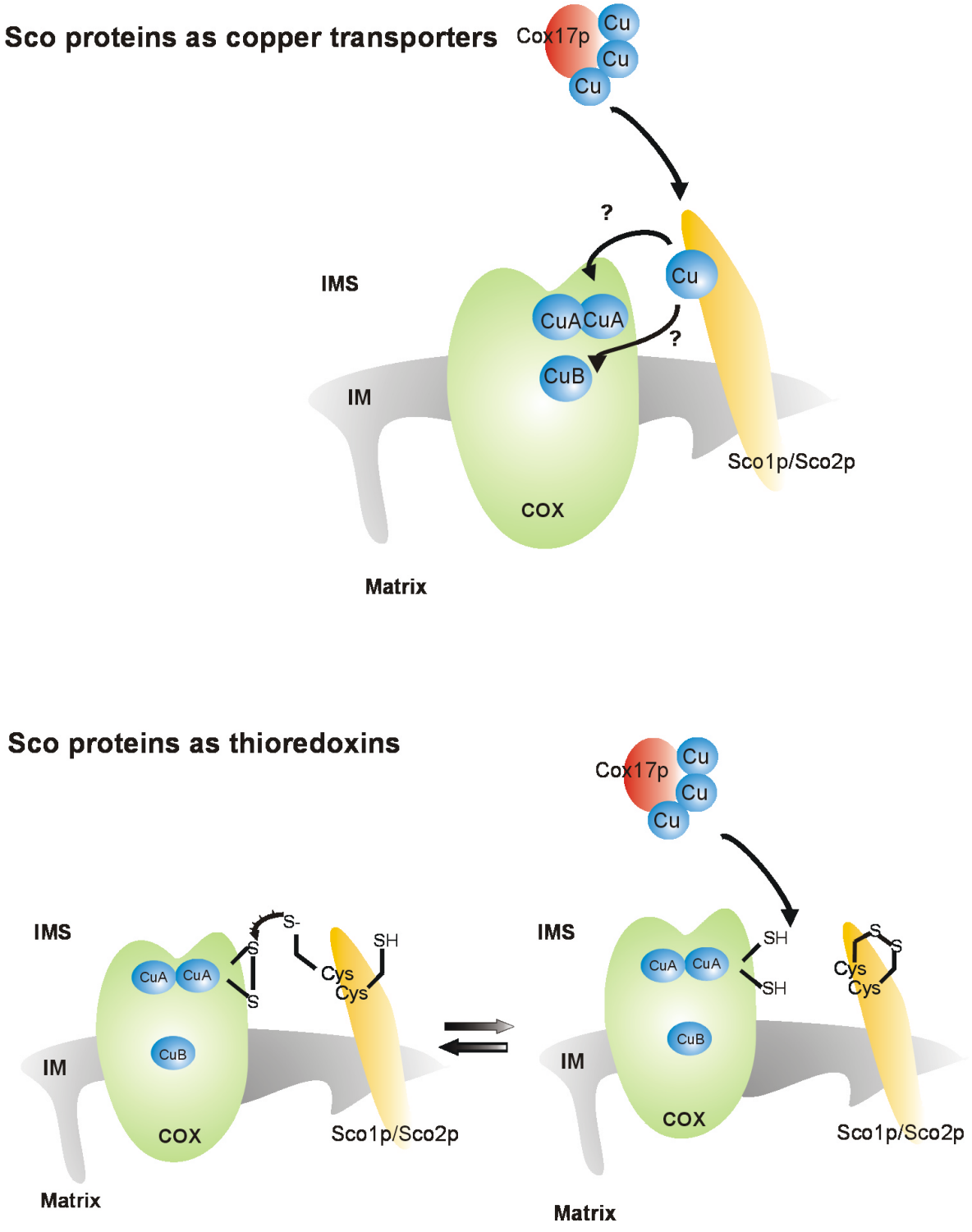

Fig. 37. Two models for the function of Sco proteins.
Sco proteins are involved in the insertion of copper in COX. Sco proteins could perform this function in two ways. In the upper picture, Sco proteins are shown as copper chaperones which acquire copper for example from Cox17p and transfer it to COX. In the lower picture, Sco proteins are shown as thioredoxins which reduce the disulfide bonds of the metal binding motif of COX, permitting the insertion of copper from Cox17p.

4.3.1 hSco proteins bind copper

To fulfil the role of copper chaperones, Sco proteins must be able to bind copper. In this work it has been shown that hSco2p and hSco1p bind copper with two different analyses, the atom emission spectroscopy and the atom absorption spectroscopy. To analyse copper binding, the C-terminal portions of both proteins were purified with affinity chromatography in PBS-DTT by using the GST system. The reducing condition was chosen to assure the specificity of copper binding. In the case of hCcsp it was shown that the protein contains copper sites in excess in an aerobic (oxidising) environment but approaches the expected ratio of 2 coppers per protein under reducing conditions [164]. Proteins derived from a further purification step with gel exclusion chromatography were not used for the analysis because it was observed that multiple purification steps reduce the metal content of the protein. The atomic emission spectroscopy performed in this work shows that hSco proteins specifically bind copper. No other metals could be identified in the proteins purified from bacteria grown without addition of copper in the medium. To determine metal binding specificity of hSco proteins other methods could be used, like metal-chelate chromatography on resin equilibrated with different heavy metals [48]. The specific affinity for copper reflects the inability of the metal binding site of the domain to conform to the preferred ligation geometry of other metals. Treatment of the fusion protein, eluted from the glutathione affinity column in the absence of DTT, with the Cu(I) specific chelator BCS gives an orange colour indicative of the $Cu(I)(BCS)_2^-$ complex (data not shown). This suggests that copper is bound in the +1 oxidation state. The +1 oxidation state of copper has been so far described for all copper chaperones.

With the atomic absorption analysis hSco2p was shown to bind copper with a stoichiometry of 1:1 (copper : protein) and hSco1p with a stoichiometry of 0,6:1 (copper : protein). The putative copper binding site CxxxC is present only once and a 1:1 stoichiometry is expected for both proteins. Other copper chaperones like hHah1p and yAtx1p contain one copper binding motif CxxC and were shown to bind one copper ion. WND and MNK contain each six copper binding motif and bind 6 copper ions.

The lower copper binding of hSco1p can have different reasons. First, it is possible that hSco1p binds copper as a dimer, with one copper ion bound by four cysteines. The FPLC analysis shows that the C-terminal portion of hSco1p exists as a mixture of monomers and dimers. In this work the copper content was measured without separating the monomer form from the dimer form. Second, the affinity of hSco1p to copper can be lower than that of hSco2p and copper can be lost during the purification procedure. The fact that copper is lost by

multiple purification steps suggests that copper is not tightly bound. The affinity of copper proteins to the metal is different and it depends on the protein's function. Metallothioneins (MT) have a very high affinity for copper. A weaker bond can be necessary to allow copper to be released and transferred to other proteins. Interestingly, affinity of copper binding can depend on the copper concentration in the cell. MNK has a low affinity for copper at low copper concentration, by increasing the copper concentration the affinity increases [214]. Thus, addition of a higher copper concentration in the *E. coli* medium, before induction with IPTG, could eventually result in an increase of bound copper in hSco1p. Third, it is possible that the bacterial system used in the purification led to an altered protein fold with subsequent loss of bound copper. Lutsenko *et al.* (1997) pointed to the importance of the three-dimensional structure of the MNK and WND metal binding motifs for selectivity toward copper [215]. The bacterial cytoplasm is known to be more reducing than its eukaryotic counterpart and thus it is not an ideal environment for the production of properly folded eukaryotic proteins. In the case of the purification of the MNK protein, a 0,0026 : 1 (Cu : protein) stoichiometry instead of the expected 1 : 1 was found. To overcome this problem and to obtain a functional protein, a new approach was reported [216] which required cotransfection of *E. coli* with a thioredoxin-encoding plasmid. The expression of high levels of thioredoxin seems to change the redox potential of *E. coli* cells, mimicking the environment in eukaryotic cells. This in turn facilitates proper folding of eukaryotic proteins and increases their solubility. In this case, the thioredoxin, which normally acts as a cytosolic reductant, acts as a protein oxidant [217], consistent with its ability to act as an oxidant when exported to the periplasm [218]. Moreover, new bacterial strains have been created which have an oxidising cytoplasm [219]. Another possibility is in the *in vitro* loading of copper after protein purification. This system was used to determine the *in vitro* stoichiometry of WND and MNK [157]. Fourth, it is possible that the system used for the purification interferes with the properties of the protein. GST is an obligate dimer and it was shown to influence the stoichiometry of copper in yCox17p [117]. Moreover, it is possible that the protein cannot acquire the preferred ligation geometry of copper while it is bound to the column matrix. Recently, the copper stoichiometry of ySco1p has been determined [208]. ySco1p binds 1 copper ion per monomer. Because hSco1p can complement the Δ*ysco1* strain in chimeric constructs with ySco1p, it can be expected that the human gene, too, can bind copper with this stoichiometry.

4.3.1.1 Structure of the copper binding domain

To identify the ligands involved in copper binding, site direct mutagenesis was performed. Thiol groups of cysteine residues are reactive Aa side chains forming complexes of varying stability with many metal ions. In many cases cysteine residues have been described as copper ligands. A CxxC motif has been found in the copper chaperones hHah1p, yCcc2p, Atx1p, WND, MNK and in other metal binding proteins including zinc finger proteins, ferrodoxins and metallothioneins. The CxxxC motif has been identified as a copper binding site so far only in Cox2p. The involvement of the CxxxC motif of hSco proteins in the copper binding was clearly shown in this work by the dramatic decrease of the copper content in the purified C-terminal portion of mutants carrying alanines in place of cysteines. This was observed for both proteins in the atomic emission spectroscopy and for hSco2p also with the atom absorption spectroscopy. The stoichiometry for hSco2p(C)Δcys was 0,2 mole of copper per mole of protein. The presence of residual copper hints at the presence of further copper ligands. Copper can acquire different geometry. Atx1p can adopt a two or three coordinate copper ligand site involving the conserved cysteines and either a methionine or an exogenous thiol, like GSH [154]. X-ray absorption spectroscopy studies indicate that Cu(I) is two-coordinate in WND [220]. EXAFS (X-ray absorption fine structure spectroscopy) analysis suggests the presence in hCcsp of a binuclear cysteine-bridged dicopper cluster in which each copper is coordinated by three cysteine ligands. The other hSco ligands are expected to bind copper weakly to allow changes in geometry necessary for the copper transfer. ySco1p carries two further cysteines, but they are not essential for the protein function [203]. hSco2p has a cysteine before the copper binding motif and hSco1p has no further cysteines. A possible ligand in Sco proteins is the histidine at position 260 in hSco1p, 224 in hSco2p and 239 in ySco1p. This histidine is highly conserved and it was shown to be essential for the protein function in yeast and in bacteria [104, 179]. Moreover, the environment of this histidine remembers the environment of the two cysteines of the CxxxC motif containing a lot of acidic residues. The presence of a negative charge around the metal binding site is perhaps important for controlling the affinity or the geometry of the site. The trigonal coordination of Cu has been recently confirmed for ySco1p with EXAFS analysis and the conserved histidine at position 239 was identified as the third ligand [208]. The H239A mutant protein bound 0.14 ± 0.1 Cu per protein. In *hSCO2* patients, a mutation in a serine next to the conserved histidine (S225F) is associated with lethal COX deficiency. Atom emission analysis made in this work shows that this mutant protein is able to bind copper. Quantification of the copper bound was not performed but the atomic

emission data show that a dramatic reduction of copper content such as those observed in mutants lacking cysteines is unlikely. The S225F mutation could interfere with the structure of the coordination sphere of copper. Structural changes associated with altered geometries of the Zn and copper binding site of Sod1p are associated with alterations in the reactivity of the wild type enzyme, probably resulting from an altered copper binding affinity [221]. Histidines as copper ligands have been described, for example, for Cox1p, Cox2p and hSod1p. Further experiments, like EXAFS, are planned to identify the coordination state of the copper centre in hSco1p and hSco2p.

In a recent model, transfer of copper involves docking of the two partner proteins with the metal binding sites in close proximity and consequent formation of two- and three-coordinate intermediates in which the copper ion is coordinated simultaneously from the ligand of the chaperone and of the recipient protein [154]. This process requires the ability of the copper centre of the chaperone to change its coordination sphere to become accessible from the ligand of the recipient (see Fig. 38).

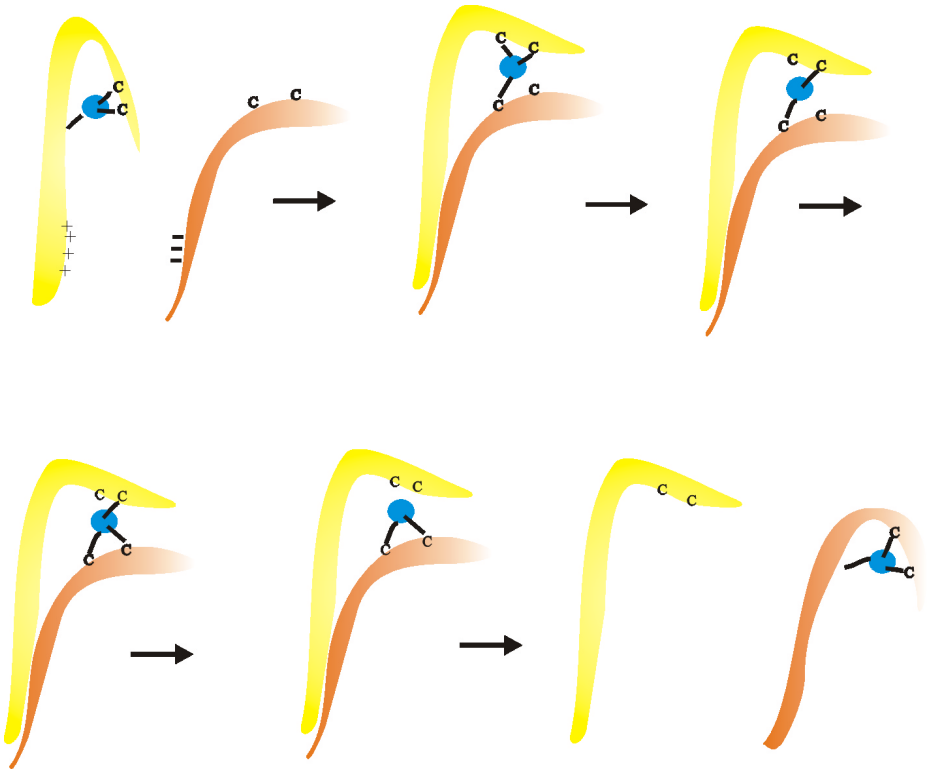

Fig. 38. Model of copper transfer between the chaperone and its partner protein.
The copper chaperone (yellow) binds copper (blue) for example with a trigonal geometry involving two cysteines (C) and another ligand. The docking process between the chaperone and its partner (red) involves electrostatic interactions between a domain of the chaperone containing for example positive residues (+) and a domain of the partner containing for example negative residues (-). The copper centre of the chaperone changes its conformation to become accessible for the ligands of the recipient. Two- and three-coordinate intermediates are formed leading to a transfer of the metal centre to the recipient protein, which can thus acquire its normal fold.

The metal binding domain has to be at the surface of the protein, accessible for ligand exchange reactions. An interesting question is the accessibility of the cysteines residues of the CxxxC motif. The solvent accessibility can be deduced from the ability of the cysteines to be oxidised and reduced. The accessible SH groups can be determined using Ellman's reagent [222]. Preliminary studies have shown that hSco2p is sensitive against oxygen from the air and that the protein can be reduced by incubating in DTT-containing buffer (data not shown). This means that the cysteine residues are readily accessible. The SH/protein ratio has yet to be investigated. The accessibility of the metal centre is in accord with the three-dimensional structure of Sco proteins suggested by Chinenov [176]. The proposed thioredoxin fold permits the exposition of the two essential cysteines at a junction site between a loop and a helix (Fig. 39). A similar structure, but with another succession of the ß-sheet and α-helices, was found in a variety of proteins that bind inorganic ions and also in copper metallochaperones.

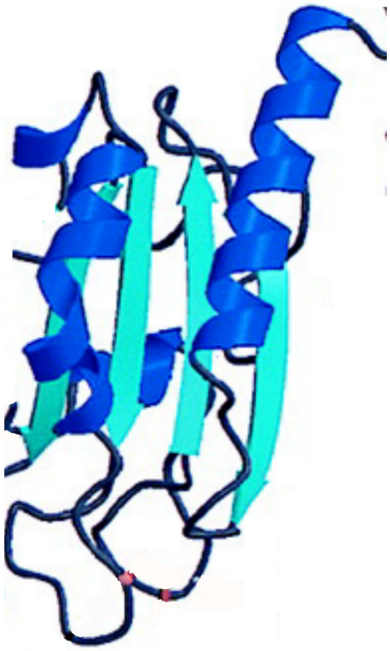

Fig. 39. Accessibility of the cysteine residues in the metal binding site of hSco proteins.
The structural motif of the thioredoxin fold consists of a four-stranded central β-sheet and three-flanking α-helices which are arranged in the order ß-α-ß-α-ß-ß-α. The two cysteines (in red) of the metal binding site are solvent accessible (in part taken from [223]).

Interestingly, copper transfer is facilitated by hydrogen bond interaction between a threonine in hHah1p near the metal binding motif and a cysteine of the metal binding site in WND [224]. A threonine at a distance of two Aa from the CxxxC motif is conserved in hSco proteins and ySco1p. Site direct mutagenesis of this threonine could elucidate its function.

The E140K mutation in hSco2p changes a negative residue to a positive. Atom emission analysis performed in this work shows that the E140K mutant protein is still able to bind copper. Quantification of the bound copper was not carried out, but clearly the amount of bound copper is not dramatically reduced. The influence of this mutation could be explained by a deformation of the metal binding site. The coordination of metal in protein involves normally the transfer of electrons of ligands to the outer orbitals of the metal. This causes an accumulation of a partial negative charge on the metal and the presence of a positive Aa near the copper site could contribute to an extreme stabilisation of the bond impeding the delivery to another protein. It would be interesting to elucidate the affinity with which copper is bound in the mutant protein. Patients carrying the E140K mutation show an accumulation of copper as deduced from the increasing copper uptake and normal copper retention [110]. This could mean that copper is imported in the mitochondria, transferred to hSco proteins, but it can be more difficult to deliver it to COX. The cell responds by increasing the copper uptake and copper concentrates in mitochondria reaching a toxic concentration. The E140K mutation, if engineered in ySco1p, shows no effect on COX assembly [109]. However, COX activity is slightly reduced and a small reduction was also observed in the steady-state level of the mutant protein [109]. In human mitochondria this slight reduction might be just enough to be deleterious in the complete absence of any other functional hSco2p. Deleterious consequences can accumulate in time leading to a later appearance of the disease. The latter development of the lethal COX deficiency is typical of patients carrying the homozygous E140K mutation.

The P174L mutation, which was found in *hSCO1* patients and which was shown in this work to affect the assembly of COX, is next to the CxxxC motif. This mutation was suggested to interfere with the structure of the metal binding site [108]. Interestingly, respiratory growth of transformants expressing K2L, but not K1L, can be rescued by adding copper to the growth medium. The effect of copper could result from a copper-induced alteration in the overall structure, which overcomes the interference of the P174L mutation with the three-dimensional structure of the CxxxC-containing domain. This interpretation could also account for the suppression of the temperature-sensitive growth phenotype of K1-transformants by addition of copper to the YPGly medium. Alternatively - if the P174L mutation lowers the binding affinity

of the protein for copper - an elevated copper concentration may be required to allow loading of the protein with copper. The inability of copper to complement the K1L mutation may reflect a suboptimal ability of K1 to substitute for ySco1p. This hypothesis is confirmed by the lower COX activity of K1 transformants, which require copper to reach a wild-type like growth behaviour. The K2 chimera is, therefore, the best construct to characterise hSco1p mutations in the yeast model. The P174L mutation represents the first example of a COX assembly mutant which can be complemented by adding copper. This finding strongly confirms the importance of Sco proteins in the copper pathway. Interestingly, in the strain carrying the K2L construct, the level of Cox1p and Cox2p is less reduced than in the null mutant. The COX activity is 30 % of the wild type, suggesting that the mutated protein is able to permit the assembly of a small quantity of COX. Therefore, the P174L mutation only partially impairs the function of the K2L construct and its function can be completely restored by adding copper.

Positive Aa residues could be involved in stabilising the metal centre. Clusters of lysine residues have been described as a conserved motif in other human and yeast copper chaperones [155]. NMR and structural analyses show that positive residues are located near the metal binding site in Atx1p [154, 225] and are important in the activity of the metallochaperone. Positive residues in the vicinity of the metal binding site in hHah1p have been shown to be important for metal transfer by creating an electrostatic potential gradient that favours the movement of the positively charged copper ion [151]. In the case of Atx1p, a lysine was suggested to affect the kinetics or thermodynamics of copper/protein interaction through hydrogen binding to a coordinate cysteine sulfur atom. This lysine is predicted to partially neutralise the net negative charge that results from a coordination of two cysteinate anions to Cu(I) and would, thereby, stabilise the copper chaperone complex. A working hypothesis is that allosteric conformation changes at this lysine may occur during docking of the chaperone with its partner Ccc2p [154]. A cluster of charged Aa is localised at the extreme C-terminal portion of hSco proteins and could be implicated in this stabilisation process.

In hSod1p, mutations in a histidine ligand is associated with FALS-disease and mutant hSod1p is devoid of copper. In this case it was suggested that the hCcsp interaction with an impaired hSod1p target results in an inappropriate release of free copper [226]. It would be interesting to test if all patient cells accumulate copper and if this copper is in a free or bound form.

4.3.2 hSco proteins have no thioredoxin activity

The affinity-purified C-terminal portions of hSco proteins have also been used in an enzymatic test to determine if the two proteins can act as thiol-disulfide oxidoreductase. The function of Sco proteins as thioredoxin was deduced from the similarity of Sco proteins to bacterial thiol-disulfide reductases [176]. Thioredoxins are able to reduce the disulfide bridges of insulin faster than DTT. Reduction of insulin in presence of NADPH and thioredoxin reductase is a widely used method to test the thiol-disulfide oxidoreductase activity. Both hSco proteins were not able to reduce insulin, whereas a human thioredoxin, used as a positive control, was. It can be argued that the recombinant proteins from *E. coli* don't have the same properties as the authentic human proteins. However, copper binding and enzymatic analysis of eukaryotic proteins have often been performed using the bacterial system for the purification. Purification of only the soluble part of the protein is also a common procedure in functional analysis [136, 227]. Insulin is a widely used substrate, because of the ability of a thioredoxin to substitute for another with similar redox potential *in vivo* [228]. Another substrate used to test the thioredoxin activity is lipoic acid, which is reduced slower by thioredoxin as compared to insulin [229]. The insulin test was, however, shown to be ineffective in the case of two periplasm-exposed proteins, HelXp and Ccl2p, involved in the thioreduction pathway of cytochrome *c* in *Rhodobacter capsulatus*. *In vitro* studies with these purified proteins indicate that although neither can reduce insulin, HelXp can reduce the Ccl2p cysteine residues which in turn are oxidised by an apocytochrome *c* peptide containing the CxxCH domain [230]. Therefore, it can be supposed that, in the case of Sco proteins, too, the specific substrate has to be added to detect a thiol-disulfide oxidoreductase activity. Thioredoxins have been shown to be essential in the biogenesis of periplasm exposed proteins in bacteria. Thioredoxins-like proteins can reduce cysteine bridges in the cytoplasm, which has reducing properties, or oxidise proteins in the periplasm, which has oxidant properties. The ability of thioredoxins to reduce or to oxidise depends on its redox properties and thioredoxins have been identified with reducing properties in periplasm [134]. In eukaryotes, thioredoxins have also been found in mitochondria where they are important in the defence against oxidative damage and stress, acting as hydrogen donor for peroxiredoxines which catalyse the reduction of H_2O_2 [231, 232]. So far only one mammalian mitochondrial thioredoxin [136] and thioredoxin reductase [233] have been identified. An interesting question is whether a thioredoxin system is required in the biogenesis of the OXPHOS system. Formation of disulfide bonds during folding of proteins in mammalian cells occurs in the lumen of the ER. The unique GSH/GSSG ratio (3:1) within the

lumen of this compartment is thought to provide it with a redox potential that - in contrast to cytosol (100:1) - is oxidising enough to favour disulfide bonds [234]. Moreover, the ER lumen contains a variety of chaperones that assist and accelerate the folding reactions [235]. Cytoplasm is generally considered to be too reducing to allow the formation of disulfide bonds. However, proteins from vaccinia virus (vv) are able to form disulfide bonds in the cytoplasm of infected cells [236]. Since the redox state of cytoplasm of vv infected cells remain normal, these proteins probably possess an inherent property to acquire disulfide bonds. *In vitro* studies have shown that the formation of intramolecular disulfide bonds depends on the conformation as well as on the inherent disulfide oxidation-reduction potential of the protein [237]. The disulfide bond formation of the vv proteins under cytosolic (reducing) condition can be rationalised by assuming that the redox potential of the these proteins themselves must be higher than the cytosolic redox potential and that the conformation of the proteins favours the intramolecular bonding and folding. These data show that the equilibrium between disulfide bonds and sulfhydryl is a complicated pathway which can be independent on the redox state of the compartment and which can occur spontaneously or catalysed by chaperones. In yeast the only genes found to be necessary for cytochrome *c* biogenesis are the heme lyases. So far disulfide reductase activity of the heme lyase was not shown and it is thus possible that the cysteines of apocytochrome *c* and COX are already in a reduced state without requiring assisting proteins.

4.4 Interaction analysis of hSco proteins

4.4.1 Interaction between hSco1p, hSco2p and Cox2p.

The results of the functional analysis strongly hint at the conclusion that the two hSco proteins act as copper chaperones. Sco proteins could transfer copper to Cox1p and/or Cox2p. To test if hSco proteins are involved in the transfer of copper to Cox2p, interaction was studied using affinity chromatography and coimmnunoprecipitation. With the affinity chromatography analysis no interaction was detected. It is possible that the *in vitro* test is not the best system to study this interaction because only the C-terminal portion of hSco proteins fused to GST was used in the test. The TM could be important for the protein-protein interaction and the N-terminal portion may be necessary for the correct protein folding. Interestingly, the N-terminal

portions of hSco1p and hSco2p are very different and bacterial Sco homologues like SenC and YpmQ lack the N-terminal portion. It could be useful to repeat the test fusing the soluble part of Cox2p to GST and incubating it with lysate of HeLa cells expressing a tagged version of the full version of hSco proteins. Moreover, as GST is an obligate dimer, it can alter the properties of the fused proteins. Therefore, it may be advantageous to use another tag like chitin binding protein or maltose binding protein.

The results of the coimmunoprecipitation show a very weak interaction only between hSco1p and Cox2p. Perhaps the interaction between hSco2p and Cox2p was too weak to be detected. The interaction could be transient and, therefore, hard to detect. This possibility was suggested for the interaction between hHah1p and WND and MNK, respectively. The transient nature of the interaction would permit diffusion-driven movement of cellular copper via association and dissociation of hHah1p with the ATPases. Such an interaction is consistent with immunofluorescence data which reveal no detectable hHah1p concentrated at the trans-Golgi network and by coimmunoprecipitation studies which indicated that only 3-5 % of hHah1p coprecipitate with the ATPases [152]. Moreover, a transient interaction between ySco1p and Cox2p was postulated [208]. Detergent-solubilized mitochondrial lysates were subjected to size exclusion chromatography and column fractions analysed by SDS-PAGE and Western blotting. ySco1p eluted in fractions corresponding to a molecular mass larger than 200 kDa. The fractions containing ySco1p also contained Cox2p. However, if mitochondrial lysates from strains lacking Cox2p were analysed under the same conditions, the size of the ySco1p containing complex was unaffected, suggesting that these two proteins were not in the same complex [208]. However, interaction between ySco1p and Cox2p was detected in the immunoprecipitation test [104].

In this work about 1 mg of mitochondria was used for the *in vivo* test. In the case of the immnunoprecipitation of hSco1p-EGFP, the cell line HeLa 17A3 was used, which express hSco1p-EGFP stably. For the immunoprecipitation of hSco2p-EGFP, transfected HeLa cells were used. Because the transformation efficiency is about 50 %, only half of the used mitochondria will contain hSco2p-EGFP. Perhaps it can be useful in further experiments to use more mitochondria to detect the interaction. One other problem can be the tag used for the immunodetection of hSco proteins. EGFP is a 27 kDa protein, and it could destroy the structure of the hSco proteins or interfere with the conformation necessary for the protein-protein interaction. Smaller tags like AU5 or HA could be used in the place of EGFP. The HA epitope seems not to be suitable because preliminary studies showed that the antibody against

HA recognise a lot of unspecific bands in HeLa cell lysate. Moreover, it can be expected that only copper-lacking Cox2p can interact with hSco proteins. If all proteins contain bound Cu(I), the interaction may be destabilised. Therefore, it might be useful to remove copper from COX. A copper chelator widely used to test copper dependent interaction is BCS. BCS was used to reveal the interaction between hHah1p and MNK. In this case the interaction was copper-dependent and immunoprecipitation was performed from lysate from cells grown in the presence of BCS or in the presence of high copper concentration [152]. However, it cannot be excluded that starvation of copper with BCS leads to an instable COX complex. Another possibility may be to grow the cells in a medium with a small quantity of copper and add copper immediately prior to the immunoprecipitation to have a higher amount of assembling COX complexes.

4.4.2 Interaction between hSco1p, hSco2p and hCox17p.

ySCO1 and *ySCO2* can rescue a *ycox17* null mutant [84]. Since a Δ*ysco1* strain is not rescued by *yCOX17*, ySco1p is likely to act downstream of yCox17p [84]. Cox17p could target copper specifically to mitochondria and transfer the metal to Sco proteins. yCox17p binds three copper ions forming a polycopper cluster [115]. This cluster exhibits many features of the copper thiolate cluster of the Cup1 metallothionein [238]. Each molecule forms a cluster with trigonal Cu coordination by cysteinyl thiolates and the clusters are pH-stable. The difference consists in the lability to ligand exchange reactions using BCS. Two of the three Cu ions are very reactive to exogenous ligands, showing that yCox17p is implicated in copper transfer rather than acting as a metal-scavenging protein in the mitochondria. Interaction between hSco1p, hSco2p and hCox17p was detected only in the absence of DTT in the affinity chromatography assay. The importance of DTT in the interaction probably did not result from a negative influence of DTT on the structure of the proteins. DTT should not demetallate the proteins, because it is a weak Cu(I) chelator. Moreover, the stoichiometry of yCox17p was demonstrated using proteins purified in the presence of DTT [115] and in this work the stoichiometry of hSco1p and hSco2p was performed in PBS-DTT. yCox17p was shown to form oligomer complexes [115]. The oligomerisation state was independent of the presence of DTT. The importance of DTT rather consists in its reducing properties. If the interaction between Sco proteins and Cox17p occurs via disulphide bridges, DTT could disrupt this interaction. This idea is supported by the observation that the interaction between hSco

proteins and hCox17p is stronger in the presence of copper. Copper, like other transition metals, can catalyse the formation of unspecific disulfide bridges in aerobic conditions. Interaction between yCox17p and ySco proteins was demonstrated in the yeast system *in vitro* [203]. Again, it can be postulated that the presence of a very large tag like EGFP (27 kDa versus 8 kDa of hCox17p) destroys the native structure of hCox17p. EGFP dimerises at high concentration and because of the very high expression of hCox17p-EGFP in Hela cells, it can be expected that the EGFP part of the fusion protein form dimers and can induce a non-native conformation of hCox17p, thereby altering the properties of the polycopper cluster. Moreover, the oligomeric state of Cox17p in mitochondria could be an important feature for the interaction with Sco proteins and the formation of oligomers could be impaired by the presence of EGFP.

An interesting question is why overexpression of ySco proteins is able to complement a *ycox17* deletion mutant. Sco proteins, if overexpressed, could bind copper directly in the cytoplasm and overcome the absence of Cox17p. Moreover, the published null allele of *yCOX17* is a disruptant with three-fourth of the protein including 6 of the 7 cysteines still disposable [86]. Perhaps the remaining protein could bind copper with a reduced affinity and more copper (the strain can be complemented too with a copper rich medium) or more partner protein could be required to reach a good efficiency of the copper delivery. The question remains open if other copper transporters for the mitochondria exist. Cu chaperones appear to be particularly important at low concentration of extracellular copper. Under elevated copper concentration their contribution to Cu transport is reduced, possibly because of the increasing role of non specific Cu-binding carriers. The Cu/Zn-superoxide dismutase activity, for example, was restored by addition of Cu (but not by addition of other metal cations) to the growth medium of yeast strains lacking the ySod1p chaperone Lys7p [239]. GSH is a highly abundant thiol agent in mammalian cells and can form very stable complexes with Cu(I). GSH was found to be a more efficient copper donor to the copper-free enzyme Cu/Zn-superoxide dismutase than other low molecular weight Cu(I) complexes *in vitro* [240]. Evidence was obtained for the occurrence of a Cu(I)-GSH protein intermediate in the reconstitution process. On the contrary, copper-thionein was unable to reconstitute Cu/Zn-superoxide dismutase. Copper-GSH complexes were detected in hepatoma cells over-loaded with copper [241]. A majority of the cytoplasmic copper (more than 60 %) was isolated as a GSH complex. Kinetic studies of ^{67}Cu uptake showed that GSH bound ^{67}Cu before the metal was complexed by MT. These results support a model of copper metabolism in which the metal is complexed by GSH soon after

entering the cell. The complexed metal is then transferred to higher molecular weight components such as metallothioneins, where it is stored, and as Cu/Zn-superoxide dismutase [242]. Because the outer mitochondrial membrane is porous to small molecules, it is possible that Cu(I)-GSH can act as a copper transporter for this compartment. Moreover, recent studies suggest that the transfer of metals from MT to an acceptor is possible and GSH facilitates such transfer reaction [243, 244]. These data suggest that MT could prevent metal toxicity and/or donate the metal to metalloproteins. MT have been shown to localise inside mitochondria when copper is in excess [245]. How Cox17p enters mitochondria is not clear because the outer membrane is porous only for small molecules up to a size of 12 kDa [246] whereas yCox17p is shown to be a dimer in the cytoplasm with a MW of 16 kDa [115]. Moreover, transport of copper in other compartments, like the secretory pathway, is a very controlled mechanism and it can be expected that in mitochondria, too, a specific copper pump is required. Indeed it was demonstrated that a form of the WND is localised in the mitochondria [48]. WND is localised normally in the Golgi and has a MW of 160 kDa. A version of 140 kDa was detected in mitochondria of cultured hepatic cells and human tissues. The 140 kDa WND product is formed as a result of proteolytic cleavage at the N-terminal portion of the full length WND. The cleavage of the WND protein presumably removes one or two of the six metal-binding repeats from the N-terminal domain [48]. WND and the other copper pump MNK have been shown to move from their localisation in the Golgi in the presence of high concentration of copper [148, 149]. If a parallel copper pathway exist in mitochondria, Sco proteins would be able to receive copper from proteins other than Cox17p. Possibly the alternative way is switched on in the absence of Cox17p. It will be interesting to look for other copper containing proteins in mitochondria. Homologues of Cox17p were not found in bacteria [179] and deletion of the bacterial Sco homologue YpmQ from *Bacillus subtilis* can be overcome by supplementing the growth medium with copper [179]. This finding can reflect the simpler structure of prokaryotic cells.

4.4.3 Homomerisation and heterodimerisation of hSco proteins.

Affinity chromatography analysis performed in this work shows that the carboxyl-terminal portion of hSco proteins can form homomeric complexes. Because HeLa cell lysates were used in the experiments as the source of the tagged hSco proteins, it is not excluded that complex formation is mediated by other proteins present in the lysate. The interaction - whether direct or indirect - does not require the CxxxC motif, as shown by the formation of homomeric complexes by the hScoΔcys mutant proteins. A further analysis with gel filtration chromatography of the affinity purified hSco proteins leads to the conclusion that hSco1p forms dimers directly because the protein eluted from the column as a 1:1 mixture of monomer and dimer and no other component could be detected. In contrast hSco2p eluted mostly as a monomer, with a small amount of dimer. This result can hint at the conclusion that other factors can be involved in the dimerisation of hSco2p or that the C-terminal portion alone is not sufficient to promote the dimerisation. In the *in vitro* assay hSco2p is present as a full-length construct fused to EGFP and as a GST fusion of the C-terminal portion. Therefore, the presence of one N-terminal portion could be sufficient to promote the formation of the dimer. The dimeric state of hSco proteins is in agreement with the recent finding that ySco1p form oligomers complexes. In this case, too, it was proposed that the formation of the oligomers requires the presence of the N-terminal portion [208]. Dimerisation of copper binding proteins is not without precedent: recently it was reported that the copper enzyme superoxide dismutase as well as its chaperone Ccsp form homo- and heterodimers [165]. Dimerisation of yCcsp was copper dependent *in vitro* [161]. The homodimerisation of hSco2p could explain the correlation between genotype and phenotype in the patients. As outlined in the introduction, all patients have a common mutation and a further stop mutation or point mutation. People carrying only one mutation do not present a phenotype, showing that a single wild type copy is sufficient. Patients with two E140K mutations have a milder phenotype, in that they develop the disease at a later time point. Possibly hSco2p with the E140K mutation still can homomerise. Patients with a further point mutation live only for three months, and patients with a further stop mutation only for few days. In these cases the presence of the E140K mutant allele is no longer sufficient to allow assembly of COX. Probably the E140K mutant protein can dimerise with itself, but significant percentage will homomerise with the other mutated protein leading to an inactive dimer. This suggests that the functionality of the hSco2p(E140K) mutant form is disturbed by the presence of a further mutant protein and that dimerisation is important for the protein activity.

In this work, the hSco2p(E140K) and hSco2p(S225F) mutant forms were shown to be stable as EFGP fusions, however their stability can derive from the presence of the EGFP tag. It was observed that the concentration of the hSco2p(E140K) mutant form in the GST construct was somewhat reduced, suggesting an effect of the E140K mutation on the stability of the protein. It was demonstrated that the E140K and S225F mutations do not lead to a mislocalisation of the two proteins. Mutants carrying the E140K mutation and the S225F mutation can dimerise with the wild type protein and with each other. This supports the idea that the mutations do not influence the dimerisation, but rather the formation of an active dimer. Moreover these mutations could interfere with the heterodimerisation process. The importance of dimerisation in copper delivery has been discussed for yCcsp (Lys7p) and yCox17p. In the case of Lys7p, dimerisation of the protein is induced by the presence of copper [161]. On the basis of (a) observations that full-length Lys7p can be dimeric in both crystalline and solute environments [162], (b) features in the Lys7p structure that suggest a putative docking site for an ySod1p dimer with a Lys7p dimer [247], and (c) the spatial arrangement of the putative copper delivery domain(s) in the dimeric Lys7p structure [162], a model for Lys7p-ySod1p interaction and copper delivery was suggested. It implicates a dimer-dimer interaction that obviates the need to disrupt the very stable ySod1p homodimer and that allows simultaneous copper ion delivery to both ySod1p subunits [247]. Bovine COX exists as a dimer [248] with the two copper centres separated by 74 Å. The dimer interface is formed by Cox4p which also forms a tight interaction with Cox2p [248]. Heaton *et al.* (2001) [115] suggested that the Cu_A site formation, if the Cu insertion into Cu_A takes place in the assembled COX complex, may involve the dimeric COX complex. Thus the oligomeric state of Cox17p may be important in the Cu(I) delivery to two Sco molecules docked on Cox2p at the dimer interface.
The copper chaperone Ccsp directly interacts with copper/zinc superoxide dismutase [165]. Interestingly, Ccsp has a high degree of similarity to Sod1p, reminiscent of the situation with hSco1p and hSco2p. In effect, hSco1p and hSco2p were shown to form heterodimers *in vivo* and *in vitro*. Again no data are available to determine if the interaction is direct or mediated from other factors present in the lysate of HeLa cells.

Docking of proteins involves generally electrostatic interaction. This interaction was described for hHah1p and WND [151] as well as for Atx1p and Ccc2p [249]. In this case the docking process was supposed to involve electrostatic interactions between the basic face of the metallochaperone and the corresponding acid face in its target protein [225]. The R175W

mutation in hSco2p is localised in a cluster of charged amino acids and could interfere with the protein-protein interactions. This mutation was not examined in this work, analysis of its copper binding and homodimerisation properties are planned. Interestingly, other clusters of charged Aa are localised near the TM and at the extreme C-terminal portion of Sco proteins. Both were shown to be essential for ySco1p function [203]. The interaction between Cox2p and hSco proteins, both membrane proteins, could involve the TM and the positive charge of hSco proteins next to the TM could mediate the protein recognition. Another chaperone/target recognition mechanism implies a structural similarity between the two partner proteins, as described for Ccsp and Sod1p. Sco proteins exhibit sequence homology with a 20 Aa portion of the Cu_A domain of COX centred around the pair of cysteine residues of the copper binding site but the structural similarity is too limited to support this mechanism.

A schematic overview of domains possibly involved in the action of Sco proteins is given in Fig. 40.

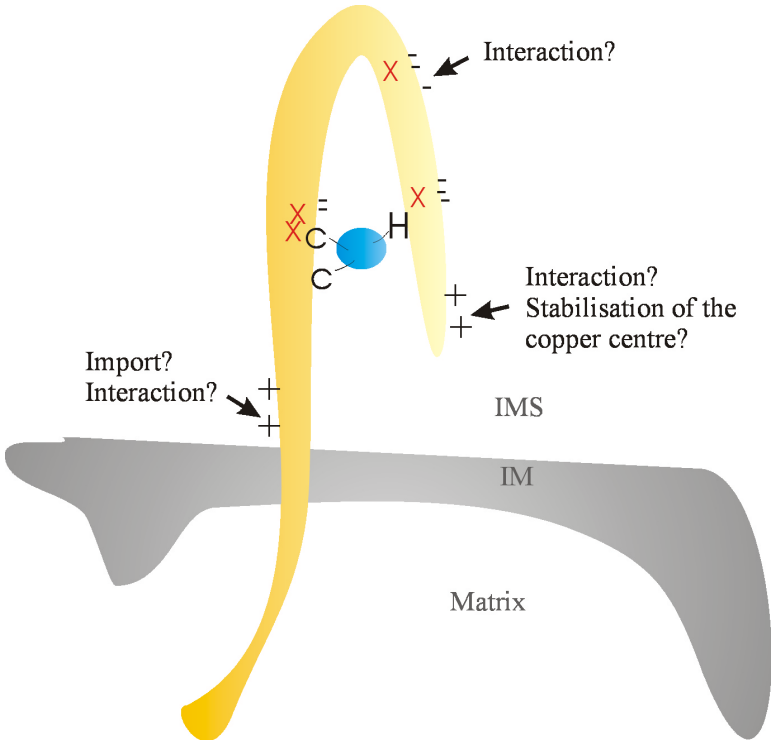

Fig. 40. Schematic presentation of important domains of hSco proteins.
hSco proteins (yellow) are probably localised in the inner mt membrane (IM, grey). The C-terminal portion could protrude in the intermembrane space (IMS) and the N-terminal portion is in the matrix, as described for ySco1p. Copper (blue) is possibly bound by two cysteine residues (C) and one histidine (H). Positively (+) and negatively (-) charged domains are indicated. Mutation identified in human COX deficiency are shown with a red X. The possible role of the different domains is indicated.

4.5 Role of hSco1p and hSco2p

The results of the functional analysis strongly suggest that the two hSco proteins bind copper. No thioredoxin activity was detected and it can be proposed that hSco proteins act as copper chaperones.

Sco proteins could transfer copper to Cox1p and or Cox2p. In this work only the interaction between hSco proteins and Cox2p was analysed. A weak interaction *in vivo* was found between hSco1p and Cox2p. In yeast, an interaction between ySco2p and Cox2p was also found [203], but it cannot be excluded that the high homology between ySco1p and ySco2p led to an unspecific interaction or that the yeast and the human systems are not identical.

Several indications suggest that Sco proteins deliver copper to Cox2p. First, the deletion of the *Bacillus subtilis* Sco1 homologous YpmQ suppresses the activity of the cytochrome *c* oxidase but not of a second oxidase, the menaquinol oxidase, which only contains a Cu_B centre [179]. Second, the S225F mutation, when engineered in ySco1p, led to a partial COX assembly, with reduction of only Cox2p [92]. The insertion of Cu_B requires the Cox11p protein. In *Rhodobacter sphaeroides*, the deletion of the respective gene led to a cytochrome *c* oxidase containing Cu_A but lacking Cu_B [87]. Deletion of *yCOX11* eliminates the accumulation of detectable COX in the mitochondrial membrane [250]. Cox11p has a conserved CxC motif which resembles the metal binding region of other metal chaperones and can act in the binding of copper. It cannot be excluded that Cox11p receives copper from Sco proteins. However, a role for Cox11p in the formation of Cu_B does not require it to bind copper. It was also proposed that by interacting with Cox1p, Cox11p permits a conformation receptive for copper delivery by a different protein [87]. It would be interesting to test copper binding of Cox11p and the eventual interaction between Cox17p and Sco proteins and Cox11p. The different pathways of copper insertion for Cu_A and Cu_B can reflect the different structural features of the two copper centres. For example, Cu_A is located in an aqueous environment exposed domain about 5 Å from the surface of the protein, whereas Cu_B is bound within a transmembrane helix of Cox1p at a distance of about 15 Å from the closest water-exposed surface of the protein [248, 251]. Assembly of Cu_B occurs either in the matrix where Cox1p is synthesised, or in the membrane. The analysis of the orientation of Cox11p and Sco proteins could help to reveal whether the incorporation of copper takes place, before, in the matrix side, or after the assembly of Cox1p and Cox2p. The extra membrane domain of ySco1p faces the intermembrane space. This conclusion is supported by the sensitivity of ySco1p to proteinase K in mitoplasts but not in intact mitochondria [113]. This suggests that the proposed copper

binding site of ySco1p and the copper site of Cox2p face the same mitochondrial compartment. Such a localisation would be in accord with the proposed model in which Cox17p targets copper specifically to mitochondria by transferring the metal to Sco1p. In this work, an interaction with hCox17p was not found. However, as discussed above, the condition of the *in vitro* assay are possibly not optimal to test this interaction. Cox17p remains, therefore, a good candidate for the transfer of copper to Sco proteins, even though it cannot be excluded that other copper transporters, like WND, exist in human mitochondria. Sco proteins could also be carriers that transport copper to the matrix. This theory would be in agreement with the recently described oligomerisation state of ySco1p [208] which would allow to the Sco proteins to form a pore in the inner membrane. If copper addition occurs after membrane insertion of Cox2p, a role of Sco1p as a copper transferase would be more attractive than the pore model. The S225F mutant, engineered in ySco1p (S240F), is the first reported yeast COX assembly mutant that can partially complete the assembly pathway without complete proteolytic loss of the catalytic core of the molecule [92]. The S240F mutant selectively lacks Cox2p and it was proposed that the absence of the Cu_A centre led to unoccupied sites that are susceptible to proteases. Unlike GR20, the strain bearing the S240F allele has a stable mutated ySco1 protein, suggesting a stabilising influence of ySco1p on the assembling holoenzyme. These results suggest that ySco1p acts perhaps at the last step in the assembly pathway since all of the other subunits of the holoenzyme are present and assembled. However, it cannot be excluded that copper is inserted but with a wrong coordination, allowing the assembly of the others subunits but not protecting Cox2p from degradation.

The presence of two homologues raises the question whether they have the same function. The diversity of the phenotypes resulting from *hSCO1* and *hSCO2* mutations suggest that the proteins do not have the same role. So far mutations in two other assembly factors have been correlated with COX deficiency and in each case the phenotype is different even though in all cases the COX activity is reduced, pointing to a different mechanism of COX impairment. Moreover, these mutations have different effects on the COX assembly: while the concentration of all COX-subunits except for Cox5ap and Cox5bp is strongly reduced in *hSURF1* patients [98], mutations in the *hCOX10* gene preferentially affect the level of Cox2p [80]. In patients with *hSCO2* mutations, immunohistochemistry revealed a severe reduction of Cox1p and Cox2p, while Cox4p and Cox5ap were less affected [95]. The pathogenic *hSCO1* mutation, if introduced in a ySco1p/hSco1p chimera, affect the level of Cox1p and Cox2p (this work). Different assembly profiles are typical of COX deficiencies and reflect the genes which

are potentially involved. Some patients have normal levels of all COX subunits and are classified as candidates for mutations in nuclear encoded structural genes. Other patients have reduced levels of several subunits and are classified as assembly mutants [252]. The decreased steady-state level of the subunits observed in patients is likely the result of proteolytic degradation of unassembled or misfolded subunits. Studies in yeast have revealed the existence of an ATP-dependent proteolytic pathway responsible for the clearing of unassembled and improperly folded polypeptides in the various subcompartments of mitochondria [175]. This proteolytic system is responsible for the rapid degradation of COX subunits in yeast strains unable to complete assembly of the holo-enzyme due to a lack of one of the subunits or of assembly-assisting proteins [253]. In yeast COX assembly mutants are characterised by a selective degradation of the mitochondrially encoded subunits 1 and 2, while the nuclearly encoded subunits are normally present at or near wild type levels. The proteolytic system appears to be conserved in mammals [45]. Low levels of nuclear-encoded COX subunits have been found in human cell lines that do not express the mtDNA encoded subunits [254] and it was demonstrated that these low steady-state levels are the result of an increased turnover rate [255]. Furthermore, it was shown that the reduced COX content in fibroblasts cultures from patients with COX deficiency suffering from Leigh syndrome was the result of an elevated rate of degradation [172]. In most patients the steady-state levels of subunits 4, 5a and 5b were less affected. Subunit 4 appears to have an intrinsic stability and is present at 40 % of control values in human cell cultures depleted of mtDNA [256]. Subunits 5a and 5b do not span the inner membrane and are located on the matrix site of the enzyme complex [62]. These subunits may already be folded prior to assembly making them less prone to proteolytic degradation.

hSURF1, *hCOX10* and *hSCO1* mutations lead to an overall decrement of the COX activity, only *hSCO2* patients show a tissue specific reduction with strong involvement of myoblasts and skeletal muscle. *hSURF1* mutations cause lesions in cerebral basal ganglia, known as Leigh syndrome. Age at onset is usually between 8 and 14 months. *hSCO2* mutations are associated with hypertrophic cardiomyopathy. Age at onset is generally between birth and the first months of life with death occurring between 1 and 6 months. Interestingly, *hSCO2* patients carrying the E140K mutation show a normal development in the first months, later they develop a Leigh syndrome and the fatal cardiomyopathy occurs in the final stadium. In these patients a predominant involvement of the peripheral nervous system was observed and it was hypothesised that the progressive cardiomyopathy in *hSCO2* patients is not necessarily an early symptom of this disorder, but it may be indicative of a specific aerobic energy supply

threshold for cardiac function [110]. Threshold effect of mitochondrial mutations is a well investigate process [257]. Mitochondrial cytopathies present usually a tissue specificity. Even if a mutation is present in all tissues, only some will be affected and show a pathology. The tissue specificity can be explained with the expression of the defect in OXPHOS complexes that present individual biochemical thresholds. The value of this threshold for a given OXPHOS complex can vary according to the tissue; thus different tissues will display different sensitivities to a defect in an OXPHOS complex. A classification of tissues according to their response to a OXPHOS complex deficiency and, therefore, to their threshold values has been proposed [258]. For a given OXPHOS complex, the lower the threshold value in a tissue, the more sensitive this tissue is to a defect of this complex. For complex IV threshold values in the muscle and in the heart are lower than in the kidney and brain. For example, it was shown that an 80 % decrease in COX activity will induce a small decrease in mitochondrial respiration in liver, while the respiration drops to 40 % in heart mitochondria [258].

Little information is available for *hSCO1* mutations because so far they were found only in two boys from the same family. However, the course of the disease was very fast, with death after 4 days from the birth in one case. The combined data from patients lead to the conclusion that both *hSCO* genes are essential for COX assembly. The different involvement of tissues addresses the question if both proteins are expressed in all tissues. Northern blot analysis shows that both genes are expressed in the same tissues [95], but a post-translational regulation could be postulated. There is no direct relation between steady-state transcript and protein levels. Mechanism ensuring post-transcriptional or post-translational regulation must, therefore, be envisioned to account for the discrepancy between these two parameters. In human, three nuclear coded subunits of COX (6a, 7a and 8) occur as tissue-specific isoforms. COX presents different kinetic parameters according to its L (liver) and H (heart) isoform composition [259]. Subunit 6a has potential regulatory function [72, 260] controlling COX activity in response to ATP binding. Mutations in such tissue- and developmental-specific subunits have been proposed to account for some COX deficiencies [261, 262]. Mutations in nuclear genes have so far not been reported, but they are strongly suspected to account for COX deficiencies [252]. Specific isoforms could optimise the enzymatic activity to the metabolic demands of different tissues. In analogy, hSco1p and hSco2p could represent isoforms of high and low energy requiring tissues.

Even though fibroblasts are less affected than myoblasts in *hSCO2* patients, they still show a reduction of 50 % of the reference value, indicating an influence of hSco2p. It could be

supposed that hSco1p represents the general way for copper delivery and that hSco2p is a redundant protein in those tissues which do not require high energy, but it is indispensable in tissues with a high energy demand. This would explain why in yeast the deletion of *ySCO2* does not have any effect on the respiration and why *hSCO1* mutations lead to an overall COX deficiency, whereas *hSCO2* mutations lead to a tissue specific COX activity reduction. Because both proteins were shown to homomerise, it is possible that the transfer of copper requires the formation of dimers. The presence of an assembled COX complex, lacking only Cox2p [92], suggests that Cu_A is inserted in a last step of the assembling process, when COX is already a dimer. Dimer or higher complexes of Sco would be required to interact with the COX dimers. Alternatively, hSco dimers can be required to transfer at the same time two copper atoms to the two-copper centre of Cox2p. Since oligomerization of Cox17p is important for its function [115], the possibility exists that Cu(I) ions are donated from the Cox17p tetramer to the Sco1p oligomer.

The detection of heterodimers complexes *in vivo* and *in vitro* underlines the importance of the interaction between the two homologues. hSco1p dimers could receive copper inefficiently from a mitochondrial copper chaperone like hCox17p or more efficiently from hSco2p dimers, which may represent a high affinity binding site for hCox17p. In fibroblast, the less efficient copper transfer from the chaperone to hSco1p is sufficient for the COX activity. The transfer of copper from hSco2p to hSco1p becomes indispensable in high energy requiring tissues or under conditions of limiting copper. Research in yeast has shown that the respiration competence of a Δ*ysco2* strain is reduced in a medium poor of copper (Lode, personal communication). In the case of hCcsp, it was shown that a domain of the protein acts as sequestering site only under the condition of copper limitation [161], and another domain as translocation site. The sequestering site transfers the copper to the translocation site via a three coordinate intermediate. A comparable situation could be represented in mitochondria by hSco1p/hSco2p heterodimers. It can be expected that this specific copper pathway can be bypassed in high copper condition by the presence of unspecific copper carriers like GSH.

Assembly of COX may differ in high and low energy requiring tissues. The finding that *hSURF1* mutations cause an overall COX deficiency shows that at least some of the assembly steps are identical in the various tissues. hSurf1p is possibly implicated in the insertion of Cox1p and Cox2p in the holoenzyme, a process that can be the same in all tissues. The formation of the copper centres, instead, can require a more efficient pathway in tissues like brain and heart. In these tissues more COX complexes have been expected to be produced and

the copper disposability can be a limiting parameter. This hypothesis is supported by the tissue distribution profile of *hCOX17* mRNA. Hybridisation signals were detected in all tissue RNA samples, but they were drastically more intense in heart, kidney and brain [263]. The tissue distribution profile of *hCOX17* mRNA is quite different from that of *hHAH1* [145] and *hCCS* [160]. The mRNA of these cytosolic chaperones has the same abundance in all tissues. The mRNA distribution profile of *hSCO1* and *hSCO2* overlaps with that of *hCOX17*. This suggests that in high requiring energy tissues the copper transport pathway is more active.

The presence of a parallel copper transfer pathway for high energy demand tissues cannot be excluded. Different routes of copper transport could be used in different tissues. This possibility was, for example, proposed in the case of MNK, because the mRNA transcripts were found in all tissues except in liver [264]. In analogy, hSco2p could receive copper specifically from a so far unidentified copper transporter which is expressed in high energy requiring tissues and transfer it to hSco1p.

A model for the function of the hSco proteins under several conditions is represented in Fig. 41.

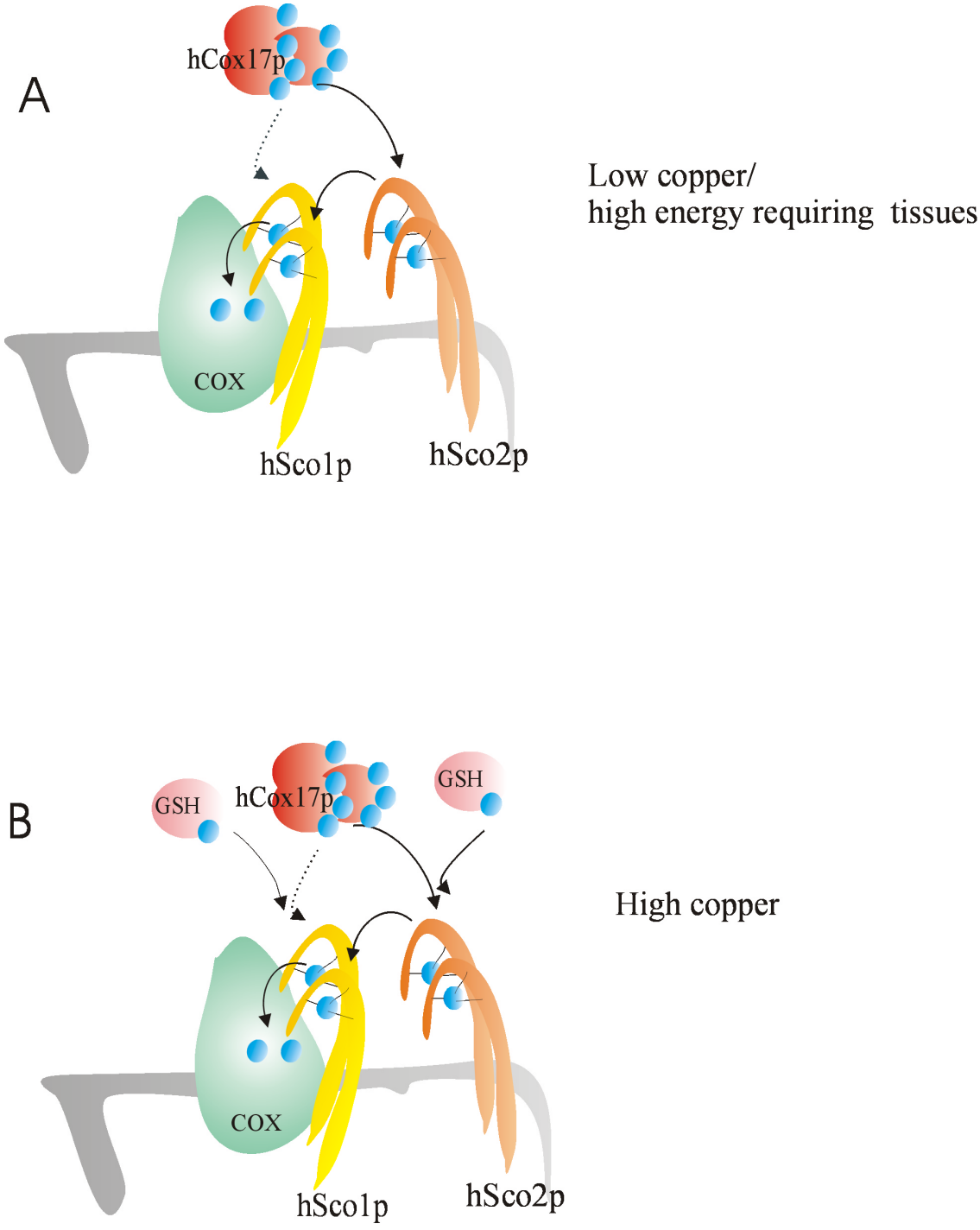

Fig. 41. Possible mechanisms of copper transfer from Sco proteins to COX.
A. Copper (in blue) is imported in the mitochondria by hCox17p which forms oligomers and transfers copper to the high affinity hSco2p-dimer and, partially, to the low affinity hSco1p-dimer. hSco2p-dimers transfer copper selectively to hSco1p-dimers. The specific transfer of copper from hSco2p dimers to hSco1p-dimers is indispensable in condition of low copper and/or in high-requiring energy tissues. hSco1p-dimers interact with COX through the TM portion and transfer two copper ions to the dicopper centre of Cox2p. **B**. In the presence of high amount of copper, hSco1p can receive copper from non-specific Cu-binding carriers, like GSH.

The finding that copper addition to the medium can complement the P174L mutation can provide a strategy for the early treatment of infants carrying *hSCO1* and *hSCO2* mutations. Treatment with copper-histidinate is recommended in Menkes disease and was tested with two *hSCO2* patients [110]. No beneficial effects were observed, but the copper supplementation began at a late stage of the disease, when the damages were probably irreversible. Very recently, it was shown that addition of copper-histidinate to the medium of cultured myoblasts of patients, harbouring the E140K mutation and a stop mutation at Aa position 90, completely restored COX activity [265]. This result supports the model proposed in this work, according to which hSco1p can substitute for hSco2p in the presence of high copper concentration.

5 SUMMARY

COX deficiency in human presents a plethora of phenotypes which is not surprising given the complexity of the enzyme structure and the multiple factors and many steps required for its assembly. A functional COX requires three mitochondrially encoded subunits (Cox1p, Cox2p and Cox3p), at least 10 nuclearly encoded subunits, some of which are tissue specific, and a yet unknown number of assembly factors. Mutations in four of these factors, hSco1p, hSco2p, hCox10p and hSurf1p, have been associated with lethal COX deficiency in patients.

Sco proteins, conserved from prokaryotes to eukaryotes, are probably involved in the insertion of copper in COX. The role of hSco1p and hSco2p in this process was investigated in this work. Moreover the importance of some hSco mutations found in patients was analysed.

Both *in vitro* and *in vivo* analyses show that the hSco proteins are localised in the mitochondria.

Both proteins are *per se* unable to substitute for ySco1p. However, a chimeric construct consisting of the N-terminal portion, the TM and a part of the C-terminal portion of ySco1p and the remaining C-terminal part derived from hSco1p was able to complement a *Dysco1* strain. This construct was used to define the role of a point mutation (P174L) found in the *hSCO1* gene of infants suffering from ketoacidotic coma. These mutation was shown to affect the COX activity and the levels of Cox1p and Cox2p. The fact that copper was able to suppress this mutation, strongly outlined the importance of Sco proteins in the copper insertion in COX.

The C-terminal portions of recombinant hSco1p and hSco2p were purified from *E. coli* by affinity chromatography. The purified proteins were subjected to atomic emission and absorption analyses and were shown to specifically bind copper. A stoichiometry of 1:1 for hSco2p and of 0,6:1 for hSco1p was determined.

To identify the Aa residues involved in copper binding, *in vitro* mutagenesis was performed. hSco1p and hSco2p, lacking the cysteines of the predicted metal binding site CxxxC, show a dramatic decrease in the ability to bind copper. A model for the structure of the metal binding site in hSco proteins is proposed. hSco proteins could bind copper with trigonal coordination, involving the two cysteines of the CxxxC motif and a conserved histidine.

The purified recombinant proteins were also used in an enzymatic assay to test their ability to reduce disulfide bridges, similar to thioredoxin-like proteins involved in the assembly of

bacterial COX. Both hSco proteins were not able to act as thioredoxins suggesting a role for the hSco proteins as copper chaperones.

To define the pathway of the copper transfer to COX, hSco proteins were tested for their ability to interact with hCox17p, a mitochondrial copper chaperone, and with Cox2p, which contains two copper ions. An interaction between hSco1p and Cox2p was detected.

Both hSco proteins were shown to homomerise and to form heterodimers one with each other.

Two mutations found in *hSCO2* patients suffering from hypertrophic cardiomyopathy, (E140K and S225F) were shown not to affect the copper binding properties, the intracellular localisation and the ability to form homomers.

In accordance to these data, a model is proposed in which hSco2p dimers transfer copper to hSco1p dimers. hSco1p dimers interact with COX and insert copper in the binuclear centre of Cox2p.

6 REFERENCES

1 DiMauro, S., Bonilla, E. and De Vivo, D.C. (1999) Does the patient have a mitochondrial encephalomyopathy? *J Child Neurol* **14 Suppl 1**, S23-35.

2 Anderson, S., Bankier, A.T., Barrell, B.G., de Bruijn, M.H., Coulson, A.R., Drouin, J., Eperon, I.C., Nierlich, D.P., Roe, B.A., Sanger, F., Schreier, P.H., Smith, A.J., Staden, R. and Young, I.G. (1981) Sequence and organization of the human mitochondrial genome. *Nature* **290**, 457-65.

3 Schon, E.A. (2000) Mitochondrial genetics and disease. *Trends Biochem Sci* **25**, 555-60.

4 Shitara, H., Hayashi, J.I., Takahama, S., Kaneda, H. and Yonekawa, H. (1998) Maternal inheritance of mouse mtDNA in interspecific hybrids: segregation of the leaked paternal mtDNA followed by the prevention of subsequent paternal leakage. *Genetics* **148**, 851-7.

5 Khrapko, K., Coller, H.A., Andre, P.C., Li, X.C., Hanekamp, J.S. and Thilly, W.G. (1997) Mitochondrial mutational spectra in human cells and tissues. *Proc Natl Acad Sci U S A* **94**, 13798-803.

6 Clayton, D.A., Doda, J.N. and Friedberg, E.C. (1974) The absence of a pyrimidine dimer repair mechanism in mammalian mitochondria. *Proc Natl Acad Sci U S A* **71**, 2777-81.

7 Bohr, V.A. and Anson, R.M. (1999) Mitochondrial DNA repair pathways. *J Bioenerg Biomembr* **31**, 391-8.

8 Croteau, D.L., Stierum, R.H. and Bohr, V.A. (1999) Mitochondrial DNA repair pathways. *Mutat Res* **434**, 137-48.

9 Richter, C. (1995) Oxidative damage to mitochondrial DNA and its relationship to ageing. *Int J Biochem Cell Biol* **27**, 647-53.

10 Hayashi, J., Ohta, S., Kikuchi, A., Takemitsu, M., Goto, Y. and Nonaka, I. (1991) Introduction of disease-related mitochondrial DNA deletions into HeLa cells lacking mitochondrial DNA results in mitochondrial dysfunction. *Proc Natl Acad Sci U S A* **88**, 10614-8.

11 Boulet, L., Karpati, G. and Shoubridge, E.A. (1992) Distribution and threshold expression of the tRNA(Lys) mutation in skeletal muscle of patients with myoclonic epilepsy and ragged-red fibers (MERRF). *Am J Hum Genet* **51**, 1187-200.

12 Chomyn, A., Martinuzzi, A., Yoneda, M., Daga, A., Hurko, O., Johns, D., Lai, S.T., Nonaka, I., Angelini, C. and Attardi, G. (1992) MELAS mutation in mtDNA binding site for transcription termination factor causes defects in protein synthesis and in respiration but no change in levels of upstream and downstream mature transcripts. *Proc Natl Acad Sci U S A* **89**, 4221-5.

13 Wallace, D.C. (2000) Mitochondrial defects in cardiomyopathy and neuromuscular disease. *Am Heart J* **139**, S70-85.

14 Ciafaloni, E., Ricci, E., Shanske, S., Moraes, C.T., Silvestri, G., Hirano, M., Simonetti, S., Angelini, C., Donati, M.A., Garcia, C. *et al*. (1992) MELAS: clinical features, biochemistry, and molecular genetics. *Ann Neurol* **31**, 391-8.

15 Wallace, D.C., Zheng, X.X., Lott, M.T., Shoffner, J.M., Hodge, J.A., Kelley, R.I., Epstein, C.M. and Hopkins, L.C. (1988) Familial mitochondrial encephalomyopathy (MERRF): genetic, pathophysiological, and biochemical characterization of a mitochondrial DNA disease. *Cell* **55**, 601-10.

16 Prezant, T.R., Agapian, J.V., Bohlman, M.C., Bu, X., Oztas, S., Qiu, W.Q., Arnos, K.S., Cortopassi, G.A., Jaber, L., Rotter, J.I. *et al*. (1993) Mitochondrial ribosomal RNA mutation associated with both antibiotic-induced and non-syndromic deafness. *Nat Genet* **4**, 289-94.

17 Wallace, D.C., Singh, G., Lott, M.T., Hodge, J.A., Schurr, T.G., Lezza, A.M., Elsas, L.J., 2nd and Nikoskelainen, E.K. (1988) Mitochondrial DNA mutation associated with Leber's hereditary optic neuropathy. *Science* **242**, 1427-30.

18 Huoponen, K., Vilkki, J., Aula, P., Nikoskelainen, E.K. and Savontaus, M.L. (1991) A new mtDNA mutation associated with Leber hereditary optic neuroretinopathy. *Am J Hum Genet* **48**, 1147-53.

19 Johns, D.R., Neufeld, M.J. and Park, R.D. (1992) An ND-6 mitochondrial DNA mutation associated with Leber hereditary optic neuropathy. *Biochem Biophys Res Commun* **187**, 1551-7.

20 DiMauro, S. and Andreu, A.L. (2000) Mutations in mtDNA: are we scraping the bottom of the barrel? *Brain Pathol* **10**, 431-41.

21 Keightley, J.A., Hoffbuhr, K.C., Burton, M.D., Salas, V.M., Johnston, W.S., Penn, A.M., Buist, N.R. and Kennaway, N.G. (1996) A microdeletion in cytochrome *c* oxidase (COX) subunit III associated with COX deficiency and recurrent myoglobinuria. *Nat. Genet.* **12**, 410-6.

22 Hanna, M.G., Nelson, I.P., Rahman, S., Lane, R.J., Land, J., Heales, S., Cooper, M.J., Schapira, A.H., Morgan-Hughes, J.A. and Wood, N.W. (1998) Cytochrome *c* oxidase deficiency associated with the first stop-codon point mutation in human mtDNA. *Am. J. Hum. Genet.* **63**, 29-36.

23 Hoffbuhr, K.C., Davidson, E., Filiano, B.A., Davidson, M., Kennaway, N.G. and King, M.P. (2000) A pathogenic 15-base pair deletion in mitochondrial DNA-encoded cytochrome *c* oxidase subunit III results in the absence of functional cytochrome *c* oxidase. *J. Biol. Chem.* **275**, 13994-4003.

24 Comi, G.P., Bordoni, A., Salani, S., Franceschina, L., Sciacco, M., Prelle, A., Fortunato, F., Zeviani, M., Napoli, L., Bresolin, N., Moggio, M., Ausenda, C.D., Taanman, J.W. and Scarlato, G. (1998) Cytochrome *c* oxidase subunit I microdeletion in a patient with motor neuron disease. *Ann. Neurol.* **43**, 110-6.

25 Bruno, C., Martinuzzi, A., Tang, Y., Andreu, A.L., Pallotti, F., Bonilla, E., Shanske, S., Fu, J., Sue, C.M., Angelini, C., DiMauro, S. and Manfredi, G. (1999) A stop-codon mutation in the human mtDNA cytochrome *c* oxidase I gene disrupts the functional structure of complex IV. *Am J Hum Genet* **65**, 611-20.

26 Clark, K.M., Taylor, R.W., Johnson, M.A., Chinnery, P.F., Chrzanowska-Lightowlers, Z.M., Andrews, R.M., Nelson, I.P., Wood, N.W., Lamont, P.J., Hanna, M.G., Lightowlers, R.N. and Turnbull, D.M. (1999) An mtDNA mutation in the initiation codon of the cytochrome *c* oxidase subunit II gene results in lower levels of the protein and a mitochondrial encephalomyopathy. *Am. J. Hum. Genet.* **64**, 1330-9.

27 Rahman, S., Taanman, J.W., Cooper, J.M., Nelson, I., Hargreaves, I., Meunier, B., Hanna, M.G., Garcia, J.J., Capaldi, R.A., Lake, B.D., Leonard, J.V. and Schapira, A.H. (1999) A missense mutation of cytochrome oxidase subunit II causes defective assembly and myopathy. *Am J Hum Genet* **65**, 1030-9.

28 Tiranti, V., Corona, P., Greco, M., Taanman, J.W., Carrara, F., Lamantea, E., Nijtmans, L., Uziel, G. and Zeviani, M. (2000) A novel frameshift mutation of the mtDNA *COIII* gene leads to impaired assembly of cytochrome *c* oxidase in a patient affected by Leigh-like syndrome. *Hum Mol Genet* **9**, 2733-42.

29 Holt, I.J., Harding, A.E., Petty, R.K. and Morgan-Hughes, J.A. (1990) A new mitochondrial disease associated with mitochondrial DNA heteroplasmy. *Am J Hum Genet* **46**, 428-33.

30 Santorelli, F.M., Shanske, S., Macaya, A., DeVivo, D.C. and DiMauro, S. (1993) The mutation at nt 8993 of mitochondrial DNA is a common cause of Leigh's syndrome. *Ann Neurol* **34**, 827-34.

31 Harding, A.E. and Hammans, S.R. (1992) Deletions of the mitochondrial genome. *J Inherit Metab Dis* **15**, 480-6.

32 Moraes, C.T., DiMauro, S., Zeviani, M., Lombes, A., Shanske, S., Miranda, A.F., Nakase, H., Bonilla, E., Werneck, L.C., Servidei, S. *et al*. (1989) Mitochondrial DNA deletions in progressive external ophthalmoplegia and Kearns-Sayre syndrome. *N Engl J Med* **320**, 1293-9.

33 Walsh, F.B. (1969) Progressive external ophthalmoplegia (PEO). *Trans Pa Acad Ophthalmol Otolaryngol* **22**, 88-96.

34 Rotig, A., Cormier, V., Blanche, S., Bonnefont, J.P., Ledeist, F., Romero, N., Schmitz, J., Rustin, P., Fischer, A., Saudubray, J.M. *et al*. (1990) Pearson's marrow-pancreas syndrome. A multisystem mitochondrial disorder in infancy. *J Clin Invest* **86**, 1601-8.

35 Tang, Y., Schon, E.A., Wilichowski, E., Vazquez-Memije, M.E., Davidson, E. and King, M.P. (2000) Rearrangements of human mitochondrial DNA (mtDNA): new insights into the regulation of mtDNA copy number and gene expression. *Mol Biol Cell* **11**, 1471-85.

36 Moraes, C.T., Shanske, S., Tritschler, H.J., Aprille, J.R., Andreetta, F., Bonilla, E., Schon, E.A. and DiMauro, S. (1991) mtDNA depletion with variable tissue expression: a novel genetic abnormality in mitochondrial diseases. *Am J Hum Genet* **48**, 492-501.

37 Baysal, B.E., Ferrell, R.E., Willett-Brozick, J.E., Lawrence, E.C., Myssiorek, D., Bosch, A., van der Mey, A., Taschner, P.E., Rubinstein, W.S., Myers, E.N., Richard, C.W., 3rd, Cornelisse, C.J., Devilee, P. and Devlin, B. (2000) Mutations in *SDHD*, a mitochondrial complex II gene, in hereditary paraganglioma. *Science* **287**, 848-51.

38 Jin, H., May, M., Tranebjaerg, L., Kendall, E., Fontan, G., Jackson, J., Subramony, S.H., Arena, F., Lubs, H., Smith, S., Stevenson, R., Schwartz, C. and Vetrie, D. (1996) A novel X-linked gene, *DDP*, shows mutations in families with deafness (DFN-1), dystonia, mental deficiency and blindness. *Nat Genet* **14**, 177-80.

39 Koehler, C.M., Leuenberger, D., Merchant, S., Renold, A., Junne, T. and Schatz, G. (1999) Human deafness dystonia syndrome is a mitochondrial disease. *Proc Natl Acad Sci U S A* **96**, 2141-6.

40 de Lonlay, P., Valnot, I., Barrientos, A., Gorbatyuk, M., Tzagoloff, A., Taanman, J.W., Benayoun, E., Chretien, D., Kadhom, N., Lombes, A., de Baulny, H.O., Niaudet, P., Munnich, A., Rustin, P. and Rotig, A. (2001) A mutant mitochondrial respiratory chain assembly protein causes complex III deficiency in patients with tubulopathy, encephalopathy and liver failure. *Nat Genet* **30**, 30.

41 Harding, A.E. (1981) Friedreich's ataxia: a clinical and genetic study of 90 families with an analysis of early diagnostic criteria and intrafamilial clustering of clinical features. *Brain* **104**, 589-620.

42 Campuzano, V., Montermini, L., Molto, M.D., Pianese, L., Cossee, M., Cavalcanti, F., Monros, E., Rodius, F., Duclos, F., Monticelli, A. *et al*. (1996) Friedreich's ataxia: autosomal recessive disease caused by an intronic GAA triplet repeat expansion. *Science* **271**, 1423-7.

43 Campuzano, V., Montermini, L., Lutz, Y., Cova, L., Hindelang, C., Jiralerspong, S., Trottier, Y., Kish, S.J., Faucheux, B., Trouillas, P., Authier, F.J., Durr, A., Mandel, J.L., Vescovi, A., Pandolfo, M. and Koenig, M. (1997) Frataxin is reduced in Friedreich ataxia patients and is associated with mitochondrial membranes. *Hum Mol Genet* **6**, 1771-80.

44 Rotig, A., de Lonlay, P., Chretien, D., Foury, F., Koenig, M., Sidi, D., Munnich, A. and Rustin, P. (1997) Aconitase and mitochondrial iron-sulphur protein deficiency in Friedreich ataxia. *Nat Genet* **17**, 215-7.

45 Casari, G., De Fusco, M., Ciarmatori, S., Zeviani, M., Mora, M., Fernandez, P., De Michele, G., Filla, A., Cocozza, S., Marconi, R., Durr, A., Fontaine, B. and Ballabio, A. (1998) Spastic paraplegia and OXPHOS impairment caused by mutations in paraplegin, a nuclear-encoded mitochondrial metalloprotease. *Cell* **93**, 973-83.

46 Tzagoloff, A., Yue, J., Jang, J. and Paul, M.F. (1994) A new member of a family of ATPases is essential for assembly of mitochondrial respiratory chain and ATP synthetase complexes in *Saccharomyces cerevisiae*. *J Biol Chem* **269**, 26144-51.

47 Bull, P.C., Thomas, G.R., Rommens, J.M., Forbes, J.R. and Cox, D.W. (1993) The Wilson disease gene is a putative copper transporting P-type ATPase similar to the Menkes gene. *Nat Genet* **5**, 327-37.

48 Lutsenko, S. and Cooper, M.J. (1998) Localization of the Wilson's disease protein product to mitochondria. *Proc Natl Acad Sci U S A* **95**, 6004-9.

49 The Huntington's Disease Collaborative Research Group. (1993) A novel gene containing a trinucleotide repeat that is expanded and unstable on Huntington's disease chromosomes. *Cell* **72**, 971-83.

50 Tao, T. and Tartakoff, A.M. (2001) Nuclear relocation of normal huntingtin. *Traffic* **2**, 385-94.

51 Gu, M., Gash, M.T., Mann, V.M., Javoy-Agid, F., Cooper, J.M. and Schapira, A.H. (1996) Mitochondrial defect in Huntington's disease caudate nucleus. *Ann Neurol* **39**, 385-9.

52 Rosen, D.R., Siddique, T., Patterson, D., Figlewicz, D.A., Sapp, P., Hentati, A., Donaldson, D., Goto, J., O'Regan, J.P., Deng, H.X. *et al*. (1993) Mutations in Cu/Zn superoxide dismutase gene are associated with familial amyotrophic lateral sclerosis. *Nature* **362**, 59-62.

53 Gurney, M.E., Pu, H., Chiu, A.Y., Dal Canto, M.C., Polchow, C.Y., Alexander, D.D., Caliendo, J., Hentati, A., Kwon, Y.W., Deng, H.X. *et al*. (1994) Motor neuron degeneration in mice that express a human Cu,Zn superoxide dismutase mutation. *Science* **264**, 1772-5.

54 Browne, S.E., Bowling, A.C., Baik, M.J., Gurney, M., Brown, R.H., Jr. and Beal, M.F. (1998) Metabolic dysfunction in familial, but not sporadic, amyotrophic lateral sclerosis. *J Neurochem* **71**, 281-7.

55 Okado-Matsumoto, A., Myint, T., Fujii, J. and Taniguchi, N. (2000) Gain in functions of mutant Cu,Zn-superoxide dismutases as a causative factor in familial amyotrophic lateral sclerosis: less reactive oxidant formation but high spontaneous aggregation and precipitation. *Free Radic Res* **33**, 65-73.

56 Baker, M., Litvan, I., Houlden, H., Adamson, J., Dickson, D., Perez-Tur, J., Hardy, J., Lynch, T., Bigio, E. and Hutton, M. (1999) Association of an extended haplotype in the *tau* gene with progressive supranuclear palsy. *Hum Mol Genet* **8**, 711-5.

57 Goedert, M., Spillantini, M.G., Jakes, R., Rutherford, D. and Crowther, R.A. (1989) Multiple isoforms of human microtubule-associated protein tau: sequences and localization in neurofibrillary tangles of Alzheimer's disease. *Neuron* **3**, 519-26.

58 Sergeant, N., Wattez, A. and Delacourte, A. (1999) Neurofibrillary degeneration in progressive supranuclear palsy and corticobasal degeneration: tau pathologies with exclusively exon 10; isoforms. *J Neurochem* **72**, 1243-9.

59 Mailliot, C., Sergeant, N., Bussiere, T., Caillet-Boudin, M.L., Delacourte, A. and Buee, L. (1998) Phosphorylation of specific sets of tau isoforms reflects different neurofibrillary degeneration processes. *FEBS Lett* **433**, 201-4.

60 Albers, D.S. and Augood, S.J. (2001) New insights into progressive supranuclear palsy. *Trends Neurosci* **24**, 347-53.

61 Calhoun, M.W., Thomas, J.W. and Gennis, R.B. (1994) The cytochrome oxidase superfamily of redox-driven proton pumps. *Trends Biochem Sci* **19**, 325-30.

62 Tsukihara, T., Aoyama, H., Yamashita, E., Tomizaki, T., Yamaguchi, H., Shinzawa-Itoh, K., Nakashima, R., Yaono, R. and Yoshikawa, S. (1996) The whole structure of the 13-subunit oxidized cytochrome c oxidase at 2.8 Å. *Science* **272**, 1136-44.

63 Schlerf, A., Droste, M., Winter, M. and Kadenbach, B. (1988) Characterization of two different genes (cDNA) for cytochrome *c* oxidase subunit VIa from heart and liver of the rat. *Embo J* **7**, 2387-91.

64 Seelan, R.S. and Grossman, L.I. (1991) Cytochrome *c* oxidase subunit VIIa isoforms. Characterization and expression of bovine cDNAs. *J Biol Chem* **266**, 19752-7.

65 Lightowlers, R., Ewart, G., Aggeler, R., Zhang, Y.Z., Calavetta, L. and Capaldi, R.A. (1990) Isolation and characterization of the cDNAs encoding two isoforms of subunit CIX of bovine cytochrome *c* oxidase. *J Biol Chem* **265**, 2677-81.

66 Schillace, R., Preiss, T., Lightowlers, R.N. and Capaldi, R.A. (1994) Developmental regulation of tissue-specific isoforms of subunit VIa of beef cytochrome *c* oxidase. *Biochim Biophys Acta* **1188**, 391-7.

67 Bratton, M.R., Pressler, M.A. and Hosler, J.P. (1999) Suicide inactivation of cytochrome *c* oxidase: catalytic turnover in the absence of subunit III alters the active site. *Biochemistry* **38**, 16236-45.

68 Taanman, J.W. (1997) Human cytochrome *c* oxidase: structure, function, and deficiency. *J Bioenerg Biomembr* **29**, 151-63.

69 Napiwotzki, J., Shinzawa-Itoh, K., Yoshikawa, S. and Kadenbach, B. (1997) ATP and ADP bind to cytochrome *c* oxidase and regulate its activity. *Biol Chem* **378**, 1013-21.

70 Arnold, S., Goglia, F. and Kadenbach, B. (1998) 3,5-Diiodothyronine binds to subunit Va of cytochrome-*c* oxidase and abolishes the allosteric inhibition of respiration by ATP. *Eur J Biochem* **252**, 325-30.

71 Frank, V. and Kadenbach, B. (1996) Regulation of the H+/e- stoichiometry of cytochrome *c* oxidase from bovine heart by intramitochondrial ATP/ADP ratios. *FEBS Lett* **382**, 121-4.

72 Huttemann, M., Frank, V. and Kadenbach, B. (1999) The possible role of isoforms of cytochrome *c* oxidase subunit VIa in mammalian thermogenesis. *Cell Mol Life Sci* **55**, 1482-90.

73 Taanman, J.W. and Capaldi, R.A. (1992) Purification of yeast cytochrome *c* oxidase with a subunit composition resembling the mammalian enzyme. *J Biol Chem* **267**, 22481-5.

74 Schatz, G. (1996) The protein import system of mitochondria. *J Biol Chem* **271**, 31763-6.

75 Van Dyck, L. and Langer, T. (1999) ATP-dependent proteases controlling mitochondrial function in the yeast *Saccharomyces cerevisiae*. *Cell Mol Life Sci* **56**, 825-42.

76 Nijtmans, L.G., de Jong, L., Artal Sanz, M., Coates, P.J., Berden, J.A., Back, J.W., Muijsers, A.O., van der Spek, H. and Grivell, L.A. (2000) Prohibitins act as a membrane-bound chaperone for the stabilization of mitochondrial proteins. *Embo J* **19**, 2444-51.

77 Preuss, M., Leonhard, K., Hell, K., Stuart, R.A., Neupert, W. and Herrmann, J.M. (2001) Mba1, a novel component of the mitochondrial protein export machinery of the yeast *Saccharomyces cerevisiae*. *J Cell Biol* **153**, 1085-96.

78 Hell, K., Neupert, W. and Stuart, R.A. (2001) Oxa1p acts as a general membrane insertion machinery for proteins encoded by mitochondrial DNA. *Embo J* **20**, 1281-8.
79 Tzagoloff, A., Nobrega, M., Gorman, N. and Sinclair, P. (1993) On the functions of the yeast *COX10* and *COX11* gene products. *Biochem Mol Biol Int* **31**, 593-8.
80 Valnot, I., von Kleist-Retzow, J.C., Barrientos, A., Gorbatyuk, M., Taanman, J.W., Mehaye, B., Rustin, P., Tzagoloff, A., Munnich, A. and Rotig, A. (2000) A mutation in the human heme A:farnesyltransferase gene (*COX10*) causes cytochrome *c* oxidase deficiency. *Hum Mol Genet* **9**, 1245-9.
81 Mashkevich, G., Repetto, B., Glerum, D.M., Jin, C. and Tzagoloff, A. (1997) *SHY1*, the yeast homolog of the mammalian *SURF-1* gene, encodes a mitochondrial protein required for respiration. *J Biol Chem* **272**, 14356-64.
82 Zhu, Z., Yao, J., Johns, T., Fu, K., De Bie, I., Macmillan, C., Cuthbert, A.P., Newbold, R.F., Wang, J., Chevrette, M., Brown, G.K., Brown, R.M. and Shoubridge, E.A. (1998) SURF1, encoding a factor involved in the biogenesis of cytochrome *c* oxidase, is mutated in Leigh syndrome. *Nat Genet* **20**, 337-43.
83 Poyau, A., Buchet, K. and Godinot, C. (1999) Sequence conservation from human to prokaryotes of Surf1, a protein involved in cytochrome *c* oxidase assembly, deficient in Leigh syndrome. *FEBS Lett* **462**, 416-20.
84 Glerum, D.M., Shtanko, A. and Tzagoloff, A. (1996) *SCO1* and *SCO2* act as high copy suppressors of a mitochondrial copper recruitment defect in *Saccharomyces cerevisiae*. *J Biol Chem* **271**, 20531-5.
85 Rentzsch, A., Krummeck-Weiss, G., Hofer, A., Bartuschka, A., Ostermann, K. and Rödel, G. (1999) Mitochondrial copper metabolism in yeast: mutational analysis of Sco1p involved in the biogenesis of cytochrome *c* oxidase. *Curr Genet* **35**, 103-8.
86 Glerum, D.M., Shtanko, A. and Tzagoloff, A. (1996) Characterization of *COX17*, a yeast gene involved in copper metabolism and assembly of cytochrome oxidase. *J Biol Chem* **271**, 14504-9.
87 Hiser, L., Di Valentin, M., Hamer, A.G. and Hosler, J.P. (2000) Cox11p is required for stable formation of the Cu(B) and magnesium centers of cytochrome *c* oxidase. *J Biol Chem* **275**, 619-23.
88 Nijtmans, L.G., Taanman, J.W., Muijsers, A.O., Speijer, D. and Van den Bogert, C. (1998) Assembly of cytochrome-*c* oxidase in cultured human cells. *Eur J Biochem* **254**, 389-94.
89 Wielburski, A. and Nelson, B.D. (1983) Evidence for the sequential assembly of cytochrome oxidase subunits in rat liver mitochondria. *Biochem J* **212**, 829-34.
90 Taanman, J.W. and Williams, S.L. (2001) Assembly of cytochrome *c* oxidase: what can we learn from patients with cytochrome *c* oxidase deficiency? *Biochem Soc Trans* **29**, 446-51.
91 Wielburski, A. and Nelson, B.D. (1984) Heme *a* induces assembly of rat liver cytochrome *c* oxidase subunits I--III in isolated mitochondria. *FEBS Lett* **177**, 291-4.
92 Dickinson, E.K., Adams, D.L., Schon, E.A. and Glerum, D.M. (2000) A human *SCO2* mutation helps define the role of Sco1p in the cytochrome oxidase assembly pathway. *J Biol Chem* .
93 Forsha, D., Church, C., Wazny, P. and Poyton, R.O. (2001) Structure and function of Pet100p, a molecular chaperone required for the assembly of cytochrome *c* oxidase in *Saccharomyces cerevisiae*. *Biochem Soc Trans* **29**, 436-41.
94 Nijtmans, L.G., Artal Sanz, M., Bucko, M., Farhoud, M.H., Feenstra, M., Hakkaart, G.A., Zeviani, M. and Grivell, L.A. (2001) Shy1p occurs in a high molecular weight complex

and is required for efficient assembly of cytochrome *c* oxidase in yeast. *FEBS Lett* **498**, 46-51.

95 Papadopoulou, L.C., Sue, C.M., Davidson, M.M., Tanji, K., Nishino, I., Sadlock, J.E., Krishna, S., Walker, W., Selby, J., Glerum, D.M., Coster, R.V., Lyon, G., Scalais, E., Lebel, R., Kaplan, P., Shanske, S., De Vivo, D.C., Bonilla, E., Hirano, M., DiMauro, S. and Schon, E.A. (1999) Fatal infantile cardioencephalomyopathy with COX deficiency and mutations in *SCO2*, a COX assembly gene. *Nat Genet* **23**, 333-7.

96 Pequignot, M.O., Dey, R., Zeviani, M., Tiranti, V., Godinot, C., Poyau, A., Sue, C., Di Mauro, S., Abitbol, M. and Marsac, C. (2001) Mutations in the *SURF1* gene associated with Leigh syndrome and cytochrome *c* oxidase deficiency. *Hum Mutat* **17**, 374-81.

97 Poyau, A., Buchet, K., Bouzidi, M.F., Zabot, M.T., Echenne, B., Yao, J., Shoubridge, E.A. and Godinot, C. (2000) Missense mutations in *SURF1* associated with deficient cytochrome *c* oxidase assembly in Leigh syndrome patients. *Hum Genet* **106**, 194-205.

98 von Kleist-Retzow, J.C., Vial, E., Chantrel-Groussard, K., Rotig, A., Munnich, A., Rustin, P. and Taanman, J.W. (1999) Biochemical, genetic and immunoblot analyses of 17 patients with an isolated cytochrome *c* oxidase deficiency. *Biochim Biophys Acta* **1455**, 35-44.

99 Yao, J. and Shoubridge, E.A. (1999) Expression and functional analysis of *SURF1* in Leigh syndrome patients with cytochrome *c* oxidase deficiency. *Hum Mol Genet* **8**, 2541-9.

100 Buchwald, P., Krummeck, G. and Rödel, G. (1991) Immunological identification of yeast SCO1 protein as a component of the inner mitochondrial membrane. *Mol Gen Genet* **229**, 413-20.

101 Horvath, R., Lochmüller, H., Stucka, R., Yao, J., Shoubridge, E.A., Kim, S.H., Gerbitz, K.D. and Jaksch, M. (2000) Characterization of human *SCO1* and *COX17* genes in mitochondrial cytochrome-c-oxidase deficiency. *Biochem Biophys Res Commun* **276**, 530-3.

102 Krummeck, G. and Rödel, G. (1990) Yeast *SCO1* protein is required for a post-translational step in the accumulation of mitochondrial cytochrome *c* oxidase subunits I and II. *Curr Genet* **18**, 13-5.

103 Krummeck, G. (1992) Das mitochondriale SCO1 Protein von *Saccharomyces cerevisiae*: Untersuchungen zur Expression, Topologie und Funktion. *Thesis, Ludwig-Maximilians-Universität München* .

104 Lode, A., Kuschel, M., Paret, C. and Rödel, G. (2000) Mitochondrial copper metabolism in yeast: interaction between sco1p and cox2p. *FEBS Lett* **485**, 19-24.

105 Petruzzella, V., Tiranti, V., Fernandez, P., Ianna, P., Carrozzo, R. and Zeviani, M. (1998) Identification and characterization of human cDNAs specific to *BCS1*, *PET112*, *SCO1*, *COX15*, and *COX11*, five genes involved in the formation and function of the mitochondrial respiratory chain. *Genomics* **54**, 494-504.

106 Schulze, M. and Rödel, G. (1988) *SCO1*, a yeast nuclear gene essential for accumulation of mitochondrial cytochrome *c* oxidase subunit II. *Mol Gen Genet* **211**, 492-8.

107 Schulze, M. and Rödel, G. (1989) Accumulation of the cytochrome *c* oxidase subunits I and II in yeast requires a mitochondrial membrane-associated protein, encoded by the nuclear *SCO1* gene. *Mol. Gen. Genet.* **216**, 37-43.

108 Valnot, I., Osmond, S., Gigarel, N., Mehaye, B., Amiel, J., Cormier-Daire, V., Munnich, A., Bonnefont, J.P., Rustin, P. and Rotig, A. (2000) Mutations of the *SCO1* gene in mitochondrial cytochrome *c* oxidase deficiency with neonatal-onset hepatic failure and encephalopathy. *Am J Hum Genet* **67**, 1104-9.

109 Jaksch, M., Ogilvie, I., Yao, J., Kortenhaus, G., Bresser, H.G., Gerbitz, K.D. and Shoubridge, E.A. (2000) Mutations in *SCO2* are associated with a distinct form of hypertrophic cardiomyopathy and cytochrome *c* oxidase deficiency. *Hum Mol Genet* **9**, 795-801.

110 Jaksch, M., Horvath, R., Horn, N., Auer, D.P., Macmillan, C., Peters, J., Gerbitz, K.D., Kraegeloh-Mann, I., Muntau, A., Karcagi, V., Kalmanchey, R., Lochmüller, H., Shoubridge, E.A. and Freisinger, P. (2001) A Homozygous Mutation in *SCO2* (G1541A), a Cytochrome-*c*-Oxidase Assembly Gene, causes a Novel Phenotype. *Neurology* **in press**.

111 Sue, C.M., Karadimas, C., Checcarelli, N., Tanji, K., Papadopoulou, L.C., Pallotti, F., Guo, F.L., Shanske, S., Hirano, M., De Vivo, D.C., Van Coster, R., Kaplan, P., Bonilla, E. and DiMauro, S. (2000) Differential features of patients with mutations in two COX assembly genes, *SURF-1* and *SCO2*. *Ann Neurol* **47**, 589-95.

112 Amaravadi, R., Glerum, D.M. and Tzagoloff, A. (1997) Isolation of a cDNA encoding the human homolog of *COX17*, a yeast gene essential for mitochondrial copper recruitment. *Hum Genet* **99**, 329-33.

113 Beers, J., Glerum, D.M. and Tzagoloff, A. (1997) Purification, characterization, and localization of yeast Cox17p, a mitochondrial copper shuttle. *J Biol Chem* **272**, 33191-6.

114 Heaton, D., Nittis, T., Srinivasan, C. and Winge, D.R. (2000) Mutational analysis of the mitochondrial copper metallochaperone Cox17. *J Biol Chem* **275**, 37582-7.

115 Heaton, D.N., George, G.N., Garrison, G. and Winge, D.R. (2001) The mitochondrial copper metallochaperone Cox17 exists as an oligomeric, polycopper complex. *Biochemistry* **40**, 743-51.

116 Punter, F.A., Adams, D.L. and Glerum, D.M. (2000) Characterization and localization of human *COX17*, a gene involved in mitochondrial copper transport. *Hum Genet* **107**, 69-74.

117 Srinivasan, C., Posewitz, M.C., George, G.N. and Winge, D.R. (1998) Characterization of the copper chaperone Cox17 of *Saccharomyces cerevisiae*. *Biochemistry* **37**, 7572-7.

118 Glerum, D.M. and Tzagoloff, A. (1994) Isolation of a human cDNA for heme A:farnesyltransferase by functional complementation of a yeast *cox10* mutant. *Proc Natl Acad Sci U S A* **91**, 8452-6.

119 Murakami, T., Reiter, L.T. and Lupski, J.R. (1997) Genomic structure and expression of the human heme A:farnesyltransferase (*COX10*) gene. *Genomics* **42**, 161-4.

120 Nobrega, M.P., Nobrega, F.G. and Tzagoloff, A. (1990) *COX10* codes for a protein homologous to the *ORF1* product of *Paracoccus denitrificans* and is required for the synthesis of yeast cytochrome oxidase. *J Biol Chem* **265**, 14220-6.

121 Glerum, D.M., Koerner, T.J. and Tzagoloff, A. (1995) Cloning and characterization of *COX14*, whose product is required for assembly of yeast cytochrome oxidase. *J Biol Chem* **270**, 15585-90.

122 Barros, M.H., Carlson, C.G., Glerum, D.M. and Tzagoloff, A. (2001) Involvement of mitochondrial ferredoxin and Cox15p in hydroxylation of heme O. *FEBS Lett* **492**, 133-8.

123 Souza, R.L., Green-Willms, N.S., Fox, T.D., Tzagoloff, A. and Nobrega, F.G. (2000) Cloning and characterization of *COX18*, a *Saccharomyces cerevisiae* PET gene required for the assembly of cytochrome oxidase. *J Biol Chem* **275**, 14898-902.

124 Hell, K., Tzagoloff, A., Neupert, W. and Stuart, R.A. (2000) Identification of Cox20p, a novel protein involved in the maturation and assembly of cytochrome oxidase subunit 2. *J Biol Chem* **275**, 4571-8.

125 McEwen, J.E., Hong, K.H., Park, S. and Preciado, G.T. (1993) Sequence and chromosomal localization of two *PET* genes required for cytochrome *c* oxidase assembly in *Saccharomyces cerevisiae*. *Curr Genet* **23**, 9-14.
126 Arner, E.S. and Holmgren, A. (2000) Physiological functions of thioredoxin and thioredoxin reductase. *Eur J Biochem* **267**, 6102-9.
127 Holmgren, A. (1989) Thioredoxin and glutaredoxin systems. *J Biol Chem* **264**, 13963-6.
128 Martin, J.L. (1995) Thioredoxin - a fold for all reasons. *Structure* **3**, 245-50.
129 Fabianek, R.A., Hennecke, H. and Thony-Meyer, L. (2000) Periplasmic protein thiol:disulfide oxidoreductases of *Escherichia coli*. *FEMS Microbiol Rev* **24**, 303-16.
130 Bardwell, J.C., McGovern, K. and Beckwith, J. (1991) Identification of a protein required for disulfide bond formation *in vivo*. *Cell* **67**, 581-9.
131 Beckett, C.S., Loughman, J.A., Karberg, K.A., Donato, G.M., Goldman, W.E. and Kranz, R.G. (2000) Four genes are required for the system II cytochrome *c* biogenesis pathway in *Bordetella pertussis*, a unique bacterial model. *Mol Microbiol* **38**, 465-81.
132 Loferer, H. and Hennecke, H. (1994) Expression, purification and functional properties of a soluble form of *Bradyrhizobium japonicum* TlpA, a thioredoxin-like protein. *Eur J Biochem* **223**, 339-44.
133 Bott, M., Bolliger, M. and Hennecke, H. (1990) Genetic analysis of the cytochrome *c*-aa3 branch of the *Bradyrhizobium japonicum* respiratory chain. *Mol Microbiol* **4**, 2147-57.
134 Loferer, H., Wunderlich, M., Hennecke, H. and Glockshuber, R. (1995) A bacterial thioredoxin-like protein that is exposed to the periplasm has redox properties comparable with those of cytoplasmic thioredoxins. *J Biol Chem* **270**, 26178-83.
135 Pedrajas, J.R., Kosmidou, E., Miranda-Vizuete, A., Gustafsson, J.A., Wright, A.P. and Spyrou, G. (1999) Identification and functional characterization of a novel mitochondrial thioredoxin system in *Saccharomyces cerevisiae*. *J Biol Chem* **274**, 6366-73.
136 Spyrou, G., Enmark, E., Miranda-Vizuete, A. and Gustafsson, J. (1997) Cloning and expression of a novel mammalian thioredoxin. *J Biol Chem* **272**, 2936-41.
137 Halliwell, B. and Gutteridge, J.M. (1985) The importance of free radicals and catalytic metal ions in human diseases. *Mol Aspects Med* **8**, 89-193.
138 Rae, T.D., Schmidt, P.J., Pufahl, R.A., Culotta, V.C. and O'Halloran, T.V. (1999) Undetectable intracellular free copper: the requirement of a copper chaperone for superoxide dismutase. *Science* **284**, 805-8.
139 Sato, M. and Gitlin, J.D. (1991) Mechanisms of copper incorporation during the biosynthesis of human ceruloplasmin. *J Biol Chem* **266**, 5128-34.
140 Lee, J., Prohaska, J.R. and Thiele, D.J. (2001) Essential role for mammalian copper transporter Ctr1 in copper homeostasis and embryonic development. *Proc Natl Acad Sci U S A* **98**, 6842-7.
141 Dancis, A., Haile, D., Yuan, D.S. and Klausner, R.D. (1994) The *Saccharomyces cerevisiae* copper transport protein (Ctr1p). Biochemical characterization, regulation by copper, and physiologic role in copper uptake. *J Biol Chem* **269**, 25660-7.
142 Knight, S.A., Labbe, S., Kwon, L.F., Kosman, D.J. and Thiele, D.J. (1996) A widespread transposable element masks expression of a yeast copper transport gene. *Genes Dev* **10**, 1917-29.
143 Zhou, B. and Gitschier, J. (1997) *hCTR1*: a human gene for copper uptake identified by complementation in yeast. *Proc Natl Acad Sci U S A* **94**, 7481-6.
144 Kagi, J.H. (1991) Overview of metallothionein. *Methods Enzymol* **205**, 613-26.
145 Klomp, L.W., Lin, S.J., Yuan, D.S., Klausner, R.D., Culotta, V.C. and Gitlin, J.D. (1997) Identification and functional expression of *HAH1*, a novel human gene involved in copper homeostasis. *J Biol Chem* **272**, 9221-6.

146 Thomas, G.R., Forbes, J.R., Roberts, E.A., Walshe, J.M. and Cox, D.W. (1995) The Wilson disease gene: spectrum of mutations and their consequences. *Nat Genet* **9**, 210-7.
147 Tumer, Z. and Horn, N. (1998) Menkes disease: underlying genetic defect and new diagnostic possibilities. *J Inherit Metab Dis* **21**, 604-12.
148 Petris, M.J., Mercer, J.F., Culvenor, J.G., Lockhart, P., Gleeson, P.A. and Camakaris, J. (1996) Ligand-regulated transport of the Menkes copper P-type ATPase efflux pump from the Golgi apparatus to the plasma membrane: a novel mechanism of regulated trafficking. *Embo J* **15**, 6084-95.
149 Schaefer, M., Hopkins, R.G., Failla, M.L. and Gitlin, J.D. (1999) Hepatocyte-specific localization and copper-dependent trafficking of the Wilson's disease protein in the liver. *Am J Physiol* **276**, G639-46.
150 Solioz, M. and Vulpe, C. (1996) CPx-type ATPases: a class of P-type ATPases that pump heavy metals. *Trends Biochem Sci* **21**, 237-41.
151 Larin, D., Mekios, C., Das, K., Ross, B., Yang, A.S. and Gilliam, T.C. (1999) Characterization of the interaction between the Wilson and Menkes disease proteins and the cytoplasmic copper chaperone, HAH1p. *J Biol Chem* **274**, 28497-504.
152 Hamza, I., Schaefer, M., Klomp, L.W. and Gitlin, J.D. (1999) Interaction of the copper chaperone HAH1 with the Wilson disease protein is essential for copper homeostasis. *Proc Natl Acad Sci U S A* **96**, 13363-8.
153 Fu, D., Beeler, T.J. and Dunn, T.M. (1995) Sequence, mapping and disruption of *CCC2*, a gene that cross-complements the Ca(2+)-sensitive phenotype of *csg1* mutants and encodes a P-type ATPase belonging to the Cu(2+)-ATPase subfamily. *Yeast* **11**, 283-92.
154 Pufahl, R.A., Singer, C.P., Peariso, K.L., Lin, S.J., Schmidt, P.J., Fahrni, C.J., Culotta, V.C., Penner-Hahn, J.E. and O'Halloran, T.V. (1997) Metal ion chaperone function of the soluble Cu(I) receptor Atx1. *Science* **278**, 853-6.
155 Hung, I.H., Casareno, R.L., Labesse, G., Mathews, F.S. and Gitlin, J.D. (1998) HAH1 is a copper-binding protein with distinct amino acid residues mediating copper homeostasis and antioxidant defense. *J Biol Chem* **273**, 1749-54.
156 DiDonato, M., Narindrasorasak, S., Forbes, J.R., Cox, D.W. and Sarkar, B. (1997) Expression, purification, and metal binding properties of the N-terminal domain from the wilson disease putative copper-transporting ATPase (ATP7B). *J Biol Chem* **272**, 33279-82.
157 Lutsenko, S., Petrukhin, K., Cooper, M.J., Gilliam, C.T. and Kaplan, J.H. (1997) N-terminal domains of human copper-transporting adenosine triphosphatases (the Wilson's and Menkes disease proteins) bind copper selectively *in vivo* and *in vitro* with stoichiometry of one copper per metal-binding repeat. *J Biol Chem* **272**, 18939-44.
158 McCord, J.M. and Fridovich, I. (1969) Superoxide dismutase. An enzymic function for erythrocuprein (hemocuprein). *J Biol Chem* **244**, 6049-55.
159 Horecka, J., Kinsey, P.T. and Sprague, G.F., Jr. (1995) Cloning and characterization of the *Saccharomyces cerevisiae LYS7* gene: evidence for function outside of lysine biosynthesis. *Gene* **162**, 87-92.
160 Culotta, V.C., Klomp, L.W., Strain, J., Casareno, R.L., Krems, B. and Gitlin, J.D. (1997) The copper chaperone for superoxide dismutase. *J Biol Chem* **272**, 23469-72.
161 Schmidt, P.J., Rae, T.D., Pufahl, R.A., Hamma, T., Strain, J., O'Halloran, T.V. and Culotta, V.C. (1999) Multiple protein domains contribute to the action of the copper chaperone for superoxide dismutase. *J Biol Chem* **274**, 23719-25.
162 Lamb, A.L., Wernimont, A.K., Pufahl, R.A., Culotta, V.C., O'Halloran, T.V. and Rosenzweig, A.C. (1999) Crystal structure of the copper chaperone for superoxide dismutase. *Nat Struct Biol* **6**, 724-9.

163 Lamb, A.L., Wernimont, A.K., Pufahl, R.A., O'Halloran, T.V. and Rosenzweig, A.C. (2000) Crystal structure of the second domain of the human copper chaperone for superoxide dismutase. *Biochemistry* **39**, 1589-95.
164 Eisses, J.F., Stasser, J.P., Ralle, M., Kaplan, J.H. and Blackburn, N.J. (2000) Domains I and III of the Human Copper Chaperone for Superoxide Dismutase Interact via a Cysteine-Bridged Dicopper(I) Cluster. *Biochemistry* **39**, 7337-7342.
165 Casareno, R.L., Waggoner, D. and Gitlin, J.D. (1998) The copper chaperone CCS directly interacts with copper/zinc superoxide dismutase. *J Biol Chem* **273**, 23625-8.
166 Lamb, A.L., Torres, A.S., O'Halloran, T.V. and Rosenzweig, A.C. (2000) Heterodimer formation between superoxide dismutase and its copper chaperone. *Biochemistry* **39**, 14720-7.
167 Rosenzweig, A.C. and O'Halloran, T.V. (2000) Structure and chemistry of the copper chaperone proteins. *Curr Opin Chem Biol* **4**, 140-7.
168 Cormier, V., Rustin, P., Bonnefont, J.P., Rambaud, C., Vassault, A., Rabier, D., Parvy, P., Couderc, S., Parrot-Roulaud, F., Carre, M. *et al*. (1991) Hepatic failure in disorders of oxidative phosphorylation with neonatal onset. *J Pediatr* **119**, 951-4.
169 DiMauro, S., Lombes, A., Nakase, H., Mita, S., Fabrizi, G.M., Tritschler, H.J., Bonilla, E., Miranda, A.F., DeVivo, D.C. and Schon, E.A. (1990) Cytochrome *c* oxidase deficiency. *Pediatr Res* **28**, 536-41.
170 Holt, I.J., Harding, A.E., Cooper, J.M., Schapira, A.H., Toscano, A., Clark, J.B. and Morgan-Hughes, J.A. (1989) Mitochondrial myopathies: clinical and biochemical features of 30 patients with major deletions of muscle mitochondrial DNA. *Ann Neurol* **26**, 699-708.
171 Lombes, A., Nakase, H., Tritschler, H.J., Kadenbach, B., Bonilla, E., DeVivo, D.C., Schon, E.A. and DiMauro, S. (1991) Biochemical and molecular analysis of cytochrome *c* oxidase deficiency in Leigh's syndrome. *Neurology* **41**, 491-8.
172 Hayasaka, K., Brown, G.K., Danks, D.M., Droste, M. and Kadenbach, B. (1989) Cytochrome *c* oxidase deficiency in subacute necrotizing encephalopathy (Leigh syndrome). *J Inherit Metab Dis* **12**, 247-56.
173 Tiranti, V., Galimberti, C., Nijtmans, L., Bovolenta, S., Perini, M.P. and Zeviani, M. (1999) Characterization of *SURF-1* expression and Surf-1p function in normal and disease conditions. *Hum Mol Genet* **8**, 2533-40.
174 Mogi, T., Saiki, K. and Anraku, Y. (1994) Biosynthesis and functional role of haem O and haem A. *Mol Microbiol* **14**, 391-8.
175 Rep, M. and Grivell, L.A. (1996) The role of protein degradation in mitochondrial function and biogenesis. *Curr Genet* **30**, 367-80.
176 Chinenov, Y.V. (2000) Cytochrome *c* oxidase assembly factors with a thioredoxin fold are conserved among prokaryotes and eukaryotes. *J Mol Med* **78**, 239-42.
177 Smits, P.H., De Haan, M., Maat, C. and Grivell, L.A. (1994) The complete sequence of a 33 kb fragment on the right arm of chromosome II from *Saccharomyces cerevisiae* reveals 16 open reading frames, including ten new open reading frames, five previously identified genes and a homologue of the *SCO1* gene. *Yeast* **10 Suppl A**, S75-80.
178 Buggy, J. and Bauer, C.E. (1995) Cloning and characterization of *senC*, a gene involved in both aerobic respiration and photosynthesis gene expression *in Rhodobacter capsulatus*. *J Bacteriol* **177**, 6958-65.
179 Mattatall, N.R., Jazairi, J. and Hill, B.C. (2000) Characterization of YpmQ, an accessory protein required for the expression of cytochrome *c* oxidase in *Bacillus subtilis. J Biol Chem* .

180 Eraso, J.M. and Kaplan, S. (2000) From redox flow to gene regulation: role of the PrrC protein of *Rhodobacter sphaeroides* 2.4.1. *Biochemistry* **39**, 2052-62.
181 Santana, M., Kunst, F., Hullo, M.F., Rapoport, G., Danchin, A. and Glaser, P. (1992) Molecular cloning, sequencing, and physiological characterization of the *qox* operon from *Bacillus subtilis* encoding the aa3-600 quinol oxidase. *J Biol Chem* **267**, 10225-31.
182 Gray, K.A., Grooms, M., Myllykallio, H., Moomaw, C., Slaughter, C. and Daldal, F. (1994) *Rhodobacter capsulatus* contains a novel cb-type cytochrome *c* oxidase without a CuA center. *Biochemistry* **33**, 3120-7.
183 Merante, F., Petrova-Benedict, R., MacKay, N., Mitchell, G., Lambert, M., Morin, C., De Braekeleer, M., Laframboise, R., Gagne, R. and Robinson, B.H. (1993) A biochemically distinct form of cytochrome oxidase (COX) deficiency in the Saguenay-Lac-Saint-Jean region of Quebec. *Am J Hum Genet* **53**, 481-7.
184 Glerum, D.M. and Tzagoloff, A. (1998) Affinity purification of yeast cytochrome oxidase with biotinylated subunits 4, 5, or 6. *Anal Biochem* **260**, 38-43.
185 Hanahan, D. (1983) Studies on transformation of *Escherichia coli* with plasmids. *J Mol Biol* **166**, 557-80.
186 Studier, F.W. and Moffatt, B.A. (1986) Use of bacteriophage T7 RNA polymerase to direct selective high-level expression of cloned genes. *J Mol Biol* **189**, 113-30.
187 Jones, H.W., Jr., McKusick, V.A., Harper, P.S. and Wuu, K.D. (1971) George Otto Gey. (1899-1970). The HeLa cell and a reappraisal of its origin. *Obstet Gynecol* **38**, 945-9.
188 Hill, J.E., Myers, A.M., Koerner, T.J. and Tzagoloff, A. (1986) Yeast/*E. coli* shuttle vectors with multiple unique restriction sites. *Yeast* **2**, 163-7.
189 Mumberg, D., Muller, R. and Funk, M. (1995) Yeast vectors for the controlled expression of heterologous proteins in different genetic backgrounds. *Gene* **156**, 119-22.
190 Sambrook, J., Fritsch, E.F. and Maniatis, T. (1989) Molecular Cloning. A Laboratory Manual, Press: New York.
191 Pogulis, R.J., Vallejo, A.N. and Pease, L.R. (1996) *In vitro* recombination and mutagenesis by overlap extension PCR. *Methods Mol Biol* **57**, 167-76.
192 Lim, P.S., Jenson, A.B., Cowsert, L., Nakai, Y., Lim, L.Y., Jin, X.W. and Sundberg, J.P. (1990) Distribution and specific identification of papillomavirus major capsid protein epitopes by immunocytochemistry and epitope scanning of synthetic peptides. *J Infect Dis* **162**, 1263-9.
193 Sanger, F., Nicklen, S. and Coulson, A.R. (1977) DNA sequencing with chain-terminating inhibitors. *Proc Natl Acad Sci U S A* **74**, 5463-7.
194 Gietz, R.D., Schiestl, R.H., Willems, A.R. and Woods, R.A. (1995) Studies on the transformation of intact yeast cells by the LiAc/SS-DNA/PEG procedure. *Yeast* **11**, 355-60.
195 Tzagoloff, A., Akai, A. and Needleman, R.B. (1975) Assembly of the mitochondrial membrane system. Characterization of nuclear mutants of *Saccharomyces cerevisiae* with defects in mitochondrial ATPase and respiratory enzymes. *J Biol Chem* **250**, 8228-35.
196 Bradford, M.M. (1976) A rapid and sensitive method for the quantitation of microgram quantities of protein utilizing the principle of protein-dye binding. *Anal Biochem* **72**, 248-54.
197 Holmgren, A. (1979) Thioredoxin catalyzes the reduction of insulin disulfides by dithiothreitol and dihydrolipoamide. *J Biol Chem* **254**, 9627-32.
198 Tatusova, T.A. and Madden, T.L. (1999) BLAST 2 Sequences, a new tool for comparing protein and nucleotide sequences. *FEMS Microbiol Lett* **174**, 247-50.
199 Hartl, F.U., Pfanner, N., Nicholson, D.W. and Neupert, W. (1989) Mitochondrial protein import. *Biochim Biophys Acta* **988**, 1-45.

200 Claros, M.G. and Vincens, P. (1996) Computational method to predict mitochondrially imported proteins and their targeting sequences. *Eur J Biochem* **241**, 779-86.
201 Altschul, S.F., Madden, T.L., Schaffer, A.A., Zhang, J., Zhang, Z., Miller, W. and Lipman, D.J. (1997) Gapped BLAST and PSI-BLAST: a new generation of protein database search programs. *Nucleic Acids Res* **25**, 3389-402.
202 Rost, B. and Sander, C. (1993) Prediction of protein secondary structure at better than 70% accuracy. *J Mol Biol* **232**, 584-99.
203 Lode, A. (2001) Assemblierung der Cytochrom *c* Oxidase: Molekulare und biochemische Charakterisierung des mitochondrialen Sco1p aus *Saccharomyces cerevisiae* und homologer Proteine. *Thesis, TU-Dresden* .
204 Cubitt, A.B., Heim, R., Adams, S.R., Boyd, A.E., Gross, L.A. and Tsien, R.Y. (1995) Understanding, improving and using green fluorescent proteins. *Trends Biochem Sci* **20**, 448-55.
205 De Giorgi, F., Ahmed, Z., Bastianutto, C., Brini, M., Jouaville, L.S., Marsault, R., Murgia, M., Pinton, P., Pozzan, T. and Rizzuto, R. (1999) Targeting GFP to organelles. *Methods Cell Biol* **58**, 75-85.
206 Rizzuto, R., Brini, M., De Giorgi, F., Rossi, R., Heim, R., Tsien, R.Y. and Pozzan, T. (1996) Double labelling of subcellular structures with organelle-targeted GFP mutants *in vivo*. *Curr Biol* **6**, 183-8.
207 Matsuo, Y., Akiyama, N., Nakamura, H., Yodoi, J., Noda, M. and Kizaka-Kondoh, S. (2001) Identification of a novel thioredoxin-related transmembrane protein. *J Biol Chem* **276**, 10032-8.
208 Nittis, T., George, G.N. and Winge, D.R. (2001) Yeast Sco1, a protein essential for cytochrome *c* oxidase function is a Cu(I)binding protein. *J. Biol. Chem.* **in press**.
209 Herrmann, J.M. and Neupert, W. (2000) Protein transport into mitochondria. *Curr Opin Microbiol* **3**, 210-4.
210 Lee, C.M., Sedman, J., Neupert, W. and Stuart, R.A. (1999) The DNA helicase, Hmi1p, is transported into mitochondria by a C-terminal cleavable targeting signal. *J Biol Chem* **274**, 20937-42.
211 Folsch, H., Guiard, B., Neupert, W. and Stuart, R.A. (1996) Internal targeting signal of the BCS1 protein: a novel mechanism of import into mitochondria. *Embo J* **15**, 479-87.
212 Zara, V., Palmieri, F., Mahlke, K. and Pfanner, N. (1992) The cleavable presequence is not essential for import and assembly of the phosphate carrier of mammalian mitochondria but enhances the specificity and efficiency of import. *J Biol Chem* **267**, 12077-81.
213 Rossi, L., Lippe, G., Marchese, E., De Martino, A., Mavelli, I., Rotilio, G. and Ciriolo, M.R. (1998) Decrease of cytochrome *c* oxidase protein in heart mitochondria of copper-deficient rats. *Biometals* **11**, 207-12.
214 Jensen, P.Y., Bonander, N., Moller, L.B. and Farver, O. (1999) Cooperative binding of copper(I) to the metal binding domains in Menkes disease protein. *Biochim Biophys Acta* **1434**, 103-13.
215 Lutsenko, S., Petrukhin, K., Gilliam, T.C. and Kaplan, J.H. (1997) Heterologous expression of the metal-binding domains of human copper-transporting ATPases (P1-ATPases). *Ann N Y Acad Sci* **834**, 155-7.
216 Yasukawa, T., Kanei-Ishii, C., Maekawa, T., Fujimoto, J., Yamamoto, T. and Ishii, S. (1995) Increase of solubility of foreign proteins in *Escherichia coli* by coproduction of the bacterial thioredoxin. *J Biol Chem* **270**, 25328-31.

217 Stewart, E.J., Aslund, F. and Beckwith, J. (1998) Disulfide bond formation in the *Escherichia coli* cytoplasm: an *in vivo* role reversal for the thioredoxins. *Embo J* **17**, 5543-50.
218 Debarbieux, L. and Beckwith, J. (1998) The reductive enzyme thioredoxin 1 acts as an oxidant when it is exported to the *Escherichia coli* periplasm. *Proc Natl Acad Sci U S A* **95**, 10751-6.
219 Bessette, P.H., Aslund, F., Beckwith, J. and Georgiou, G. (1999) Efficient folding of proteins with multiple disulfide bonds in the *Escherichia coli* cytoplasm. *Proc Natl Acad Sci U S A* **96**, 13703-8.
220 DiDonato, M., Hsu, H.F., Narindrasorasak, S., Que, L., Jr. and Sarkar, B. (2000) Copper-induced conformational changes in the N-terminal domain of the Wilson disease copper-transporting ATPase. *Biochemistry* **39**, 1890-6.
221 Lyons, T.J., Liu, H., Goto, J.J., Nersissian, A., Roe, J.A., Graden, J.A., Cafe, C., Ellerby, L.M., Bredesen, D.E., Gralla, E.B. and Valentine, J.S. (1996) Mutations in copper-zinc superoxide dismutase that cause amyotrophic lateral sclerosis alter the zinc binding site and the redox behavior of the protein. *Proc Natl Acad Sci U S A* **93**, 12240-4.
222 Ellman, G. (1959) Tissue sulfhydryl groups. *Arch. Biochem. Biophys.* **82**, 70-77.
223 Hirotsu, S., Abe, Y., Okada, K., Nagahara, N., Hori, H., Nishino, T. and Hakoshima, T. (1999) Crystal structure of a multifunctional 2-Cys peroxiredoxin heme-binding protein 23 kDa/proliferation-associated gene product. *Proc Natl Acad Sci U S A* **96**, 12333-8.
224 Wernimont, A.K., Huffman, D.L., Lamb, A.L., O'Halloran, T.V. and Rosenzweig, A.C. (2000) Structural basis for copper transfer by the metallochaperone for the Menkes/Wilson disease proteins. *Nat Struct Biol* **7**, 766-71.
225 Rosenzweig, A.C., Huffman, D.L., Hou, M.Y., Wernimont, A.K., Pufahl, R.A. and O'Halloran, T.V. (1999) Crystal structure of the Atx1 metallochaperone protein at 1.02 Å resolution. *Structure Fold Des* **7**, 605-17.
226 Carri, M.T., Battistoni, A., Polizio, F., Desideri, A. and Rotilio, G. (1994) Impaired copper binding by the H46R mutant of human Cu,Zn superoxide dismutase, involved in amyotrophic lateral sclerosis. *FEBS Lett* **356**, 314-6.
227 Lee, K.K., Murakawa, M., Takahashi, S., Tsubuki, S., Kawashima, S., Sakamaki, K. and Yonehara, S. (1998) Purification, molecular cloning, and characterization of TRP32, a novel thioredoxin-related mammalian protein of 32 kDa. *J Biol Chem* **273**, 19160-6.
228 Chivers, P.T., Laboissiere, M.C. and Raines, R.T. (1996) The CXXC motif: imperatives for the formation of native disulfide bonds in the cell. *Embo J* **15**, 2659-67.
229 Mossner, E., Huber-Wunderlich, M., Rietsch, A., Beckwith, J., Glockshuber, R. and Aslund, F. (1999) Importance of redox potential for the *in vivo* function of the cytoplasmic disulfide reductant thioredoxin from *Escherichia coli*. *J Biol Chem* **274**, 25254-9.
230 Monika, E.M., Goldman, B.S., Beckman, D.L. and Kranz, R.G. (1997) A thioreduction pathway tethered to the membrane for periplasmic cytochromes *c* biogenesis; *in vitro* and *in vivo* studies. *J Mol Biol* **271**, 679-92.
231 Chae, H.Z., Chung, S.J. and Rhee, S.G. (1994) Thioredoxin-dependent peroxide reductase from yeast. *J Biol Chem* **269**, 27670-8.
232 Jin, D.Y., Chae, H.Z., Rhee, S.G. and Jeang, K.T. (1997) Regulatory role for a novel human thioredoxin peroxidase in NF-kappaB activation. *J Biol Chem* **272**, 30952-61.
233 Lee, S.R., Kim, J.R., Kwon, K.S., Yoon, H.W., Levine, R.L., Ginsburg, A. and Rhee, S.G. (1999) Molecular cloning and characterization of a mitochondrial selenocysteine-containing thioredoxin reductase from rat liver. *J Biol Chem* **274**, 4722-34.

234 Hwang, C., Sinskey, A.J. and Lodish, H.F. (1992) Oxidized redox state of glutathione in the endoplasmic reticulum. *Science* **257**, 1496-502.
235 Gaut, J.R. and Hendershot, L.M. (1993) The modification and assembly of proteins in the endoplasmic reticulum. *Curr Opin Cell Biol* **5**, 589-95.
236 Locker, J.K. and Griffiths, G. (1999) An unconventional role for cytoplasmic disulfide bonds in vaccinia virus proteins. *J Cell Biol* **144**, 267-79.
237 Creighton, T.E., Zapun, A. and Darby, N.J. (1995) Mechanisms and catalysts of disulfide bond formation in proteins. *Trends Biotechnol* **13**, 18-23.
238 Byrd, J., Berger, R.M., McMillin, D.R., Wright, C.F., Hamer, D. and Winge, D.R. (1988) Characterization of the copper-thiolate cluster in yeast metallothionein and two truncated mutants. *J Biol Chem* **263**, 6688-94.
239 Gamonet, F. and Lauquin, G.J. (1998) The *Saccharomyces cerevisiae LYS7* gene is involved in oxidative stress protection. *Eur J Biochem* **251**, 716-23.
240 Ciriolo, M.R., Desideri, A., Paci, M. and Rotilio, G. (1990) Reconstitution of Cu,Zn-superoxide dismutase by the Cu(I).glutathione complex. *J Biol Chem* **265**, 11030-4.
241 Freedman, J.H., Ciriolo, M.R. and Peisach, J. (1989) The role of glutathione in copper metabolism and toxicity. *J Biol Chem* **264**, 5598-605.
242 Ferruzza, S., Sambuy, Y., Ciriolo, M.R., De Martino, A., Santaroni, P., Rotilio, G. and Scarino, M.L. (2000) Copper uptake and intracellular distribution in the human intestinal Caco-2 cell line. *Biometals* **13**, 179-85.
243 Jiang, L.J., Maret, W. and Vallee, B.L. (1998) The glutathione redox couple modulates zinc transfer from metallothionein to zinc-depleted sorbitol dehydrogenase. *Proc Natl Acad Sci U S A* **95**, 3483-8.
244 Maret, W. (1994) Oxidative metal release from metallothionein via zinc-thiol/disulfide interchange. *Proc Natl Acad Sci U S A* **91**, 237-41.
245 Sakurai, H., Nakajima, K., Kamada, H., Satoh, H., Otaki, N., Kimura, M., Kawano, K. and Hagino, T. (1993) Copper-metallothionein distribution in the liver of Long-Evans cinnamon rats: studies on immunohistochemical staining, metal determination, gel filtration and electron spin resonance spectroscopy. *Biochem Biophys Res Commun* **192**, 893-8.
246 Pfaff, E., Klingenberg, M., Ritt, E. and Vogell, W. (1968) Correlation of the unspecific permeable mitochondrial space with the intermembrane space. *Eur J Biochem* **5**, 222-32.
247 Hall, L.T., Sanchez, R.J., Holloway, S.P., Zhu, H., Stine, J.E., Lyons, T.J., Demeler, B., Schirf, V., Hansen, J.C., Nersissian, A.M., Valentine, J.S. and Hart, P.J. (2000) X-ray crystallographic and analytical ultracentrifugation analyses of truncated and full-length yeast copper chaperones for SOD (LYS7): a dimer-dimer model of LYS7-SOD association and copper delivery. *Biochemistry* **39**, 3611-23.
248 Tsukihara, T., Aoyama, H., Yamashita, E., Tomizaki, T., Yamaguchi, H., Shinzawa-Itoh, K., Nakashima, R., Yaono, R. and Yoshikawa, S. (1995) Structures of metal sites of oxidized bovine heart cytochrome *c* oxidase at 2.8 Å. *Science* **269**, 1069-74.
249 Portnoy, M.E., Rosenzweig, A.C., Rae, T., Huffman, D.L., O'Halloran, T.V. and Culotta, V.C. (1999) Structure-function analyses of the ATX1 metallochaperone. *J Biol Chem* **274**, 15041-5.
250 Tzagoloff, A., Capitanio, N., Nobrega, M.P. and Gatti, D. (1990) Cytochrome oxidase assembly in yeast requires the product of *COX11*, a homolog of the *P. denitrificans* protein encoded by *ORF3*. *Embo J* **9**, 2759-64.
251 Iwata, S., Ostermeier, C., Ludwig, B. and Michel, H. (1995) Structure at 2.8 Å resolution of cytochrome *c* oxidase from *Paracoccus denitrificans*. *Nature* **376**, 660-9.

252 Hanson, B.J., Carrozzo, R., Piemonte, F., Tessa, A., Robinson, B.H. and Capaldi, R.A. (2001) Cytochrome *c* oxidase-deficient patients have distinct subunit assembly profiles. *J Biol Chem* **276**, 16296-301.

253 Nakai, T., Yasuhara, T., Fujiki, Y. and Ohashi, A. (1995) Multiple genes, including a member of the AAA family, are essential for degradation of unassembled subunit 2 of cytochrome *c* oxidase in yeast mitochondria. *Mol Cell Biol* **15**, 4441-52.

254 Marusich, M.F., Robinson, B.H., Taanman, J.W., Kim, S.J., Schillace, R., Smith, J.L. and Capaldi, R.A. (1997) Expression of mtDNA and nDNA encoded respiratory chain proteins in chemically and genetically-derived *rho*^{0} human fibroblasts: a comparison of subunit proteins in normal fibroblasts treated with ethidium bromide and fibroblasts from a patient with mtDNA depletion syndrome. *Biochim Biophys Acta* **1362**, 145-59.

255 Nijtmans, L.G., Spelbrink, J.N., Van Galen, M.J., Zwaan, M., Klement, P. and Van den Bogert, C. (1995) Expression and fate of the nuclearly encoded subunits of cytochrome-*c* oxidase in cultured human cells depleted of mitochondrial gene products. *Biochim Biophys Acta* **1265**, 117-26.

256 Taanman, J.W., Bodnar, A.G., Cooper, J.M., Morris, A.A., Clayton, P.T., Leonard, J.V. and Schapira, A.H. (1997) Molecular mechanisms in mitochondrial DNA depletion syndrome. *Hum Mol Genet* **6**, 935-42.

257 Mazat, J.P., Rossignol, R., Malgat, M., Rocher, C., Faustin, B. and Letellier, T. (2001) What do mitochondrial diseases teach us about normal mitochondrial functions...that we already knew: threshold expression of mitochondrial defects. *Biochim Biophys Acta* **1504**, 20-30.

258 Rossignol, R., Malgat, M., Mazat, J.P. and Letellier, T. (1999) Threshold effect and tissue specificity. Implication for mitochondrial cytopathies. *J Biol Chem* **274**, 33426-32.

259 Van Kuilenburg, A.B., Dekker, H.L., Van den Bogert, C., Nieboer, P., Van Gelder, B.F. and Muijsers, A.O. (1991) Isoforms of human cytochrome-*c* oxidase. Subunit composition and steady-state kinetic properties. *Eur J Biochem* **199**, 615-22.

260 Taanman, J.W., Turina, P. and Capaldi, R.A. (1994) Regulation of cytochrome *c* oxidase by interaction of ATP at two binding sites, one on subunit VIa. *Biochemistry* **33**, 11833-41.

261 DiMauro, S., Servidei, S., Zeviani, M., DiRocco, M., DeVivo, D.C., DiDonato, S., Uziel, G., Berry, K., Hoganson, G., Johnsen, S.D. *et al*. (1987) Cytochrome *c* oxidase deficiency in Leigh syndrome. *Ann Neurol* **22**, 498-506.

262 Zeviani, M., Peterson, P., Servidei, S., Bonilla, E. and DiMauro, S. (1987) Benign reversible muscle cytochrome *c* oxidase deficiency: a second case. *Neurology* **37**, 64-7.

263 Kako, K., Tsumori, K., Ohmasa, Y., Takahashi, Y. and Munekata, E. (2000) The expression of Cox17p in rodent tissues and cells. *Eur J Biochem* **267**, 6699-707.

264 Tumer, Z. and Horn, N. (1996) Menkes disease: recent advances and new insights into copper metabolism. *Ann Med* **28**, 121-9.

265 Jaksch, M., Paret, C., Stucka, R., Horn, N., Mueller-Hoecker, J., Horvath, R., Trepesch, N., Stecker, G., Freisinger, P., Thirion, C., Müller, J., Lunkwitz, R., Rödel, G., Shoubridge, E.A. and Lochmüller, A. (2001) Cytochrome *c* oxidase deficiency due to mutations in *SCO2*, encoding a mitochondrial copper chaperone, is rescued by copper in human myoblasts. *Hum Mol Gen* **in press**.

Danksagung

Am Ende meiner Arbeit möchte ich mich besonders bedanken bei

meinem Chef, Prof. Rödel für die Freiheit und die Unterstützung während meiner Arbeit,

Udo, für die unkomplizierte, lustige und kompetente Weise mit dem er mir sein Wissen in molekularbiologischen Techniken vermittelt hat,

Andreas, für das schnelle und geniale Lösen aller Computer Probleme,

Marlis, für die freundliche Mithilfe bei der Proteinreinigung,

Anja, für die vielen interessanten Diskussionen,

Frau Lunkwitz, für die anregenden Diskussionen über die Kupfer Bestimmung,

Frau Jaksch, für die Arbeits- und nicht Arbeitsgespräche beim Italiener,

Mita, für das Lesen meines Manuskriptes.

Curriculum vitae

Personal details

Name:	Claudia Paret
Title:	Dipl.-Chem.
Date of birth:	21/11/70 in Torino
Marital status:	single
Nationality:	Italian
Present address	Würzburger str 66
	01187 Dresden

Education

1984 -1989	Gymnasium in Torino
1989-1996	Study of Chemistry at the University of Torino
05/1995-07/1996	Thesis at the University of Medicine in Torino, Department of Cell and Molecular Biology (Leader: Prof. I. Perroteau)

Scientific activities and employment

11/1994-05/1995	Student practical training “Protein’s expression in yeast“, University of Medicine, Torino (Leader: Prof. P. M. Comoglio)
08/1996-01/1997	Student practical training at the Environment’s Ministry, Lyon (France)
05/1997-02/1998	Guest research at the Institute of Genetics, University of Technology Dresden (Leader: Prof. Dr. G. Rödel)
since 02/1998	PhD student at the Institute of Genetics, University of Technology Dresden (Leader: Prof. Dr. G. Rödel)

Versicherung

Hiermit versichere ich, dass ich die vorliegende Arbeit ohne unzulässige Hilfe Dritter und ohne Benutzung anderer als der angegebenen Hilfsmittel angefertigt habe. Die aus fremden Quellen direkt oder indirekt übernommenen Gedanken sind als solche kenntlich gemacht. Die Arbeit wurde bisher weder im Inland noch im Ausland in gleicher oder ähnlicher Form einer anderen Prüfungsbehörde vorgelegt.

Die vorliegende Arbeit wurde am Institut für Genetik der TU Dresden unter der wissenschaftlichen Betreuung von Herrn Prof. Dr. rer. nat. habil. G. Rödel angefertigt.

Die Promotionsordnung wird anerkannt

Dresden, den 15. Oktober 2001

Claudia Paret